Master Thesis in Geosciences

Caledonian structuring of the Silurian succession at Sundvollen, Ringerike, southern Norway

Eirik von der Fehr Hjelseth

UNIVERSITY OF OSLO

FACULTY OF MATHEMATICS AND NATURAL SCIENCES

Caledonian structuring of the Silurian succession at Sundvollen, Ringerike, southern Norway

Eirik von der Fehr Hjelseth

Master Thesis in Geosciences

Discipline: Petroleum geology and Petroleum geophysics

Department of Geosciences

Faculty of Mathematics and Natural Sciences

UNIVERSITY OF OSLO

[June 2010]

Tutor(s): Prof. Roy H. Gabrielsen (UIO) and Bjørn T. Larsen (Det Norske oljeselskap ASA)

This work is published digitally through DUO – Digitale Utgivelser ved UiO

http://www.duo.uio.no

It is also catalogued in BIBSYS (http://www.bibsys.no/english)

Acknowledgements

First of all I want to give a special thank to my supervisor Prof. Roy H. Gabrielsen for valuable support and guidance during the field work and preparation of the thesis. I also owe many thanks to my supervisor Bjørn T. Larsen for much appreciated support during this last year.

I would also like to thank Hans Henrik Halden and Hole municipality for assisting with map sheets applied in this thesis. I also would like to thank the kind people at Borgen and Rytteråker for the use of their property and nice conversations.

Thanks to Anders, Jonas and Maren and the remainder of the people in room 214 for interesting discussions and numerous coffee breaks.

I owe many thanks to my family for support and for letting me use the car during the weeks of field work.

Finally I especially would like to thank my dear Ieva for all the encouragement and support.

Abstract

The main scientific goal with this thesis is to study the configuration of the main Caledonian geological structures within the Lower Silurian succession, with emphasis on back-thrusts at Sundvollen, Ringerike in southern Norway. This involves determination of the relationship between main- and subsidiary thrusts and folding in context to the development of the Ringerike area.

Four separate deformational phases connected to the study area are identified based on analysis of the structural geological data. Phase 1 represents the oldest structures, whilst phase 4 represents the youngest. Thrust faults and folds connected to deformational phase 1 are associated with bedding-parallel shortening. The development of tight- to isoclinal, disharmonic folds with upright axial planes is defined as deformational phase 2. Structures connected to deformational phase 3 are foreland-directed thrust faults and large, open and upright folds with wavelengths in the order of hundreds of meters. The orientation of the maximum stress axes indicated by structures associated to phase 1 are generally consistent with what is known for the regional transport in the Oslo Region. The transport directions displayed by the structures comprising phases 2 and 3 are consistent with the main SSE-directed tectonic transport direction displayed in the Oslo Region (e.g Gabrielsen and Larsen in press). Deformational phase 4 comprises back-thrusts. Structures connected to this phase are low-angle thrust faults and fault-propagation-folds. The transport direction of the faults shifts gradually from N-NNW in the southern part of the study area to WNW-NW in the northernmost part. The generally gentle deformational style, characterized by large open folds as displayed in the study area, is consistent with the general structural style in the upper Cambro-Silurian succession in the Oslo Region (Morley 1987a). Back-thrusts are however the most dominant of the exposed thrust faults in the study area. All structures are situated in the Lower Silurian succession at Ringerike. Therefore are phases 1-4 formed in response to the Scandian phase, which corresponds to the main Caledonian deformation (e.g Roberts 2003).

Contents

1 Introduction

1.1 Subject

This master thesis encompasses mapping, description and interpretation of geometry and kinematics of the Caledonian structural evolution in the Sundvollen (Vik) area, Hole municipality, Ringerike area, Norway (Figure 1.1c). The study included structural mapping of the Lower Silurian Sælabonn, Rytteråker and Vik Formations, and generation of structural geological and lithostratigraphic maps and profiles. Further, to develop an analysis of the structural geological data and to prepare a syntheses and structural geological history of the study area.

The foremost scientific aim is to study the configuration of the main geological structures with emphasis on back-thrusts. This involves determination of the relationship between main- and subsidiary thrusts and folding in context to the development of the Ringerike area. The latter is described further by Gabrielsen and Larsen (in press).

1.2 Field work information

The field work comprised collection of structural geologic data and was performed over a period of four weeks, mainly from August to September 2009. The data utilized in this thesis was collected and analyzed by the writer. Before the field work commenced, professor Roy H. Gabrielsen and Bjørn T. Larsen gave a two day extensive introduction and excursion in the study area (Figure 1.1c), on land and on sea. Support and guidance were also provided when necessary during the weeks of field work. The study area is located in Hole municipality , within the Ringerike district, approximately 42 km northwest of Oslo (Figure 1.1b), making it accessible by car. Preparation and analysis of field data were performed at the University of Oslo and Det norske oljeselskap ASA in Oslo.

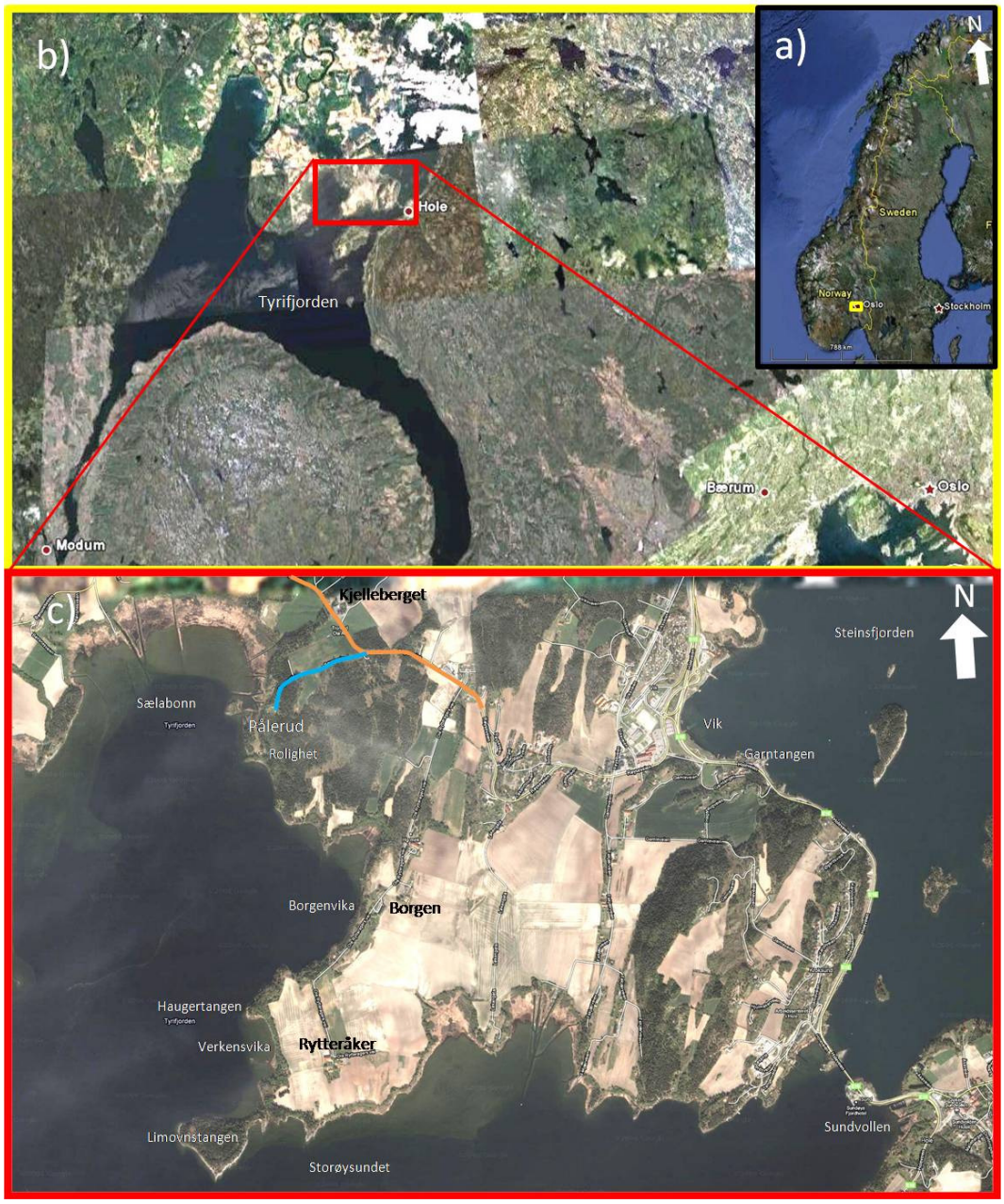

Figure 1.1: a) Satellite image of Norway and most of Sweden. b) Enlarged area from within the yellow square in image a, displaying Oslo (lower right) and Tyrifjorden. The study area is situated within red square. c) Satellite image displaying the study area. A section of Røyseveien has been marked with an orange line whilst the blue line represents a road branch with the same name. Images a. and b. from GoogleEarth™ (2010). Image c. from GoogleMaps™ (2010).

1.3 Equipment, field maps and software

Equipment

To ease access to localities situated along the shoreline, a boat was made disposable to the writer by the Department of Geosciences, University of Oslo. During the field work a Silva Expedition 15 compass was applied for measuring strike and dip of bedding- and fault planes as well as trend and plunge of fold axes and lineations. When collecting the data during this thesis the right-hand rule was applied, which means the dip is to the right of the compass when measuring the strike.

In order to place the accurate positions of localities on to a map a GPS (Global Positioning System) and the GPS on a Nokia Navigator (cell phone) were utilized.
The geological bedrock map sheet *HØNEFOSS 1815 III, M 1:50.000* (Zwaan and Larsen 2003) covers the Ringerike district and was employed in the studies. Two N5-raster map sheets, Ullern 1:5000 (Hole_municipality 2009b) and Rytteråker 1:5000 (Hole_municipality 2009a) were printed at the offices of Hole municipality and formed the basis for the structural geological maps developed by the writer during this thesis.

Software

Satellite and aerial photographs utilized in this thesis have been required from GoogleMaps™ (2010), GoogleEarth™ (2010) and *Norge i 3D*, by Norkart Virtual Globe (2010).

The stereographic projection program StereoWin© (Allmendinger 2010) was applied to plot and display measurements collected in the field. StereoWin allows the user to illustrate measurements such as strike and dip of bedding- and fault planes, trend and plunge of lineations and fold axes in several ways. Strike and dip measurements can be rotated by the program. Further, the trend and plunge of fold axes can be calculated statistically by the program, based on strike and dip measurements of bedding planes measured on a fold.

1.4 Terminology

Folds can be classified on the basis of Ramsay's (1967) fold classification. The dip isogons are lines between two bounding surfaces in the fold which exhibit equal dip. Three main classes have been identified based on the different geometries.

Class 1 – The inner arc displays more curvature than the outer arc (convergent isogons).

Class 2 – The curvature of the inner and outer arc are similar (parallel isogons).

Class 3 – The outer arc displays greater curvature than the inner arc (divergent isogons).

Additionally, Class 1 folds are divided into three sub-classes, where Class-1A folds displays thicker fold limbs compared to the hinge zone. Class-1B folds exhibit constant layer thickness, whilst Class-1C folds display thinner fold limbs compared to the hinge zone.

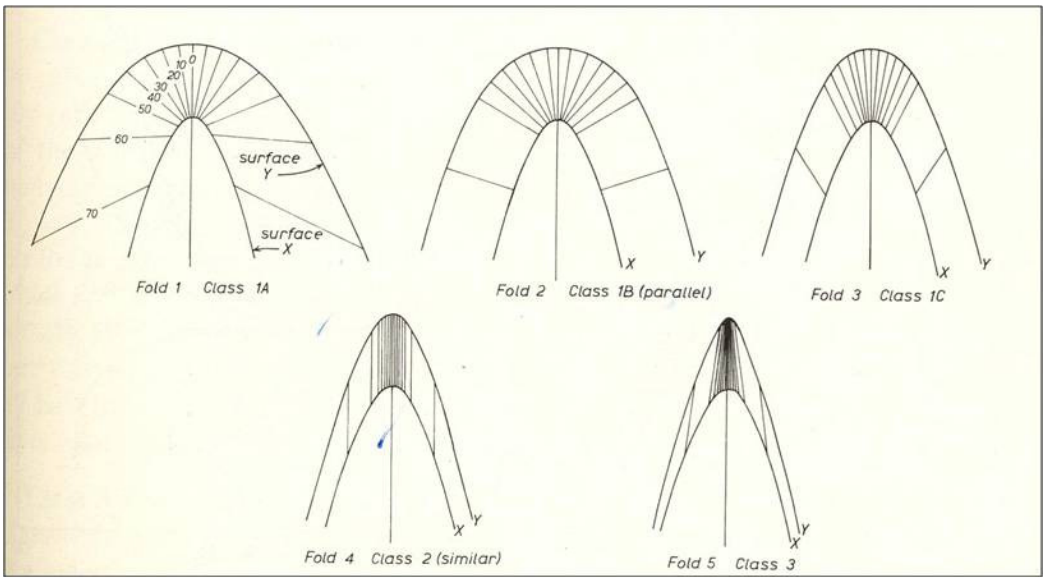

Figure 1.2: Classification of folds based on dip isogons. Figure from Ramsay (1967).

The tightness (Figure 1.3) of folds can be described based on the internal angle between two fold limbs (Davis and Reynolds 1996).

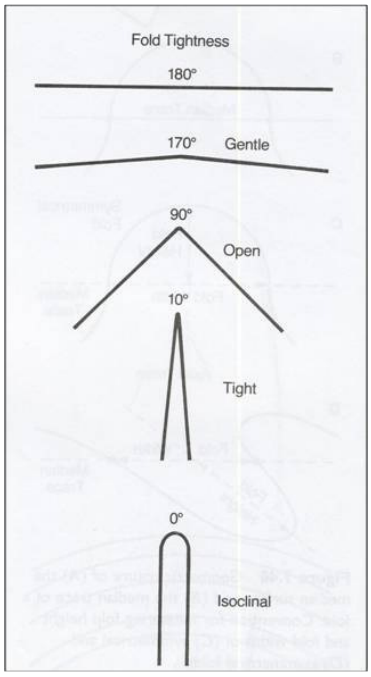

Figure 1.3: Classification of folds based on tightness. Figure from Davis and Reynolds (1996).

Fault-propagation-folds

Fault-propagation-folds are folds which develop in front of a propagating fault as it moves up a ramp (Davis and Reynolds 1996). As the propagation continues, it will cut through the previously formed folds, which are asymmetrical (Figure 1.4). Hence, an undisturbed fold will characterize the upper part and a fault will dominate the lower part (Davis and Reynolds 1996).

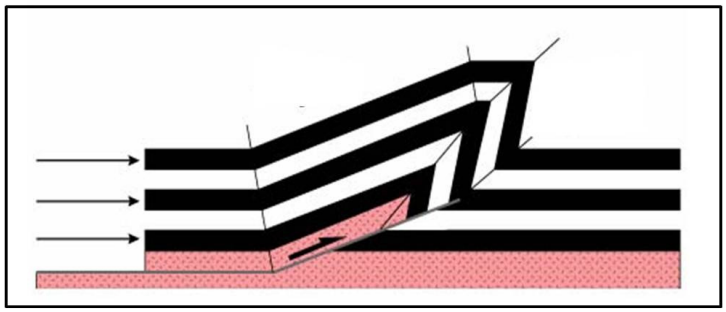

Figure 1.4: Illustration of a fault-propagation-fold. Figure from Fossen and Gabrielsen (2005).

1.5 Foreland basins

Foreland basins are elongated or arcuate depressions developed on continental crust, primarily in response to flexural loading, tied to convergent plate boundaries. Further, they are situated between the continental craton and the contractional orogenic belt (DeCelles and Giles 1996).

Two different classes of foreland basins have been suggested by Dickinson (1974). Both classes are situated on cratonic lithosphere. The first type is called a retroarc foreland basin. These are associated with ocean-continent plate collisions, where the oceanic plate underthrust the continental plate. Retroarc basins develop behind a magmatic arc (Figure 1.5a, b). A modern example is the 200 km wide Chaco foreland basin situated on top of the Brazilian shield, east of the Andes Mountains, western South America (Kearey et al. 2009). The second type, peripheral or pro-foreland basin is linked to continent-continent collision zones (Figure 1.5a), where the Indian foreland basin south of the Himalayans is an example. The Oslo Region would therefore be classified as a part of a peripheral foreland basin (Baarli 1990). The retro-foreland basin sits on the overriding plate, while the peripheral foreland basin is situated on the subducting plate. As previously mentioned, Norway, situated on the Baltic plate, was underthrust by the Laurentian plate during the evolution of the Caledonian Orogeny (Gee 1975, Roberts 2003).

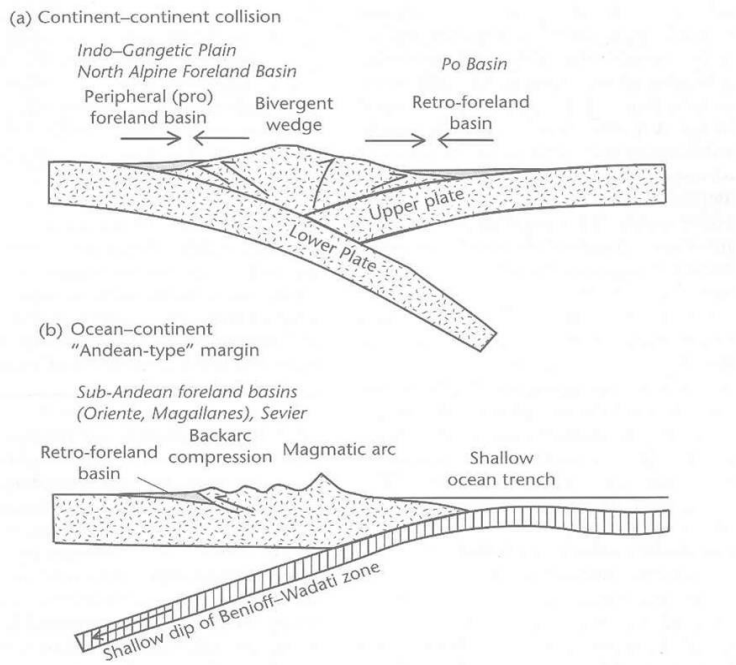

Figure 1.5: a) Continent-continent collision with the Peripheral- and retro-foreland basins. b) Ocean-continent collision and the belonging retro-foreland basin. Figure from Allen & Allen (2005).

Flexural subsidence is mainly induced by the weight of the migrating fold-thrust belt on to the continental lithosphere which causes a depression and forms a basin (Van der Pluijm and Marshak 2004). Lithospheric flexure is also induced by the subducting plates. Peripheral foreland basins may experience additional flexure caused by the weight of the dense down-going oceanic slab in front (Figure 1.6a). Although, with continuing subduction the less dense continental plate will eventually subside, and the flexural response will decrease (DeCelles and Giles 1996). Additionally, viscous coupling (Figure 1.6b) between the overlaying continental plate, mantle-wedge material and the subducting oceanic plate may cause long-wavelength (1000 km or more from the trench) flexural subsidence and uplift (around 1 km) added to Retroarc foreland basins (DeCelles and Giles 1996).

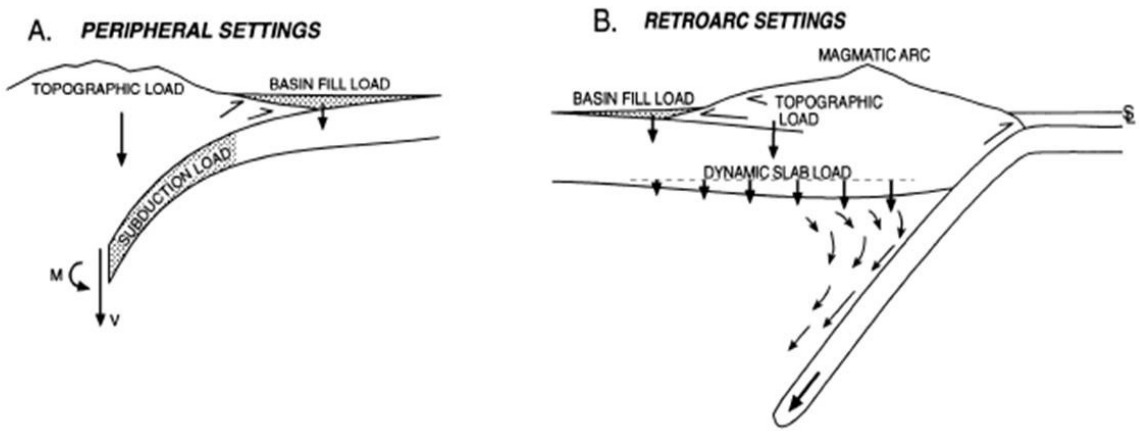

Figure 1.6: a) Peripheral foreland basin setting. b) Retroarc foreland basin setting. Figure from DeCelles and Giles (1996).

Foreland basins are asymmetrical, deepest parallel to the margin of the orogen, thinning out away from the mountain chain (Allen and Allen 2005). The longitudinal extent corresponds approximately to the length of the fold-thrust belt (DeCelles and Giles 1996). A foreland basin can be subdivided into four accommodation zones as displayed in Figure 1.7. The wedge-top, foredeep, forebulge and back-bulge, although in some instances the forebulge and back-bulge are not present or difficult to delineate (DeCelles and Giles 1996).

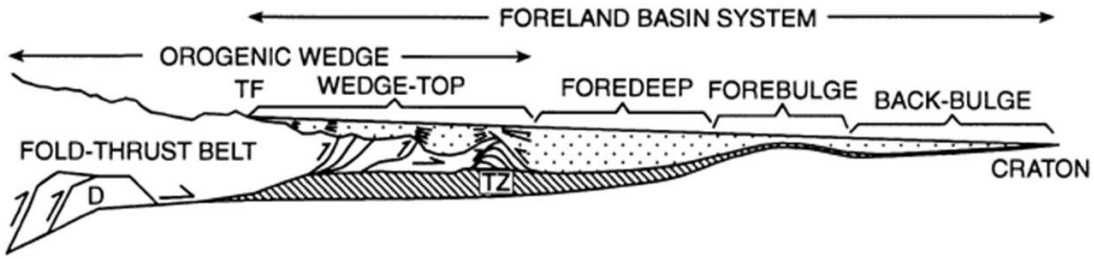

Figure 1.7: Foreland basin system displaying four depozones. Figure from DeCelles and Giles (1996)

Foreland basins receive vast amounts of synorogenic sediments from the orogenic belt, however, input from the continental interior is common, especially in the early stages of the basin evolution (Allen and Allen 2005). The majority of the sediments are deposited in the foredeep (Figure 1.7) closest to the mountain chain (DeCelles and Giles 1996).

As the fold- thrust belt propagates towards the foreland, the foredeep sediments get cannibalized by the orogenic wedge (Allen and Allen 2005). Extensive sedimentary basins also form in the interior of the orogen due to extensional or strike-slip tectonics on a local scale (Allen and Allen 2005). The sedimentary record is very important in terms of comprehending the evolutionary processes, timing and paleogeography in foreland basins (Kearey et al. 2009).

Sedimentary basins formed on top of active thrust sheets are proposed to be called piggy-back basins by Ori & Friend (1984). These basins, also named wedge-top basins (DeCelles and Giles 1996, Allen and Allen 2005) develop when a high-angled thrust ramp forms in front of the old one in a thrust sheet. Further translation of the thrust sheet results in transport (piggybacking) of the old ramp and the newly formed basin on top (Friend and Ori 1984). Piggy-back basins are often implicated in the deformational processes at the front of the thrust, and can be eroded due to exhumation of the orogenic wedge (Allen and Allen 2005). The Ringerike Group comprises Late Silurian sandstones, that were deposited in piggy-back basins (Davies et al. 2005a).

2 Regional setting

2.1 The Caledonides

From the end of Pre-Cambrian throughout the Cambrian period, the Baltic and Laurentian plates drifted apart, forming the Iapetus Ocean. During the transition from the Cambrian to the Ordovician period this process reversed, and the ocean began to close (Gee 1975). Approximately 500 million years ago, during the Cambrian period (542-488 Ma), Norway, as it is today, was part of the tectonic plate Baltica (Russia and northern Europe). At that time the plate was situated near the South Pole. The core of the Baltic plate is made up by Archean (4-2.5 billion years ago) crustal rocks and the topography was relatively flat at the time due to erosion. This is called the sub-Cambrian peneplain (Holtedahl 1953). Baltica became separated from Gondwana to the south by the Tornquist Sea and from the Laurentian (North American continent) to the west by the Iapetus Ocean. Figure 2.1 displays the plate tectonic configuration from Cambrian (500 Ma) to Late Silurian (420 Ma). The red circles on the Baltic plate represent what is believed to have been the position of Norway. It was the closing of the Iapetus Ocean and the following collision between Baltica and Laurentia (Figure 2.2) that lead to the development of the Caledonian mountain chain (Gee 1975, Hossack and Cooper 1986, *The Millennium Atlas: Petroleum Geology of the Central and Northern North Sea* 2003, Fossen et al. 2007a).

In western Scandinavia the exposed remnants of the Caledonian mountain chain can be studied over an area averaging 200 km in width, with a maximum of up to 500 km in some areas and 1800 km in length (Roberts and Gee 1985, Hossack and Cooper 1986).

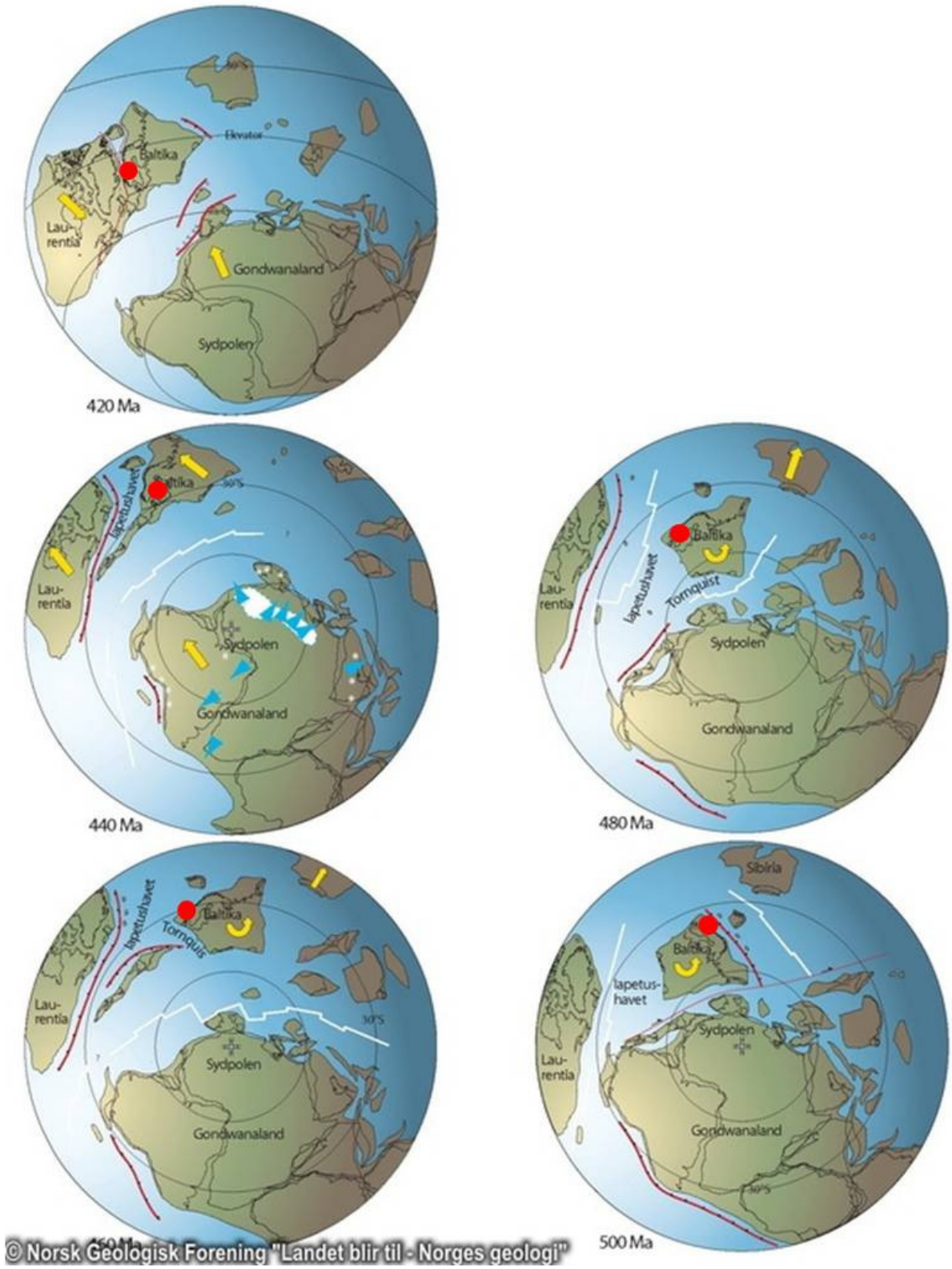

Figure 2.1: Reconstruction of the tectonic plate movement from 500 Ma (lower right) to 420 Ma (upper left). The position of Norway on the Baltic shield is marked with a red circle. Figure modified after Fossen et al. (2007a).

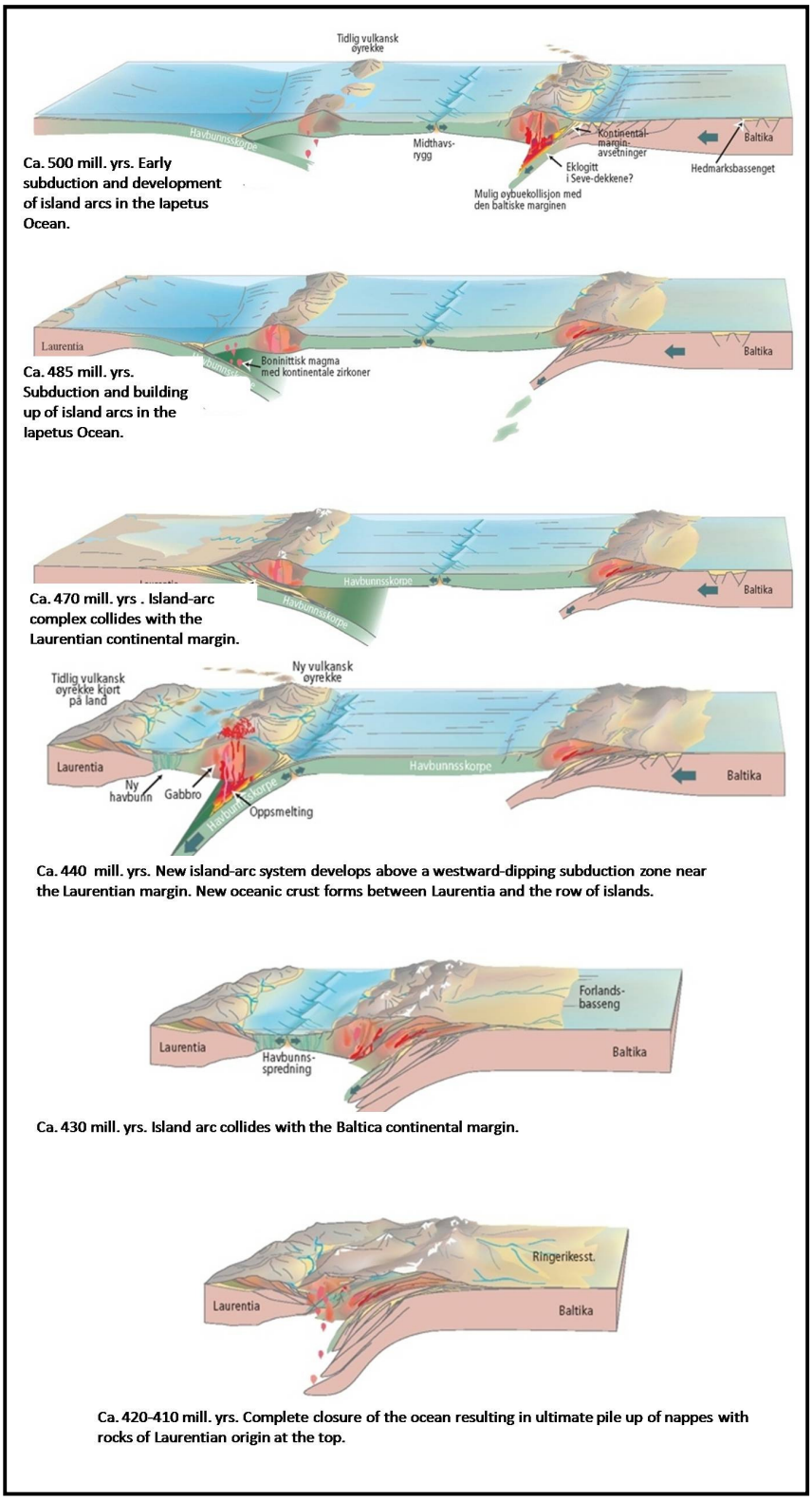

Figure 2.2: A thought evolution of the Caledonian Orogeny from ca. 500 Ma when the Iapetus Ocean began to close to 420-410 Ma when the Laurentian and Baltic continents collided. (The text on the figure is added by the writer, but taken directly from the figure in the English version) Modified after Fossen et al. (2007a).

2.2 Regional tectonostratigraphy

The tectonostratigraphy of the Caledonides can be divided into four major groups: Lower, Middle, Upper, and Uppermost Allochthons (Roberts and Gee 1985). Figure 2.3 illustrates the tectonostratigraphy in Norway today. The basement consists of autochthonous rocks from the Baltic craton with its overlaying sediments. The effect of the collision is much more severe above the basement. This is called thin-skinned deformation (Fossen et al. 2007a). The *Lower Allochthon* level consist of thrust sheets from the Baltic basement with the overlying Early Paleozoic sediments. This level was detached and transported over a basal thrust that can be traced along the front of the Scandinavian Caledonian Orogeny (Roberts and Gee 1985). The overlying group is probably made up by thrust sheets that originate from the deeper and more intensely deformed part of the Baltic crust, most likely from the margin of the continent. These units have been transported further than underlying nappe, and form the *Middle Allochthon* level (Fossen et al. 2007a). Thrust sheets derived from island arcs and the Iapetus Ocean are normally referred to as the *Upper Allochthon* level (Roberts and Gee 1985, Fossen et al. 2007a). Above lies the *Uppermost Allochthon*, which probably traces back to the Laurentian plate (Roberts 2003, Fossen et al. 2007a). The basement shows various degree of deformation due to the collision, and as one travels westwards the basement gets increasingly more deformed (Roberts and Gee 1985).

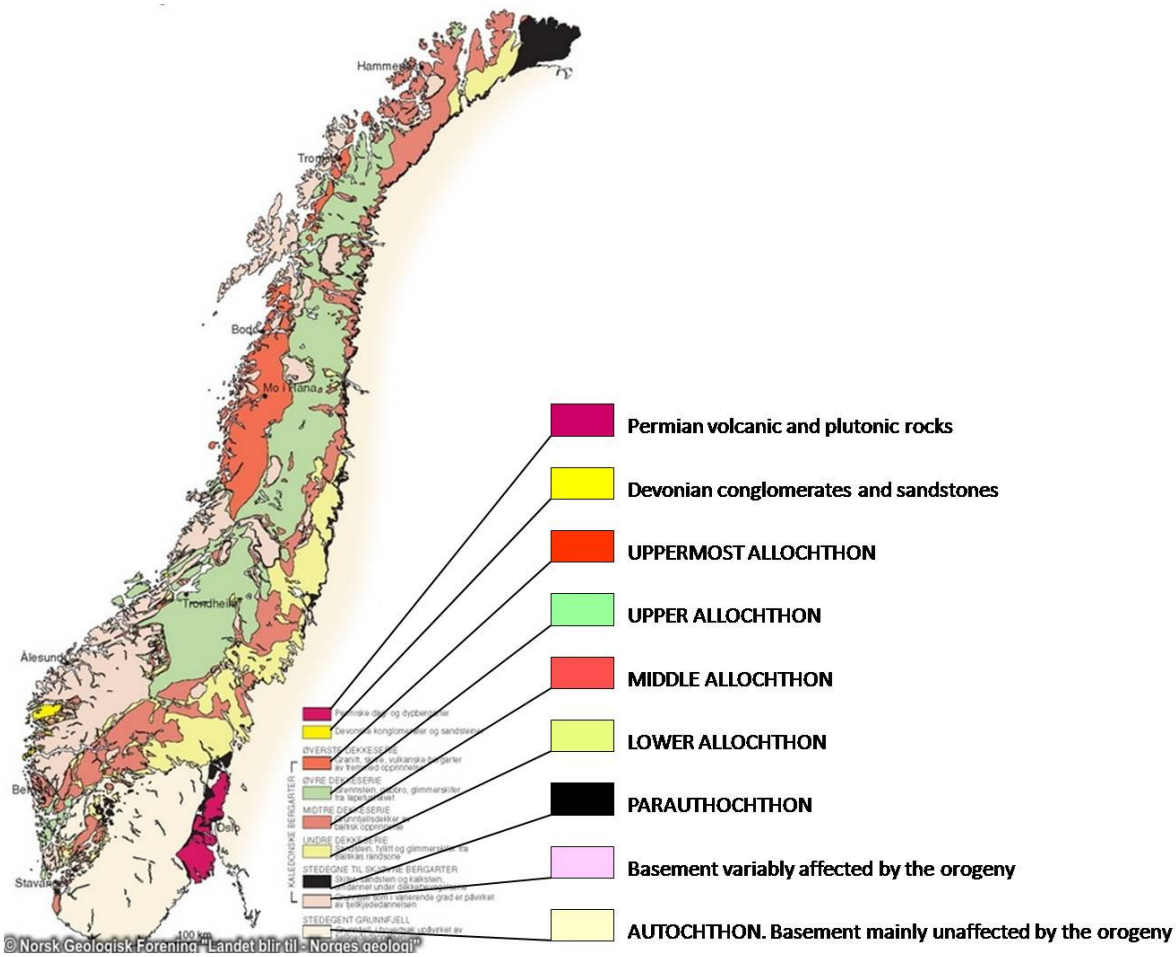

Figure 2.3: Tectonostratigraphy of the Norwegian Caledonides. Figure modified after Fossen et al. (2007a).

2.3 Direction and amount of tectonic transport

In general, it can be stated that the translation of nappes have been towards the E and SE (present coordinates) onto the Baltic plate (Gee 1975, Roberts and Gee 1985, Hossack and Cooper 1986, Fossen et al. 2007a, Gabrielsen and Larsen in press). Although in western areas the direction of transport has been towards the NE, parallel to the mountain chain (Fossen et al. 2007a). In the Oslo Region there is a shift towards a dominant SSE-direction of transport (Morley 1986a, Gabrielsen and Larsen in press), however, there are areas which display transport direction towards S (Størmer 1953, Harper and Owen 1983). Fold axes trending NE-SW in the Oslo-Asker district have also been recognized (Larsen and Olaussen 2005). According to Hossack and Cooper (1986) the thrust vectors display clockwise rotation with time caused by the oblique collision between Laurentia and Baltica.

Hossack and Cooper (1986) conclude with a minimum shortening across the Scandinavian belt of 400 km based on a balanced section stretching from Møre in western Norway, to Langesund in the southeast. The Upper- and Uppermost Allochthons have at least been transported 400 to 500 km (Gee 1975) from northwest to southeast, whilst the displacement of the parautochthon units is in the order of several tens of kilometers (Bockelie and Nystuen 1985).

2.4 Timing

The evolution of the Caledonian Orogen is seen by some authors as one continuous development (Hossack and Cooper 1986), while by others as a result of several collisions (Roberts and Sturt 1980, Roberts and Gee 1985). The development of the Caledonides have been described by Roberts (2003) through four extensive compressive/transpressive events, namely the *Finnmarkian, Trondheim, Taconian and Scandian*. Sturt et al. (1978) describes the *Finnmarkian* as a Late Cambrian to earliest Ordovician event, involving a collision between the Baltic margin and a magmatic arc, and emplacement of the Kalak nappe complex onto the Baltic plate. A recent paper by Kirkland et al. (2008) on the subject advises against the concept of a *Finnmarkian* event. According to Kirkland et al. (2008), analysis of new data contradicts the previously proposed course of events, hence invalidating the concept, but recognizes an tectonothermal accretion event in the Middle-Late Cambrian. The *Trondheim* (Early Ordovician) event is associated with subduction and collision between the Baltic plate and adjacent island arcs and microcontinents (Roberts 2003). On the Laurentian side of the Iapetus Ocean, island arc accretion took place during the mid Late Ordovician period. This is called the *Taconian* event. During the last *Scandian* event (Mid Silurian – Early Devonian), the Laurentian plate was thrust onto the Baltic plate, and the main collision between the two plates took place (Gee 1975, Hossack and Cooper 1986, Roberts 2003).

During mid Late Silurian times the final closure of the Iapetus Ocean took place (Hossack and Cooper 1986). Over a relatively short time span, perhaps as short as ten million years, the Baltic margin was brought down to depths greater than 120 km and then exhumed (Roberts 2003, Osmundsen et al. 2006). Radiometric dating of the latest developed granitic island arc complexes gives a maximum age for the final closing of the Iapetus Ocean. The youngest granites give an approximate age of 430 Ma, which indicates that the main collision was in progress at about 425 Ma (Fossen et al. 2007a).

The latest contractional deformation can be set to Early Devonian times defined on the basis of the deformed Sundvollen and Stubdal Formations of the Ringerike Group (Upper Silurian) (Gee 1975, Roberts and Gee 1985, Gabrielsen and Larsen in press), and perhaps later (Gee 1975, Andersen 1993). However, Hossack and Cooper (1986) propose that the Caledonian thrust deformation ended in Late Silurian in the Oslo Region, and that faults and folding are results of post-orogenic extensional event. The collision between the two continents was gradual oblique (Hossack and Cooper 1986, Roberts 2003) and involved major thrusting, sinistral transpressive shear together with extensional deformation (Roberts 2003).

As a consequence of the collision between Laurentia and Baltica, several extensive thrust sheets developed (Gee 1975, Roberts and Gee 1985). The nappes were mainly thrust from west to east on to the Baltic plate, and some were transported several hundred kilometers (Gee 1975, Nystuen 1981, Roberts and Gee 1985). The thrust sheets, generally displaying a westwards thinning geometry (Gee 1975), developed by in-sequence thrusting, forming a wedged-shaped pile of nappes. The wedge-shaped nappe pile tapers towards the foreland (Fossen et al. 2007a). The geometry of the thrust wedge is characteristic for a continent-continent collision (Gee 1975, Fossen and Gabrielsen 2005).

Hydrostatic pressure at the base of the nappe succession increased as the wedge got thicker due to the pile up of thrust sheets, resulting in decreasing effective normal stress, hence lowering the friction along the base (Gee 1975). At some point the transport of overriding thrust sheets stopped and translation nappe pile continued along the newly formed décollement surface, situated near the basement cover (Gee 1975). By the end of Silurian times, western Norway underwent an uplift in a rather fast paste and the tectonic transport had for the most part halted in this part of the land (Roberts and Gee 1985). However, further to the east, the frontal part of the nappe pile was prograding S-SE along the basal thrust situated over a more or less passive basement (Roberts and Gee 1985). Translation of the nappes during this last (Scandian) phase are believed to have been induced by gravitational spreading of the orogen and/or foreland directed compressive forces (Bockelie and Nystuen

1985). A possible oblique collision between Eurasian plate and Australia can be considered as a modern analogue to the development of the Caledonian Orogeny (Roberts 2003).

2.5 Caledonian extension

In Devonian times the collision forces decreased, and the continents eventually started to drift apart (Fossen et al. 2007b). As a consequence, the Caledonian mountain chain began to collapse. The initial backsliding reactivated the Caledonian basal thrust to form an extensional detachment zone, resulting in nappe translation towards the central part of orogen (Fossen and Rykkelid 1992). Further, extensional, west-dipping shear zones led to stretching of the basement (Fossen and Rykkelid 1992). Stretching and thinning of the nappes caused the deeper rocks in certain areas, situated in the root zone, to be uplifted. An example is the Nordfjord-Sogn shear zone (Fossen et al. 2007b). Figure 2.4 illustrates the evolution from the contractional regime in Silurian, via the extensional events and finally the present situation.

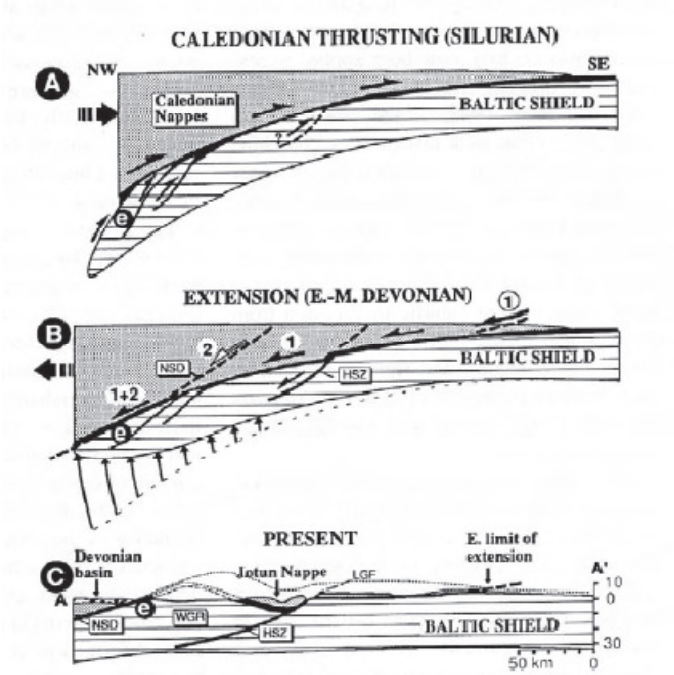

Figure 2.4: Schematic profile from NW to SE across southern Norway. From the top: A) Contraction, B) Extension and C) present time. Figure from Fossen and Rykkelid (1992).

The backsliding of the thrust wedge has been dated to have occurred approximately 400 million years ago, which also corresponds to the time when the mountains were at their

highest (Fossen et al. 2007b). However, there are signs of local extensional stretching in Nord-Trøndelag dated to about 415-422 Ma. Effects of the extension are not only observed in the central part of the orogen, but followed over 200 km eastwards, towards the foreland (Fossen and Rykkelid 1992). In southern Norway the amount of backsliding has been estimated to be 20-30 km towards the NW (Fossen et al. 2007b). According to Andersen (1993), the extensional deformation (backsliding, faulting) in the hinterland and the contractional deformation in the foreland were synchronous.

3 The Oslo Region

3.1 Introduction

The 'Oslo Region' is a geographical term tied to the area in southeastern Norway with Paleozoic rocks still preserved, separated from the surrounding high-grade metamorphic Precambrian rocks (Sundvoll and Larsen 1994). The geographical extent of the Oslo Region is limited to Ringsaker (northern Mjøsa) district to the north-northeast and Skien-Langesund district to the south-southwest, as displayed in Figure 3.1. The Oslo Region covers an area which is approximately 220 km long and 45 km wide (Størmer 1953). Within the Oslo Region the Cambrian, Ordovician and Silurian sedimentary sequences are approximately 2000 m thick (Bockelie and Nystuen 1985). The sediments were deposited in an intercratonic NNW-SSE directed depression (Størmer 1967). Above, Carboniferous and Permian sedimentary and volcanic rocks rest unconformably on them. The Cambro-Silurian rocks have also been intruded by Permian magmatic bodies (Larsen and Olaussen 2005). Major N-S to NNE-SSW striking faults borders the Oslo Region to the east and west (Larsen and Olaussen 2005).

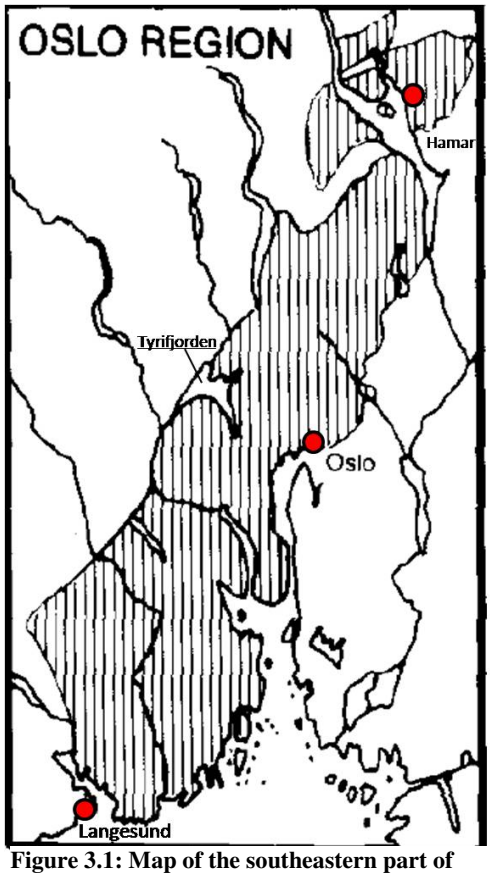

Figure 3.1: Map of the southeastern part of Norway, displaying the Oslo Region within the shaded area. Figure modified after (Sundvoll and Larsen 1994).

3.2 Sedimentary response to the Caledonian Orogeny

During Precambrian to Cambrian times, the ocean transgressed from the north and reached the Oslo Region around Mid Cambrian, forming an epicontinental sea with very low sedimentation rates. From the Mid to Late Cambrian the black Alum shale were deposited in stagnant conditions over almost the entire Baltic plate (Bockelie and Nystuen 1985, Larsen and Olaussen 2005). High sea levels characterize the Ordovician period, with the deposition of alternating mudstones and limestones (Larsen and Olaussen 2005). During the Early to Late Ordovician, the sedimentary distribution within the depression where, to a certain degree, regimented by basement tectonics (Bockelie and Nystuen 1985). The occurrence of bentonite beds within the Middle Ordovician to Lower Silurian strata represents periods of volcanic activity in the Caledonian orogenic belt (Bockelie and Nystuen 1985)

Lower Ordovician shale beds in the Oslo Region demonstrate an increase of chlorite, iron, nickel, magnesium and chromite, which is suggested by Bjørlykke (1974b) to be erosional remnants from an evolving island arc system, situated in the Trondheim Region. Influx of coarse clastic sediments into the northern Oslo Region in response to the Caledonian orogen took place during Mid-Late Ordovician times (Størmer 1967, Bjørlykke 1974a, Bockelie and Nystuen 1985). The late Mid Ordovician Elnes Formation is suggested to be the first sediments connected to the Caledonides (Gabrielsen and Larsen (in press) and references herein). The supply of minerals continued into Late Ordovician times, reflecting orogenic uplift and erosion as well as a gradually decreasing distance to the source area (Bjørlykke 1974b). In Late Ordovician coarse clastic quartz and feldspar grains were transported onto the Baltic shield possibly due to the erosion of metamorphic or magmatic rocks, or sparagmites from the Late Precambrian (Bjørlykke 1974a). Variations in the sedimentary record from the Late Ordovician suggest an extensive regression and then relatively fast sea level fluctuations and unstable basin conditions. Further, the deposition of the Lower Silurian Bærum and Hole Groups display alternating and relatively widespread carbonate ramp facies and siliciclastic wedges (Larsen and Olaussen 2005).

The orogenic uplift in Wenlockian times caused the advancement of clastic deltaic sediments (Bruflat Formation, Bærum Group) southwards towards the Oslo Region (Bjørlykke 1974a). By Ludlovian times the sediments had reached the Oslo-Asker district (Bjørlykke 1978). The sediments were deposited above Lower Silurian (Llandovery to Mid Wenlock) marine sediments, composed mainly of limestones and shales.

Towards the end of Silurian the depositional environment evolved from deltaic to tidal and brackish-water (Bockelie and Nystuen 1985), resulting in the deposition of the continental Ringerike Group sandstones in the Oslo Region (Turner 1974, Bjørlykke 1974a, Bockelie and Nystuen 1985). According to Davies et al. (2005b) the deposition took place from Late Wenlock-Early Ludlow into Pridoli. The Ringerike Group comprises four sandstone units; the Sundvollen, Stubdal, Store Arøya and Holmestrand Formations (Davies et al. 2005b). The Sundvollen (c. 500 m) and Stubdal Formations (c. 750 m), display a total thickness of about 1250 m in Ringerike (Figure 3.2), which is the type area (Turner 1974). Sundvollen Formation was most likely deposited in a coastal alluvial plain formed by meandering streams with some tidal influence, whilst the Stubdal Formation comprises mainly of fine grained braided river deposits, probably related to a distal alluvial complex (Turner 1974).

The basal part of the Ringerike Group displays a decrease in age from north to south. This reflects the southwards propagation of siliciclastic erosional sediments originated from the growing Caledonian mountains to the north (Davies et al. 2005b).

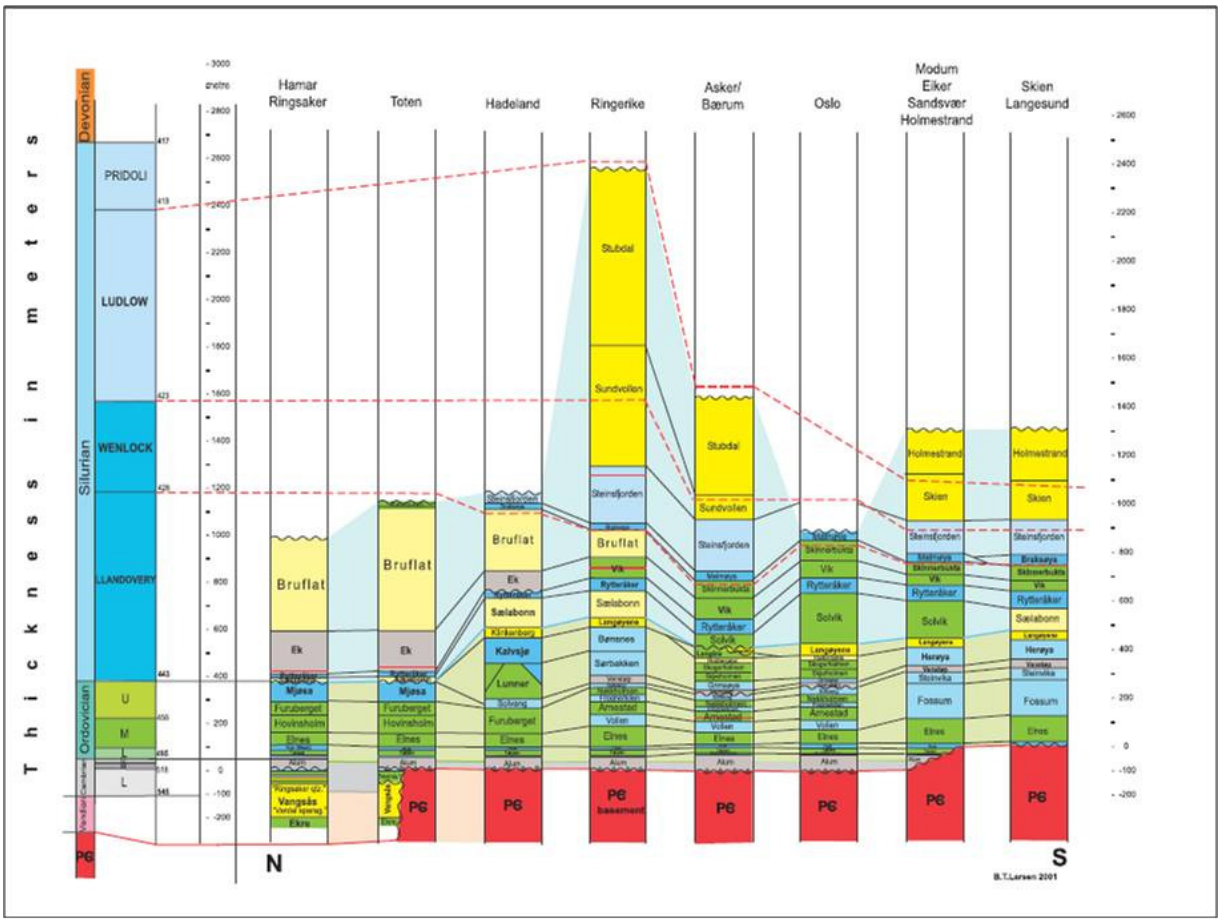

Figure 3.2: Lower Paleozoic stratigraphy including thickness and time scale from "principal major areas in the Oslo Region". Figure from Larsen and Olaussen (2005).

3.3 Tectonostratigraphy in the Oslo Region

Initially, the Caledonian nappe front was considered situated in the northern part of Lake Mjøsa, separating the Osen-Røa (Sparagmites) nappe complex of Nystuen (1981) to the north from the folded Cambro-Silurian succession to the south (Gabrielsen and Larsen in press). Oftedahl (1943) proposed a mutual basal thrust for the two, that could be traced from beneath the Osen-Røa nappe, southwards below the entire Cambro-Silurian succession of the Oslo Region. Subsequent papers (Nystuen 1981, Hossack and Cooper 1986, Morley 1986a) honors Oftedahls work.

To the north, the main detachment zone lies beneath the Late Precambrian (Hedmark Group) Sparagmite region (Nystuen 1981). In the northern part, around Lake Mjøsa the Osen-Røa thrust ramps up-section towards the south and continues as a 150 km long flat within the Cambrian Alum shale, beneath the imbricate and folded Cambro-Silurian strata of the Oslo Region (Morley 1986a).

The thrust is believed to terminate north of Langesund-Skien, as displayed in Figure 3.3 (Hossack and Cooper 1986, Morley 1986a). There is, however, no clear consensus regarding the nature of the termination. According to Oftedahl (1943) and Morley (1986a, 1986b) the Osen-Røa detachment terminates within the Alum shale as a buried horizontal thrust, whilst Hossack and Cooper (1986) believe the thrust climbs out of the sequence between the deformed rocks to the north and the undeformed rocks to the south. Nystuen (1981) calculated the displacement of the Osen-Røa nappe complex to be 200 to 400 km towards south or southeast.

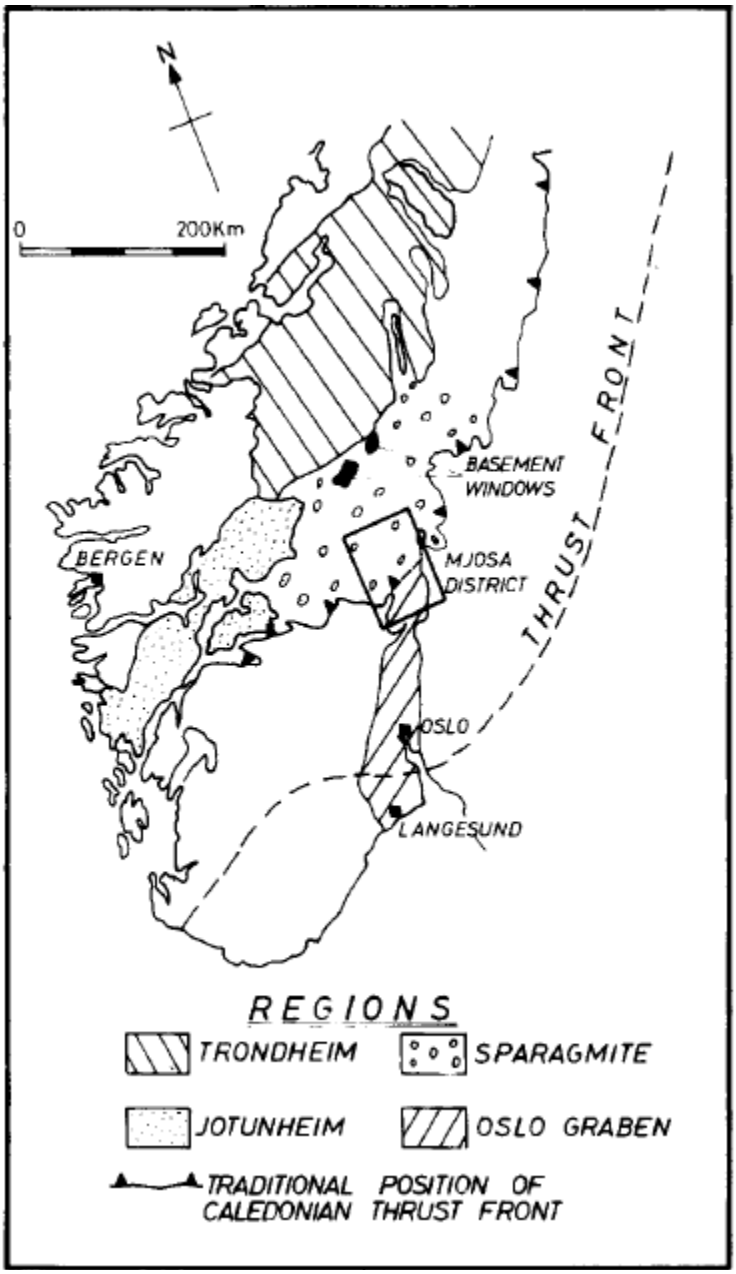

Figure 3.3: Map of the southern part of Norway displaying the locations of the tectonic regions and the proposed Caledonian trust front. Figure from (Morley 1986a).

The Cambro-Silurian strata in the Oslo Region and at the nappe front is considered to be autochthonous-parautochthonous by Bockelie & Nystuen (1985). According to Hossack & Cooper (1986) undeformed rocks appear in the southern Oslo Region, at Langesund. Morley (1986a) states that the term parautochthonous used to describe the Cambro-Silurian rocks in the Oslo Region is not valid. The reason for this is that the Osen-Røa nappe and the Oslo Region are underlain by the same thrust, as described by Nystuen (1981). Dividing the Sparagmite Region into an allochthon unit and the Oslo Region into an parautochthon unit suggests, according to Morley (1986a), that they are two separate tectonic units. The Osen-Røa nappe belongs to the Lower Allochthon. To the west, north and northwest the tectonic units of the Middle and Upper Allochthon are situated (Bockelie and Nystuen 1985). Oftedahl (1943) suggested a 50 % shortening of the Cambro-Silurian succession in the Oslo Region.

The Lower Paleozoic rocks in the Oslo Region reflect a low temperature and low pressure setting during the Caledonian deformation. Data from the Paleozoic rocks sampled around Tyrifjorden demonstrate that the succession has been subjected to temperatures in the range of 110°-200°C, indicating a burial depth of no more than 4-7 km (Fossen et al. 2007a). Studies on conodont alteration in the Oslo Region point towards an even shallower burial depth of around 2 km (Morley (1986b) and references herein).

3.4 Structural style in the Oslo Region

The Oslo Region is positioned in the distal part of the Caledonian fold-thrust belt, which is evidently reflected in the characteristic structural style (Gabrielsen and Larsen in press). Within the Oslo Region the Cambro-Silurian succession, as described by Bockelie and Nystuen (1985), exhibit folding and thrusting related to a décollement zone. Above this décollement zone or basal thrust, there are multiple detachment levels created by splay faults. In context to these levels there are " imbricate stacks, back-thrusts, duplexes, harmonic and disharmonic folds, lateral, oblique and transverse ramps, and deformed foreland basin units" (Gabrielsen and Larsen (in press) p. 5). In the Oslo Region the basement was not involved in the Caledonian deformation (Bockelie and Nystuen 1985).

In general, the deformational intensity decreases with increasing transport length and upwards in the Cambro-Silurian succession (Bockelie and Nystuen 1985, Morley 1987a, Gabrielsen and Larsen in press). Hence, contrasting deformational style within the succession can be demonstrated in the Oslo Region (Morley 1986b, Gabrielsen and Larsen in press). Several factors such as type of "lithology, thickness of the deforming unit, stress situation, basement relief, and burial depth" influence deformational style of the units involved (Gabrielsen and Larsen (in press) p. 5). Additionally, will the positions of the units within a nappe also have an effect on the deformational processes (Morley 1986b).

From north to south across the Klekken thrust (Ringerike district) there is an evident decrease in amount of shortening and structural style as described by Harper and Owen (1983) (described in detail in chapter 4). Among several suggestions Morley (1987a) mentions that an increase in thickness of the mechanical strong Ordovician strata towards the south could influence the deformational style. Further, the mechanical competent continental sandstones of the Ringerike Group (Ludlow, Upper Silurian), reaching over 1 km in thickness in certain places, have had a major effect on the uppermost part of the Cambro-Silurian succession in the Oslo Region (Gabrielsen and Larsen in press).

According to Nystuen (1983), the frontal zone of the Osen-Røa nappe complex can generally be described as an imbricate structure, whilst the northern part comprises high- and low-angle contractional faults associated with a trailing edge including open large-scale folds. Additionally, sub-horizontal flats characterize the central part (Nystuen (1983) and references herein).

3.5 The Permian Oslo Rift

Weathering and erosion of the Caledonian mountain chain characterize the period from Early-Devonian times to Late-Carboniferous. In the Oslo Region there is a hiatus of almost 100 million years, stretching from Late Silurian to Late Carboniferous (Larsen et al. 2007). Sediments deposited after the hiatus comprise continental deposits and rather limited amounts of shallow marine carbonates of the Late-Carboniferous Asker Group (Sundvoll et al. 1992).

The Oslo Rift developed due to the magmatic and tectonic events from Late Carboniferous into Permian. The area affected by the rifting covers an area of minimum 510 x 120 km in southeastern Norway, including the Skagerak Sea and parts of southwestern Sweden (Sundvoll and Larsen 1994). The Oslo Rift dies out to the south against the Tornquist zone (Sundvoll and Larsen 1994). Oslo Graben (Figure 3.4) is a term used to describe the down-faulted crustal block that comprises rocks situated within the Oslo Region and the neighboring Precambrian Kongsberg block (Sundvoll and Larsen 1994). The major faults trend NNW-SSE to NNE-SSW and throws in the order of 3 km are suggested along the NNW trending Vestfold Graben (Neumann et al. (1992) and references herein).

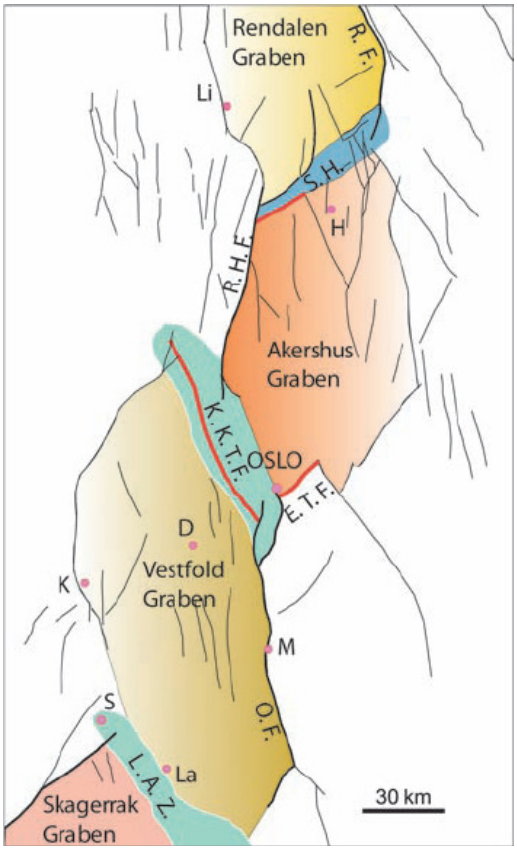

Figure 3.4: The graben segments in the Oslo Region. Figure from Larsen et al. (2008).

Since Permian to Early-Triassic times about 1-3 km of rocks have been removed by geological processes (Larsen et al. 2007). The subsidence caused by Permo-Carboniferous rifting ensured the preservation of the Cambro-Silurian succession from erosion in the Oslo Region (Fossen et al. 2007a).

4 Previous work in the Oslo Region

4.1 Introduction

The earliest geological work in the Oslo Region took place during the 19th century. As a consequence, the well preserved Lower Paleozoic rocks and fossils within the Oslo Region are acknowledged worldwide and studies within the region have provided a major contribution regarding the understanding of the geological evolution of the Caledonian Orogeny.

Several papers were published in German. The writer has chosen the paper "Caledonian structural development of the Oslo Region" written by Gabrielsen and Larsen (in press) as the main source concerning previous work performed in the Oslo Region. Since this gives an extensive summary of the previous studies in the Oslo Region regarding structural geology in context to the Caledonian Orogeny.

4.2 Previous work

In 1810 Leopold von Buch described the igneous rocks and the sediments in the Oslo Region after travelling in Norway from 1806 to 1808 (Larsen and Olaussen (2005) and references herein). Worth mentioning is Johan Kiær (1908), who founded the Silurian stratigraphy in the Oslo Region, which later was revised by Worsley et al. (1983). Figure 4.1 displays a geological map of the Silurian strata at Ringerike, including strike and dip measurements of bedding planes and faults.

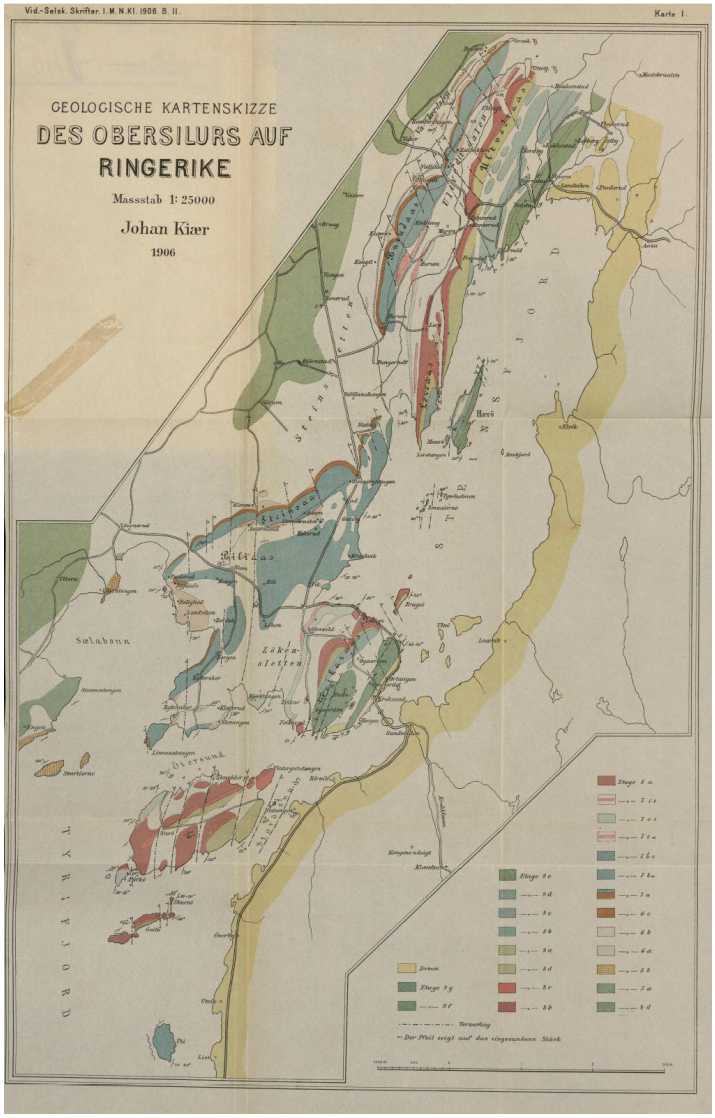

Figure 4.1: Geological map sheet displaying the Silurian strata at Ringerike. Strike and dip measurements of bedding planes and faults are also marked on the map sheet. Figure from Kiær (1908).

During the second half of the 19th century Robert I. Murchison (Gabrielsen and Larsen (in press) and references herein) and Theodor Kjerulf (1862, 1879) studied the geology in the Oslo Region, describing both faulting and folding in the area. Murchison did recognize the Silurian system in the Oslo area as early as 1844 (Larsen and Olaussen 2005). Kjerulf described the Cambro-Silurian sediments and the Permian igneous rocks and consequently published "Das Christiana Silurbecken" in 1855 (Gabrielsen and Larsen (in press) and references herein). Later Kjerulf (1862) published his work on the Ordovician strata in the Ringerike area, and proposed that intrusions initiated the shortening and the associated folding. Later he proposed that the dislocations developed prior to the intrusions (Kjerulf 1879). Figure 4.2 displays a geological profile sketched by Kjerulf from Ringerike.

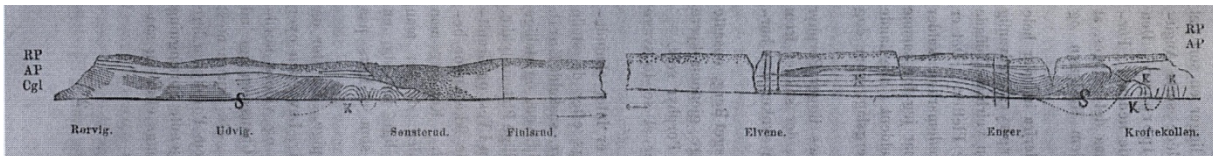

Figure 4.2: Profile from the Ringerike area, sketched by Theodor Kjerulf. Figure from Kjerulf (1862).

As stated by Gabrielsen and Larsen (in press), the important connection between the geology in the Oslo Region and the Caledonian Orogeny was first made by Waldemar C. Brøgger in the late 19th century. Brøgger concluded that the main tectonic direction was from NNW towards SSE based on the NNW dip of faults and axial surfaces, and on the ENE-WSW-trend of the Cambro-Silurian rocks. He also commented on the relationship between thrusts and folds, and produced several structural profiles from the Oslo Region. It is worth mentioning that Brøgger observed faults with a SSE-dip, which he proposed developed due to tectonic movement towards NNW, opposite to the main tectonic transport direction.

In the late 19th and early 20th century A.E. Törnebohm and K.O. Bjørlykke investigated the evolution of the Caledonian Orogeny and the effect this had on the Oslo Region by studying the central parts of the mountain chain (Gabrielsen and Larsen (in press) and references herein). O.E. Schiøtz (1902) studied the eastern part of the Sparagmite Region (Upper Proterozoic Hedmark Group in the northern Oslo Region). According to Schiøtz the Hedmark Group was deposited in a local fault-bounded 'Sparagmite basin' and came to the

conclusion that the uppermost part of the sequence had been thrust 30-40 km southwards (Schiøtz 1902).

Based on the map sheet *Hønefoss (1:100000)* developed by Brøgger and Schetelig (1872), Størmer (1934) studied the possibility of an Caledonian overthrust north of Steinsfjorden. Størmer (1934) observed Ordovician rocks emplaced on top of Late Silurian sandstone beds at Stubdal, Ringerike district. Ordovician trace fossils previously noted by Brøgger and Schetelig (1872) confirmed this (Størmer 1934). At the northern boundary of the Ringerike synclinal the Ordovician and Silurian strata revealed extensive folding and partly inverted beds. North of this line, Størmer (1934) discovered several isoclinal folds with dip towards north. Further he suggests that the Stubdal overthrust developed along the boundary between the isoclinal folds and the northern boundary of the Ringerike synclinal. According to Størmer (1934) measurements indicate displacement in the order of at least 5 km, and a N-S directed thrust. He further states that the folds within the Cambro-Silurian succession in the Oslo Region, north of the city of Drammen displays a trend towards the E or ENE (Størmer 1953).

Oftedahl (1943) concluded that the main tectonic transport in the Oslo Region was towards the SSE, particularly based on ENE-WSW trending fold axes. He also described the Cambrian Alum-shale in the Oslo Region to accommodate the main basal thrust, on which the Cambro-Silurian sediments have been thrust and folded. Further, Oftedahl (1943) suggested that the same basal thrust can traced beneath the Upper Proterozoic Sparagmite Region and estimated the total amount of shortening for the Cambro-Silurian succession and the Sparagmite Region to be in the order of 300 km.

Several papers were published during the late 20th century with the aim of understanding the effects the Caledonian Orogeny had on the Oslo Region. Nystuen (1981, 1983), Harper and Owen (1983), Bockelie & Nystuen (1985) , Hossack & Cooper (1986) and Morley (1986a, 1986b, 1987a, 1987b, 1994) were some of the most important contributers.

Harper and Owen (1983) studied the structural geology of the Ordovician rocks in the Ringerike district. The authors described the marked difference in structural style between

the areas north and south of the Klekken fault (Figure 4.3), which strikes NE-SW (Harper and Owen 1983). North of the fault, Lower and Middle Ordovician strata are extensively faulted and display steep dips towards the north. South of the Klekken fault, Middle and Upper Ordovician beds exhibit gentle folds (Harper and Owen 1983). Their interpretation is that a thrust system transported the older more deformed rocks from the north over the younger gentler deformed rocks to the south (Harper and Owen 1983). The authors describe the structure as an imbricate fan, where the floor thrust is assumed to be located within the Cambrian Alum shale. Harper and Owen (1983) mention also the possibility of the structure to be a hinterland dipping duplex, where the overthrust at Stubdal described by Størmer (1934) might be consistent with the roof thrust, however, this has not been documented. Finally, they propose that the folding of the strata occurred before the thrusting event (Harper and Owen 1983).

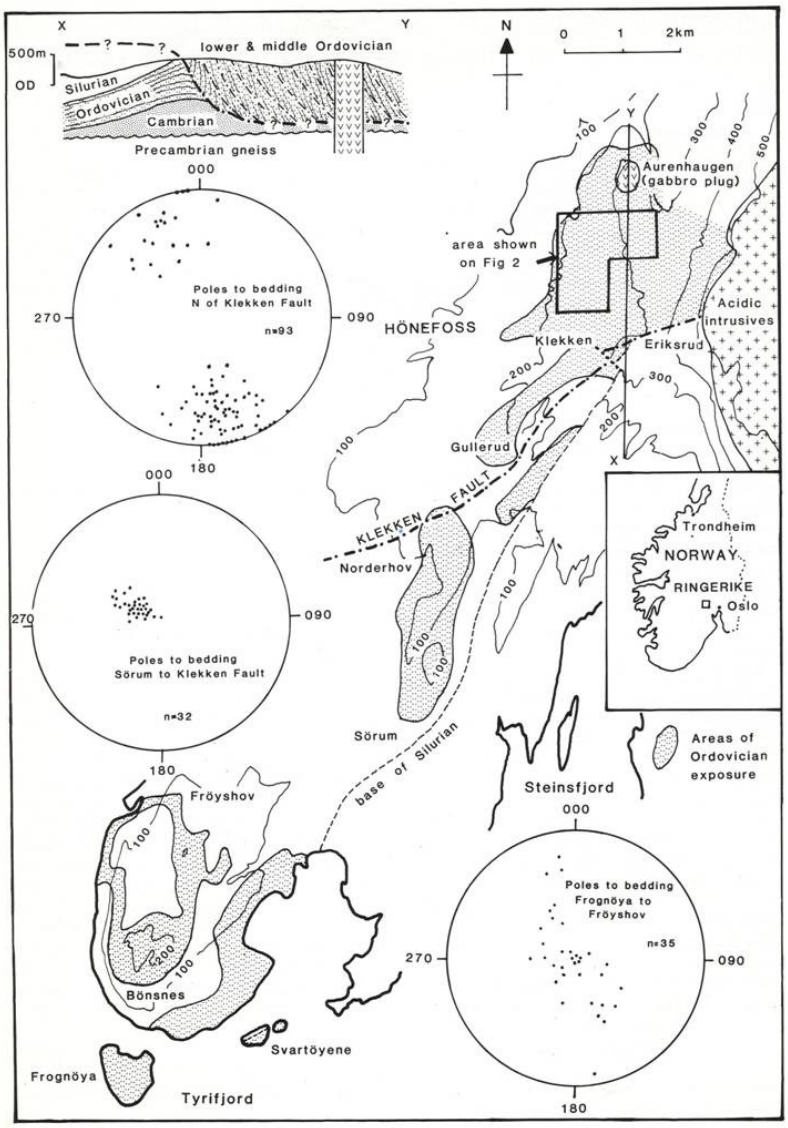

Figure 4.3: Map of the Ringerike district displaying the position of the Klekken fault. An N-S directed profile across the Klekken fault can be observed in the upper left part of the figure. Figure from Harper and Owen (1983).

When working on the structural geology in the north Hadeland district (Oslo region), Morley (1987b) described thrusts and minor folds with an ENE-WSW alignment, indicating a NNW-SSE directed shortening in the area. The NNW directed dip of most minor thrust faults in the region led Morley to the conclusion that the Osen-Røa nappe has been transported towards the SSE in the Oslo region (Morley 1987b). In addition, he noted the presence of back-thrusts. According to Morley (1987a) these are infrequent and have a small displacement in the area.

Sippel et al. (2009) published a paper regarding the paleostress field in the Oslo Region and came to the conclusion that a compressional stress field with the maximum compression directed NW-SE is due to the Caledonian Orogeny (Sippel et al. 2009). The previously mentioned paper "Caledonian structural development of the Oslo Region" by Gabrielsen and Larsen (in press) is one of the most recent studies on the topic.

Gabrielsen and Larsen state that the Late Paleozoic succession of the Oslo Region can be divided into four separate structural subareas, developed during the Caledonian Orogeny. The separation is based on "tectonic transport direction, transport length and structural style" (Gabrielsen and Larsen (in press) p .3). In addition, they define four levels that display different "structural styles and strain intensity", which are separated by major thrust faults (Gabrielsen and Larsen (in press) p .3), as illustrated in Figure 4.4.

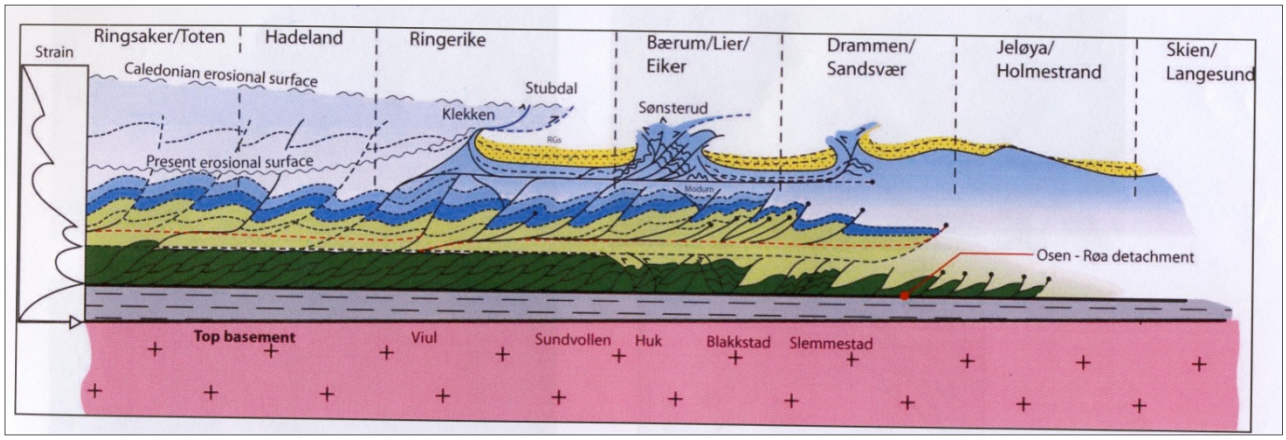

Figure 4.4: NNW-SSE cross-section of the Oslo Region illustrating the four structural levels. Figure from Gabrielsen and Larsen (in press).

5 Lithostratigraphy in Ringerike area

5.1 Introduction

The Ringerike area provides excellent localities for working with Caledonian structural geology in a foreland basin setting due to the exposure of the well preserved Cambro-Silurian succession (Zwaan and Larsen 2003). The focus has been on the area situated around the northern part of Tyrifjorden (Figure 5.1). In this chapter the general lithostratigraphy in the Ringerike district will be presented, subsequent a detailed description of the lithostratigraphy within the study area.

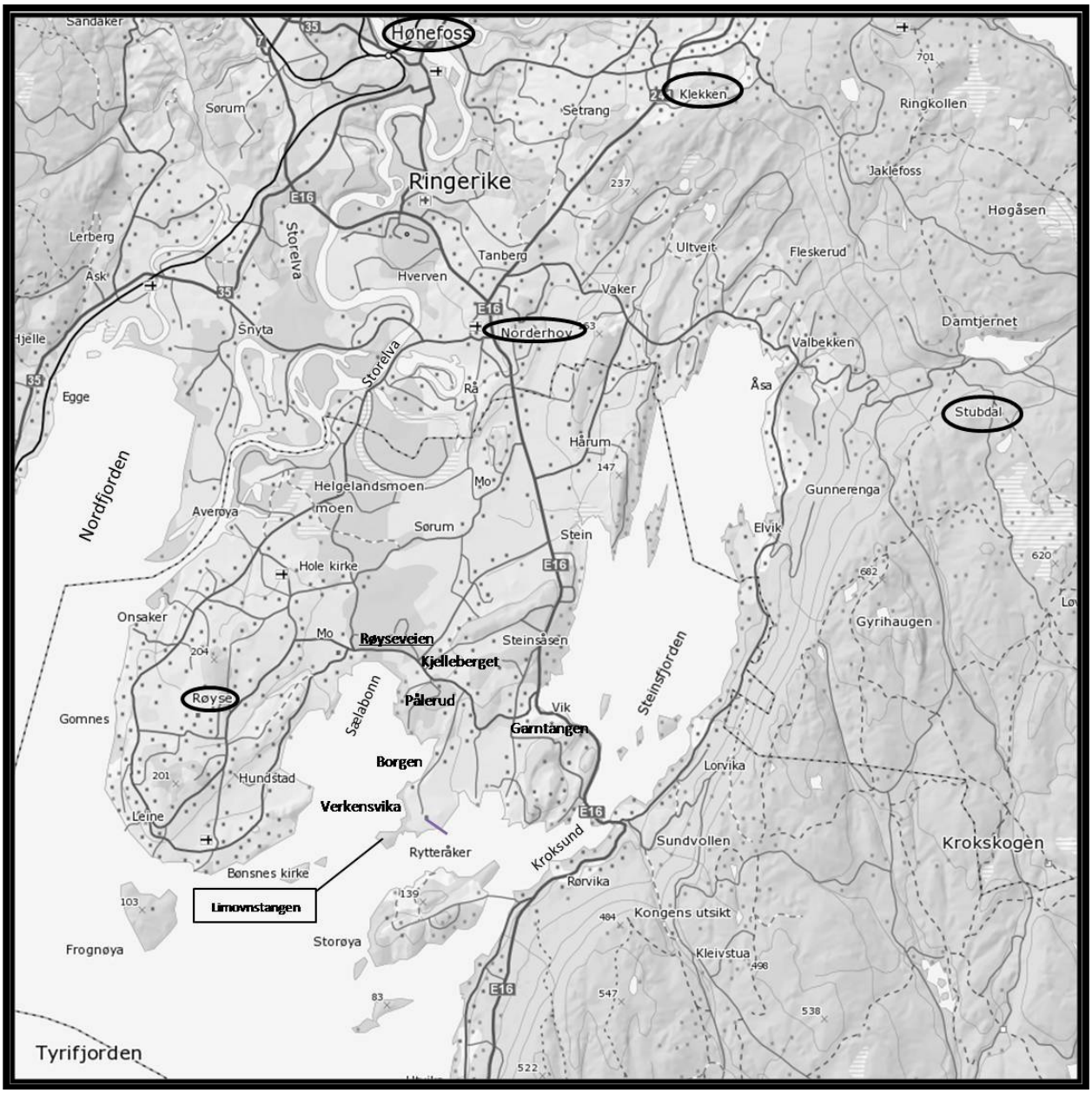

Figure 5.1: Map of the northern part of Tyrifjorden with surrounding areas. Map modified after Hole_municipality (2010).

5.2 General Lithostratigraphy in the Ringerike district

Figure 6.1 displays the eastern section of the geological map sheet *HØNEFOSS 1815 III (1:50 000)* (Zwaan and Larsen 2003), covering the Steinsfjorden area. On the basis of this map sheet a short description of the lithostratigraphy in the selected area will be given. Precambrian basement rocks are exposed along the western side of Tyrifjorden and west of the city of Hønefoss, marking the western margin of the Oslo Region. The area stretching from Nordfjorden, towards Randsfjorden and along Storelva and Randselva is covered with Quaternary deposits. East of Storelva and Randselva (north to west of Steinsfjorden), the Cambro-Silurian succession appears. The strata are up-right and tilted so that the youngest beds are found in the east.

5.3 Lithostratigraphy in the study area

The study area investigated encompasses the Early-Middle Silurian, Bærum Group (Worsley et al. 1983). Several of the formations of the Bærum Group have their type localities in or in the vicinity of the study area.

The Bærum Group comprises, in chronological order, of the Solvik, Sælabonn, Rytteråker, Vik, Ek, Bruflat, Reinsvoll and Skinnerbukta formations. The distribution of the different formations varies across the Oslo Region. The stratigraphic succession of the Bærum Group in the Ringerike district is displayed in Figure 5.2. The basal formation corresponds to the Sælabonn Formation, then Rytteråker-, Vik- and Bruflat formations above. Present in the study area are the Sælabonn, Rytteråker and Vik formations of Llandovery age.

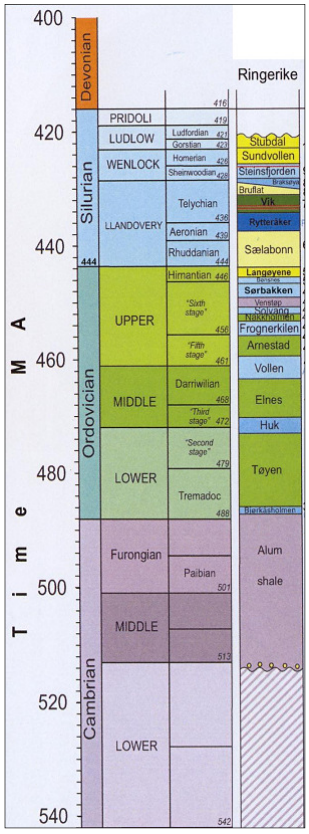

Figure 5.2: Stratigraphy in the Ringerike area. Modified after Larsen and Olaussen (2005).

The Sælabonn Formation

The Sælabonn Formation has its name from the rather small cove in the northern part of Tyrifjorden, located within the study area. The formation is approximately 110 m thick in this area and is of Early Silurian age (Worsley et al. 1983). It is not possible to observe a complete section (Figure 5.4b) of the Sælabonn Formation in one location (Worsley et al. 1983). The Sælabonn Formation comprises three members, the basal Store Svartøya, Djupvarp and the upper Steinsåsen members (Thompsen et al. 2006). The basal part of the formation can be observed on Store Svartøya (Figure 5.4a) (Worsley et al. 1983). It displays a 20 m thick section consisting of silty shales, limestones and siltstones lying above a karst surface (Worsley et al. 1983). The middle section coarsens upwards into a 50 m thick interval with medium- to thick bedded sandstone beds, interbedded with thin shale and silt layers (Worsley et al. 1983). Then it develops into upwards fining interbedded silt- and shale, with increasing limestone towards the top of the formation (Figure 5.3) (Worsley et al. 1983).

Figure 5.3: Upper part of the Sælabonn Formation exposed at the western side of Limovnstangen (Backpack as scale).

A transgression in a coastal environment took place during the deposition of the basal part of the Sælabonn Formation (Worsley et al. 1983). The middle section was deposited in a progradational coastal setting, before a new transgression took place during the upper part of the formation (Worsley et al. 1983).

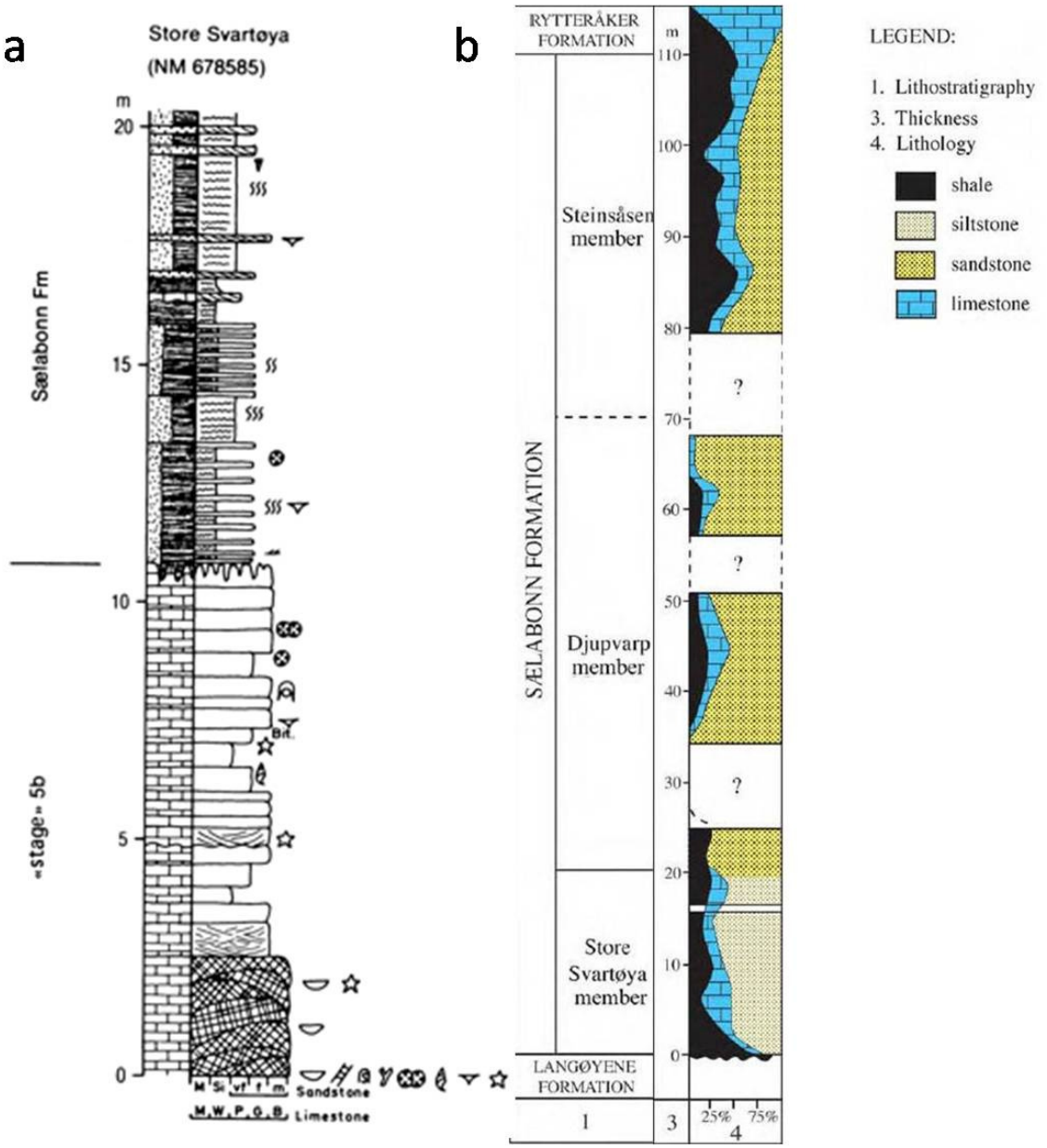

Figure 5.4: a) Sedimentological log displaying the lowermost part of the Sælabonn Formation at Store Svartøya Figure from Worsley et al. (1983). b) Stratigraphy of the entire Sælabonn Formation in the Ringerike district. From left to right: lithostratigraphy, thickness and lithology. Modified after Thompsen et al. (2006).

The Rytteråker Formation

The Rytteråker Formation (Figure 5.7) is named after the Rytteråker farm, located within the study area (Figure 5.1) (Worsley et al. 1983). In the Ringerike district the basal part of the Rytteråker Formation displays a diachronous nature and is of Early Silurian age (Llandovery) (Worsley et al. 1983). A transgressive event took place during the deposition of the upper part of the Sælabonn Formation, and as a consequence, the source areas of clastic material were submerged and the clastic supply ceased, producing the 50-52 m thick Rytteråker Formation (Worsley et al. 1983). The base of the formation is set to where limestones start to outnumber the siltstone layers at the transition between the (underlying) Sælabonn- and the Rytteråker Formation (Worsley et al. 1983). An increase in the pentamerids characterizes the lowermost 10 meters of the formation (Worsley et al. 1983). Figure 5.5a displays the pentamerids limestone at the NW-side of Limovnstangen. The next 25 meters show a transition towards thick biosparitic limestone beds, made up by crinoids and pentamerid debris (Worsley et al. 1983). Above this section it is possible to observe small bioherms (Worsley et al. 1983), as seen in (Figure 5.5b). Further, towards the top of the formation there is an increase in shale layers that are interbedded with calcareous nodules and limestone beds (Worsley et al. 1983).

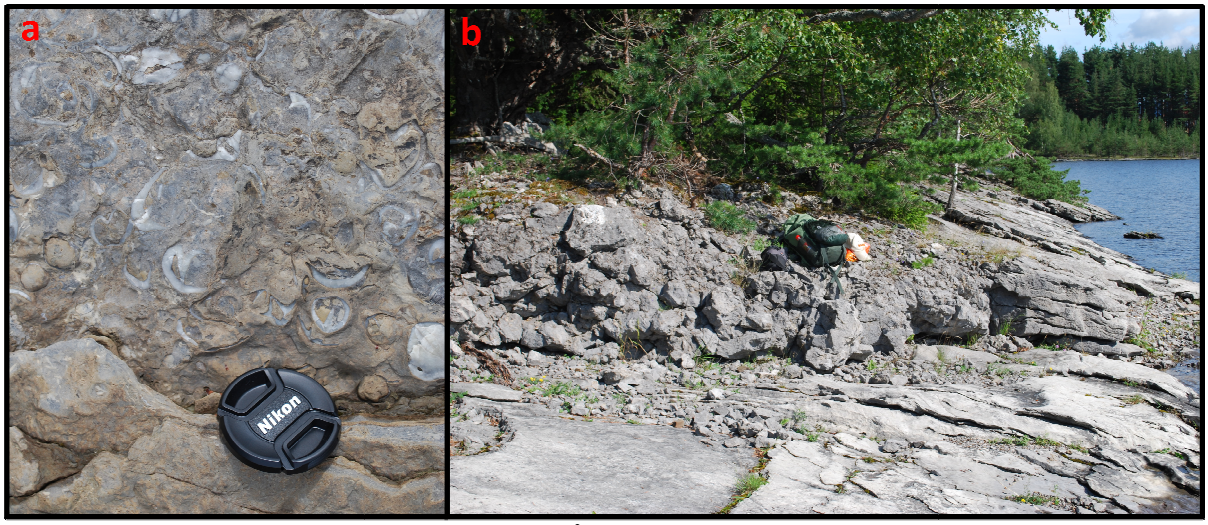

Figure 5.5: a) Pentamerids limestone of the lower Rytteråker Formation at the NW-side of Limovnstangen (Lens cap as scale). b) Bioherm in the upper middle part of the Rytteråker Formation situated on the eastern side of Limovnstangen (Backpack on top as scale).

According to Worsley et al. (1983) are the limestones of the Rytteråker Formation thought to have been deposited in rather shallow water. Further, a high energy environment characterizes the pentamerid biosparite deposits. A transgression is believed to have taken place during the development of the overlying bioherms in Ringerike (Worsley et al. 1983). The presence of benthic algae, together with corals, pentamerids and stromatoporoids points to a shallow water environment (Worsley et al. 1983).

The Vik Formation.

The Vik Formation has its name from the small community located northeast of the study area and is of Telychian age (Figure 5.2) (Worsley et al. 1983). This formation is about 80 m thick in the type area and is divided into to the Storøysundet, Garntangen and the Abborvika members (chronological order) (Worsley et al. 1983). The basal stratotype of the Vik Formation is located northwest of the Rytteråker farm (Worsley et al. 1983). The border between the Rytteråker- and Vik Formations is set to be 4 meters below the lower red shale layer of the Vik Formation (Figure 5.6), where a clear shift from limestone to shale takes place (Worsley et al. 1983).

Figure 5.6: Lowermost red shale layer of the Vik Formation, located in Verkensvika, west of the Rytteråker farm. (Logbook as scale).

The Storøysundet member is approximately 20 m in the type area and consists of two red shale layers, comprised of little but diverse fauna such as tabulate corals, brachiopods, crinoids, and stromatoporoids (Worsley et al. 1983). Interbedded grey-green shale beds can be observed together with lenses of bioclastic limestone and calcareous nodules (Worsley et al. 1983).

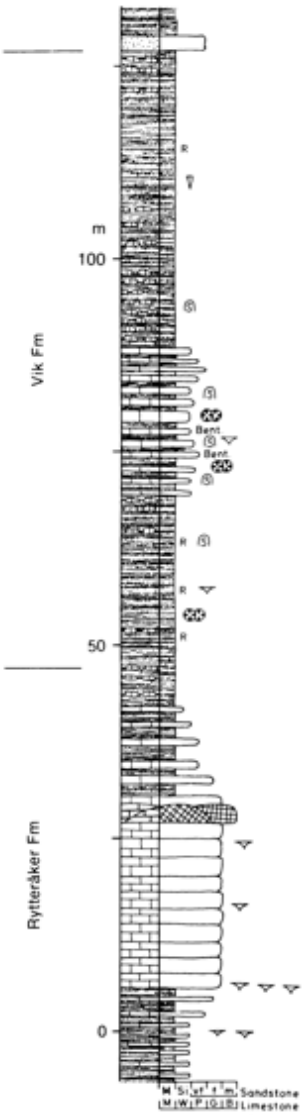

The Garntangen member is 13 m in the type area and the base has been defined where interbedded limestone begins to dominate 3 m above the upper red shale unit of the Storøysundet member (Worsley et al. 1983). The Garntangen member comprises of calcareous nodules with some occurrence of green-grey marls and thin limestone beds. The member is 25 m thick in the type area (Worsley et al. 1983).

The Abborvika member is about 35 m thick in its type location on Purkøya and the transition between the underlying Garntangen member and Abborvika member is set to where the dominant limestones decreases and calcareous grey-green shales are taking over (Worsley et al. 1983). The fauna consists of cephalopods, brachiopods and crinoids and approximately 18 m above the base there is a transition into a red shale section (Worsley et al. 1983). The uppermost 3 m of the Abborvika member comprises of green-grey shales (Worsley et al. 1983). The sharp transition to siltstones mark the transition to the overlying Bruflat Formation (Worsley et al. 1983).

Figure 5.7: Sedimentological log displaying the general section of the stratotypes of the Rytteråker and Vik Formations. Figure from Worsley et al. (1983).

The input of clastic sediments increased during the deposition of the Vik Formation. The sediments are more fine grained and indicates a deeper marine setting compared to the underlying Rytteråker Formation. The Garntangen member displays benthic fauna that indicates the presence of shallow marl banks in the type locality (Worsley et al. 1983).

6 Structural geology-Descriptive part

This chapter follows a specific scheme, where known structural features characterizing the topography in the Ringerike area, are described first. The topographic pattern in the Ringerike area (Figure 6.1b) is characterized by the undulation, reflecting the shape of the lithological units. From remote sensing the Ringerike area has been subdivided into subareas (1-4), where each subarea displays homogeneous oriented topographic lineaments (terminology after O'leary et al. (1976), which represents structural elements exposed as topographic features. These structural elements will be presented chronologically according to time of deformation. Subsequently, the focus will be narrowed down to the main study area. Associated with the study area, cross-sections, key-localities and structural maps will be presented and described.

6.1 Main topographic and structural features in the Ringerike Region

6.1.1 Caledonian structures

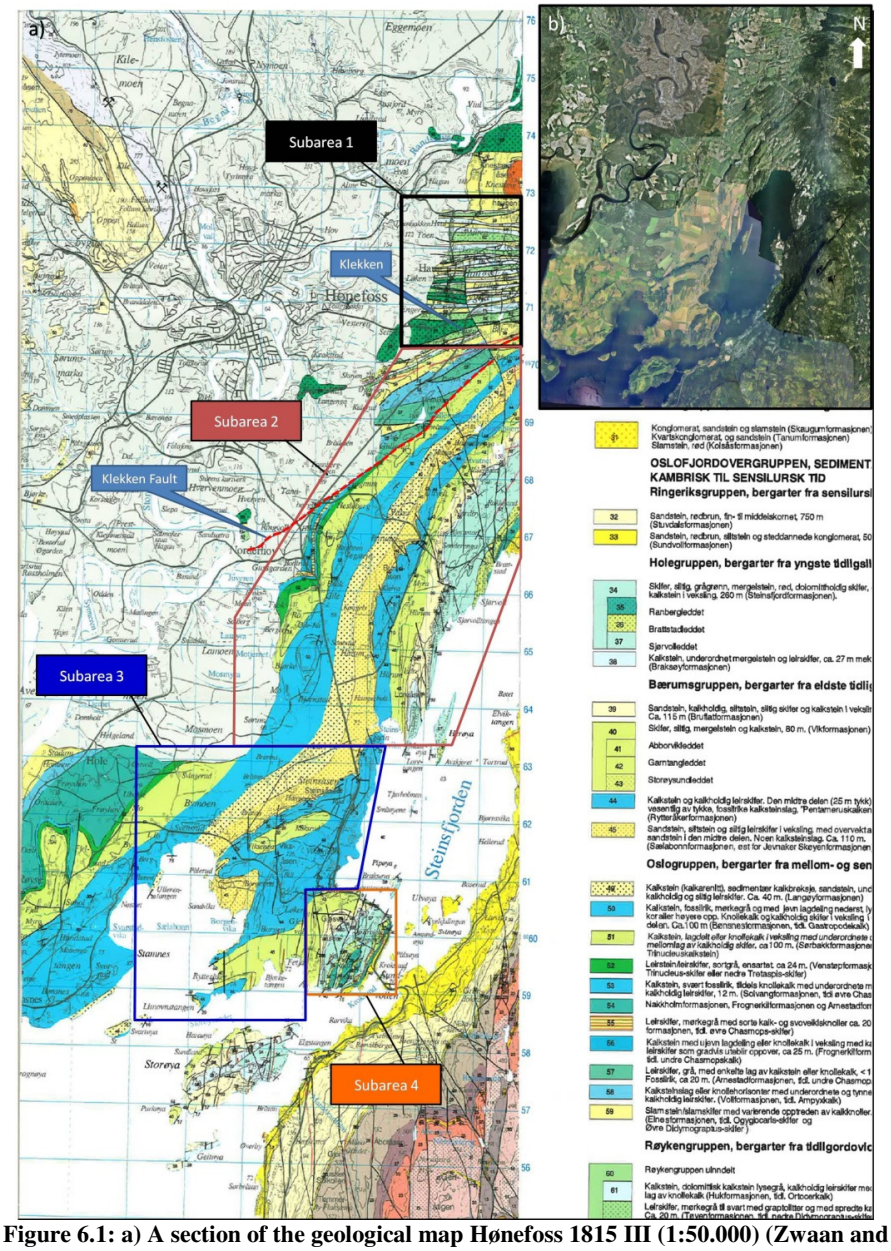

Figure 6.1: a) A section of the geological map Hønefoss 1815 III (1:50.000) (Zwaan and Larsen 2003). Subareas 1-4 have been outlined with black, maroon, blue and orange lines, respectively. The assumed Klekken fault is marked with a stippled red line. Map modified after Zwaan and Larsen (2003). b) Satellite image of the area situated around Steinsfjorden. Image from Norkart (2010).

Subarea 1.

Although not very evident, lineaments trending ENE-WSW can be observed (Figure 6.2b). These reflect the imbricate nature of the hinterland dipping Cambrian and Ordovician strata (Figure 6.2a) north of the NE-SW striking Klekken fault (Figure 6.1a), as described by Harper and Owen (1983).

Subarea 2.

Figure 6.3a displays subarea 2, covering the western side of Steinsfjorden. From the satellite image the topographic lineaments induced by the ridges are quite clear. From north to south the trend of the ridges shift gradually from NE-SW to N-S.

South of the Klekken fault (Figure 6.3c) the Ordovician and Silurian strata are tilted, striking approximately NE-SW to ENE-WSW, dipping towards (S)SE in the northern part. Farther south, towards Herøya, the strike of the bedding shifts to NNE-SSW, dipping towards ESE (seen in Figure 6.3c).

Two separate lineaments can be distinguished on the satellite image (Figure 6.3a) seen cutting through the ridges, Figure 6.3c. The western one strikes about NNW-SSE and the eastern one strikes approximately N-S.

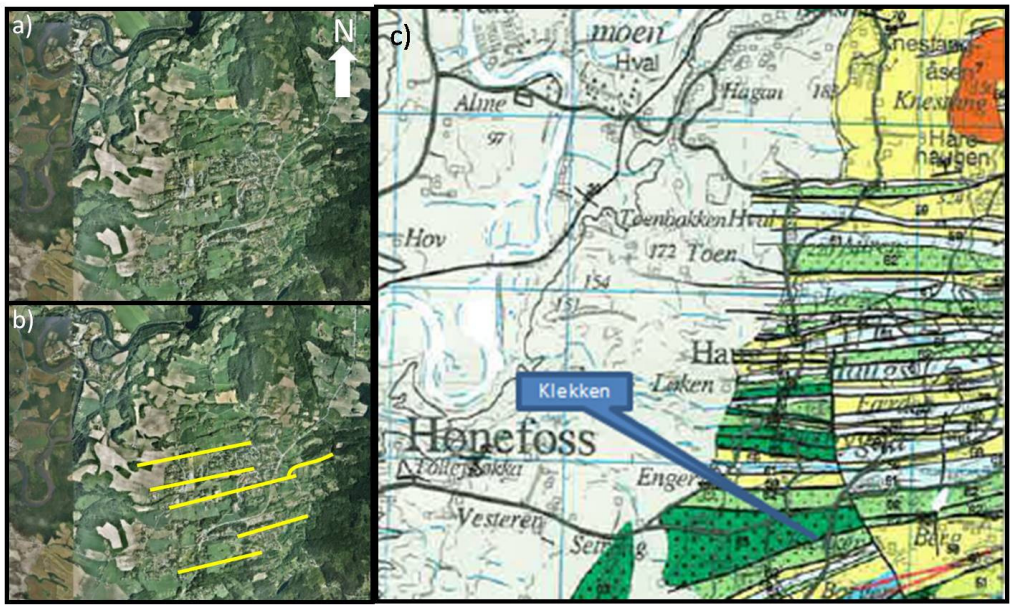

Figure 6.2: a) Satellite image of subarea 1. Image from Norkart (2010) b) Same image as a. The yellow lines mark topographic lineaments trending from about E-W to ENE-WSW. c) Section of the geological map Hønefoss 1815 III (1:50.000) (Zwaan and Larsen 2003) displaying subarea #1.

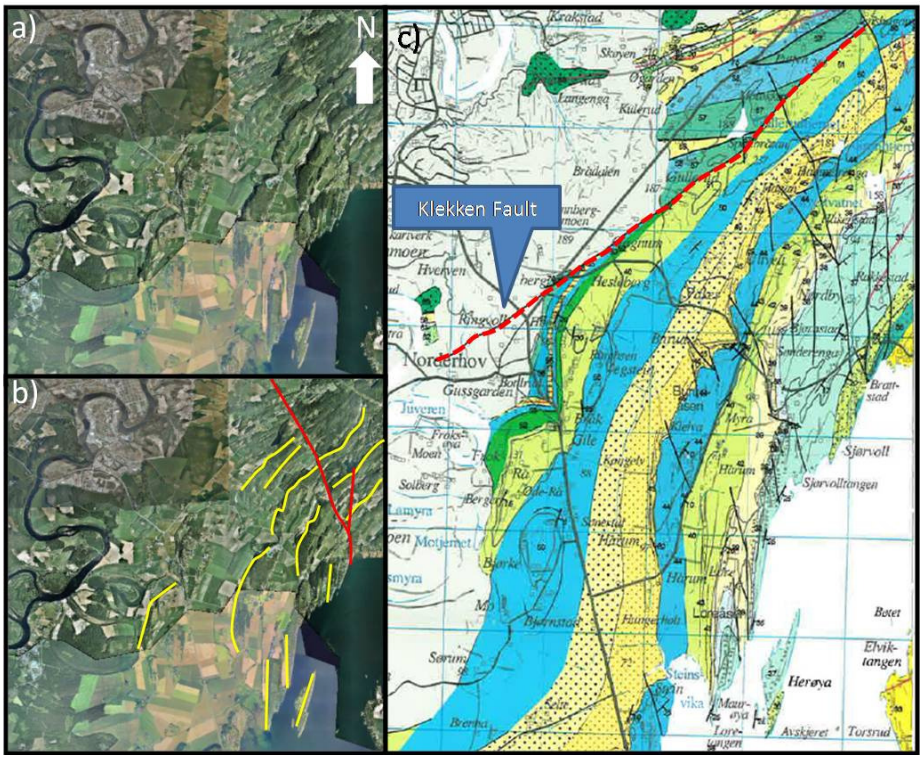

Figure 6.3: a) Satellite image of subarea 2. Image from Norkart (2010) b) Same image as in a. The yellow lines mark topographic lineaments trending from NE-SW to N-S. The red line marks two separate lineaments trending about NNW-SSE and N-S, induced by topographic lows, cutting the ridges. c) Section of the geological map Hønefoss 1815 III (1:50.000) (Zwaan and Larsen 2003) displaying subarea 2. One fault has been marked by a red line to make it more evident. This is assumed to be the Klekken fault.

Subarea 3.

Subarea 3 (Figure 6.4a) covers the area around Sælabonn and southwards including Storøya. The northern and southern part of the area is characterized by NE-SW to ENE-WSW trending ridges, where the northernmost one is Steinsåsen (Figure 6.4b).

From the geological map sheet (Figure 6.4c) it can be seen that the Silurian strata strikes mainly NE-SW, dipping towards SE and (N)NW, forming large folds trending approximately ENE-WSW.

Associated with the topographic lineaments are two synclines in the northern part of the subarea. One situated between the two northernmost ridges (Viksenga-Koksrud) (Bjørn T. Larsen, 2010, pers. comm) and the second at Rytteråker (Verkensvika), which continues into an anticline comprising Limovnstangen. The Lower Silurian beds at Storøya display strike NE-SW.

A separate set of N-S trending topographic lineaments were also identified here (Figure 6.4c).

Subarea 4.

Subarea 4 comprises the Vik peninsula. Lineaments marked in Figure 6.5b follow the most evident ridges on the peninsula trending mainly NNE-SSW. These lineaments display contrasting trend compared to Subarea 3.

The Lower Silurian beds strike approximately NNE-SSW, dipping towards ESE (Figure 6.5c). In the northern part of subarea 4, at Garntangen, Gabrielsen and Larsen (in press) describes a duplex structure which displays a top-to-east tectonic transport. The structure has been deformed by a strike-slip fault, striking NNW-SSE, which post-dates the duplex structure. The latter is believed to be of Permian age (Gabrielsen and Larsen in press).

Two N(NE)-S(SW) trending lineaments have been marked because these display a different trend and are more straight. Comparing Figure 6.5a and c, it is clear that the strike and dip of the lithological units and many of the structural elements are reflected in the topography.

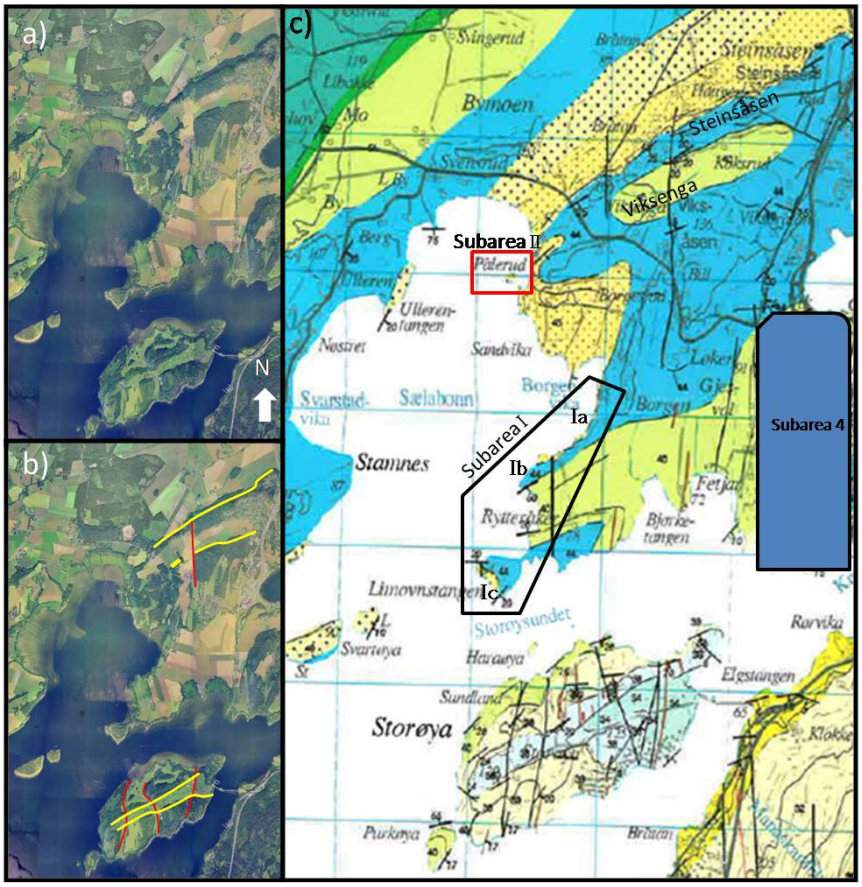

Figure 6.4:. a) Satellite image of subarea 3. Image from Norkart (2010). b) Same image as a. The yellow lines mark topographic lineaments induced by ridges, trending from approximately to (E)NE-(W)SW. The northernmost one is Steinsåsen. Red lines mark approximate N-S trending lineaments. (2010). c) Section of the geological map Hønefoss 1815 III (1:50.000) (Zwaan and Larsen 2003) displaying subarea 3. Subarea 3 has further been subdivided into areas I (black frame) and II (red frame) marked.

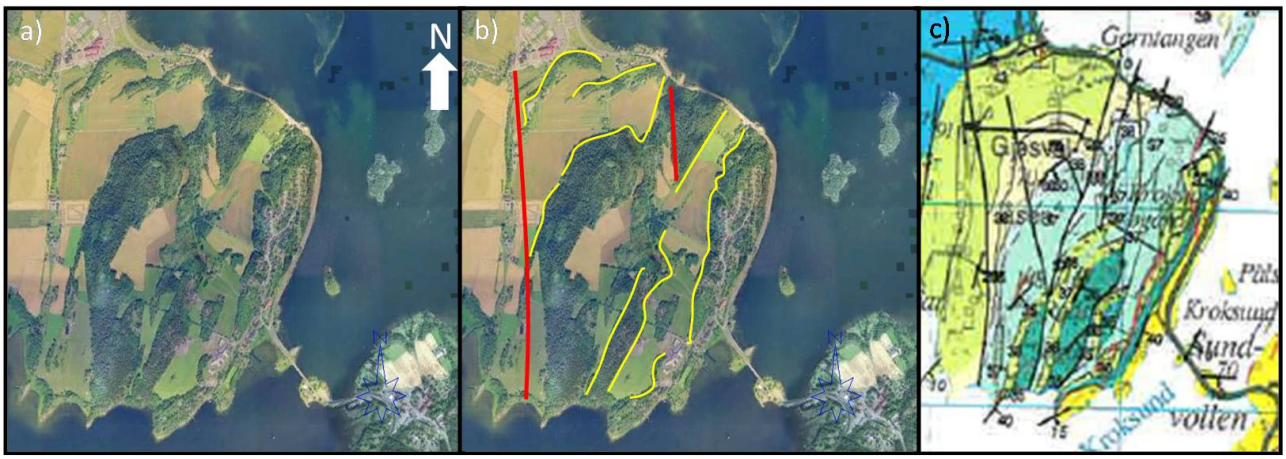

Figure 6.5:. a) Satellite image of subarea 4. Image from Norkart (2010). b) Same image as a. Yellow lines mark topographic lineaments induced by ridges, trending mainly NNE-SSW. Red lines are lineaments displaying a different trend of NNW-SSE. c) Section of the geological map Hønefoss 1815 III (1:50.000) (Zwaan and Larsen 2003) displaying subarea 4.

6.1.2 Post-Caledonian structures

Figure 6.6a displays the area around Tyrifjorden including parts of Oslo and Oslofjorden. Several pronounced topographic features characterize the landscape and have been marked in Figure 6.6b. These features can be subdivided into morphological and structural elements.

Permian lavas and magmatic bodies influence the topography in the Oslo Region. Along the eastern side of Steinsfjorden and southwards to the middle of the fjord one can follow a steep lava-cliff (Figure 6.6b). Situated between the two southern arms of Tyrifjorden is a circular, almost scallop shaped Permian named the Finnemarka batholith (Trønnes and Brandon 1992), visible on the satellite image (Figure 6.6a). Tyrifjorden was formed during the last ice-age due to glacial erosion following old river valleys (Kiær 1926). The characteristic H-shape of the fjord developed due to the presence of these tough Permian lavas and intrusive bodies. Hence guiding or "controlling" the path of the glacier, along the lava-cliff and around the Finnemarka batholith, eroding the softer Cambro-Silurian sediments (Kiær 1926, Strøm 1940). Comparing the satellite image with the geological map in Figure 6.6c, the connection between the lithology and topography is apparent. Two evident NNW-SSE trending lineaments have been identified marked in Figure 6.6b.

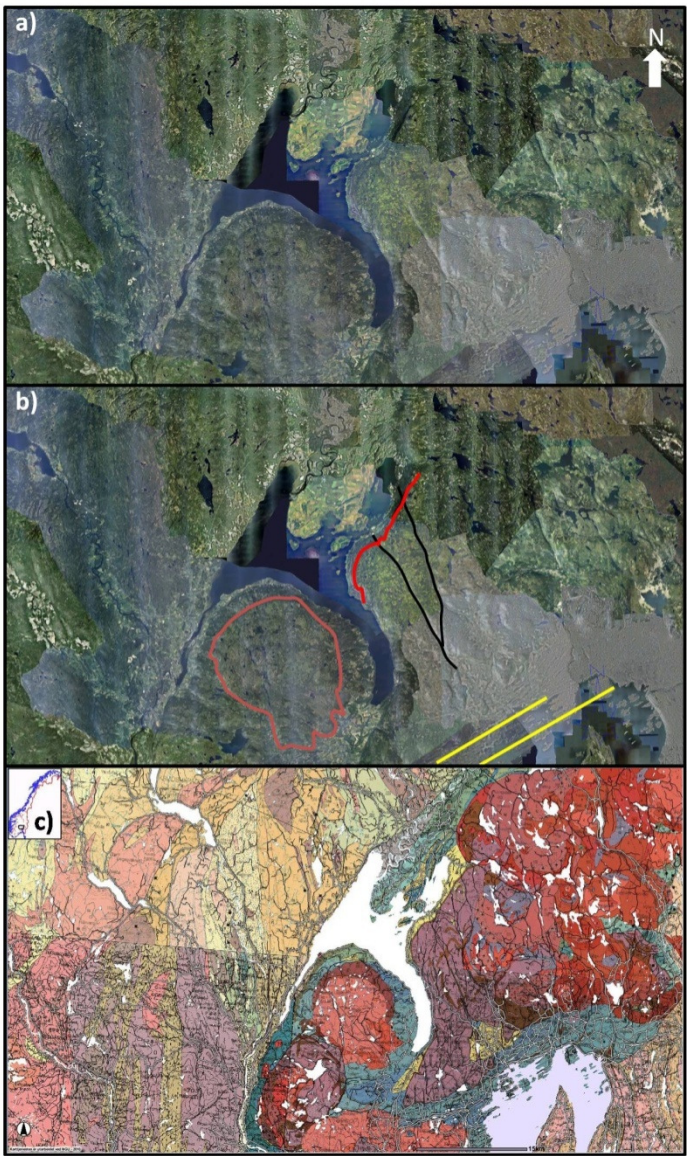

Figure 6.6: a) Satellite image displaying Tyrifjorden with Oslo and Oslofjorden to the southeast. Image from Norkart b) Same image as in a. with distinct topographic features marked. Red line = lava cliff, Maroon line = approximately circumference of the Finnemarka batholith. Black lines = NNW-SSE trending lineaments. Yellow lines = (N)NE-(S)SW trending lineaments in the northern part of the Oslofjord. c) Geological bedrock map comprising area around Tyrifjorden (middle) and parts of Oslo (lower right) and the Oslofjord. Map from (NGU 2010).

6.2 Geological description of study area, cross-sections and key-localities

Subarea 3 comprises the area of which the field work connected to this thesis was performed and has further been divided into separate geographical areas, denoted with roman numerals. The subdivision of the study area has been performed in order to separate between areas which display different structural style, into areas which display a homogeneous structural style. The subdivision is based on structural elements identified and documented during the field work. Based on these criteria two subareas, I and II, have been established. Key-localities situated within each of the subareas will be presented following a specific scheme, where the larger structures will be described first, subsequently presenting the smaller structures. Structural elements which are related to each other will be described accordingly. Cross-sections associated with Subareas I and II will be described in accordance with key-localities.

Figure 6.7 displays selected sections of the N5-raster map sheets *Ullern* (1:5000) (Hole_municipality 2009b) and *Rytteråker* (1:5000) (Hole_municipality 2009a) joined to cover the length of the study area. The positions of the cross-sections presented in this thesis are illustrated on the map.

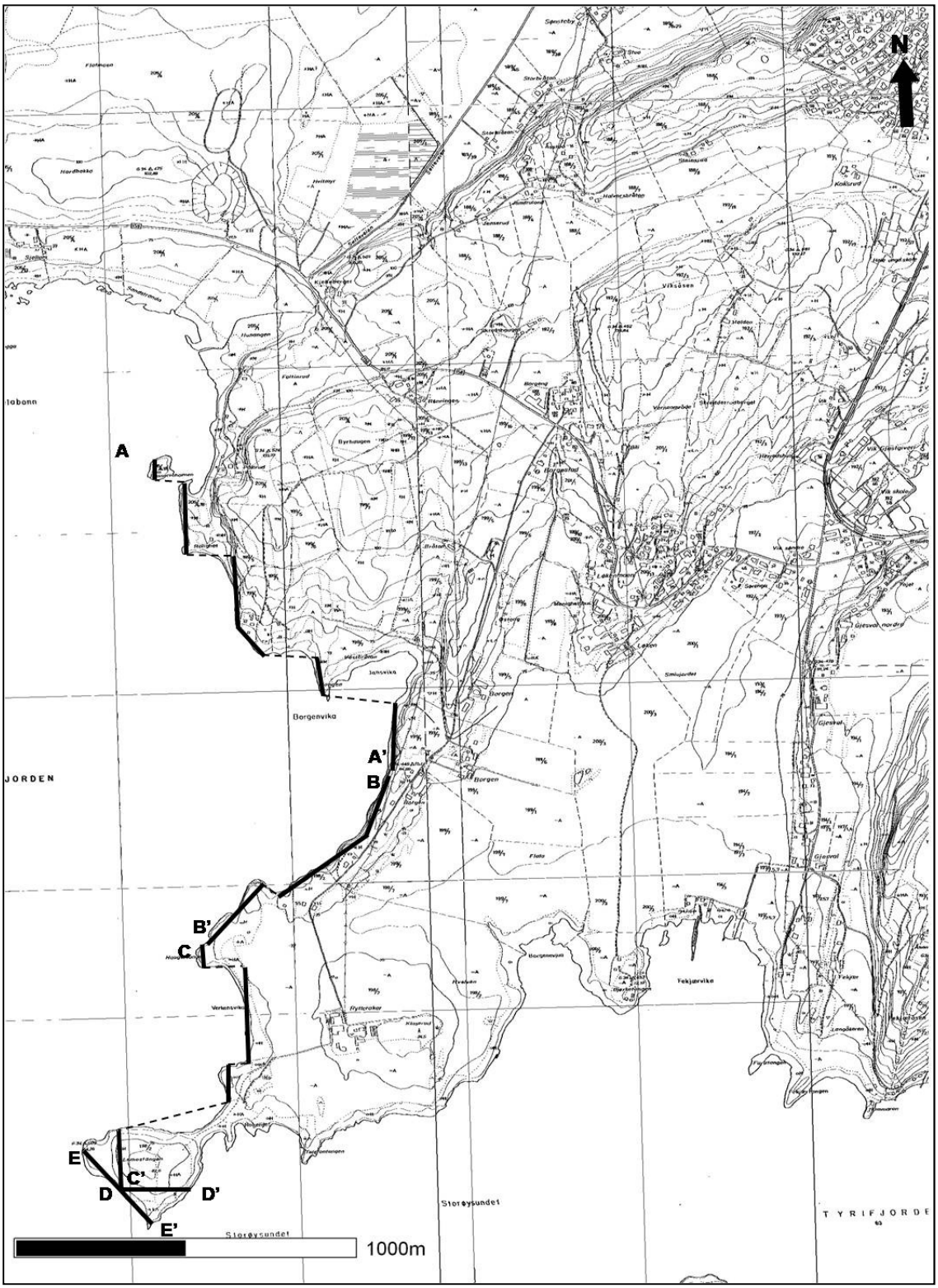

Figure 6.7: Sections of the map sheets N5-raster Ullern 1:5000 (Hole_municipality 2009b) and N5-raster Rytteråker 1:5000 (Hole_municipality 2009a) combined, displaying the eastern side of Sælabonn and Limovnstangen to the southwest. The black lines displays the orientations of cross-sections (A-A', B-B', C-C' and D-D') described in this thesis. Stippled lines illustrate the distance of extrapolation between the different segments of the cross-sections.

Cross-section A-A' stretches from Evangelieholmen in the north to Borgen (Borgenvika) in the south, estimated to approximately 950 m. Evangelieholmen displays a complex geology, comprising both Sælabonn- and Rytteråker Formations. Evangelieholmen constitutes subarea II and Borgenvika constitutes part of subarea I, which will be described later. The section (along the shoreline) between subarea I and II exhibit rather gentle tectonic deformation without any intense deformation in which the Sælabonn Formation is displayed. At Rolighet (just south of Pålerud, Figure 5.1) the strata strikes WNW-ESE, with an average dip of 23° towards NNE. South of Rolighet towards Borgen the strike of the bedding shifts from about N-S to NNE-SSW, dipping 08°-20° towards the E and ESE, with the smallest dips at Tangen varying between 2°-11°. The bedding planes situated between Evangelieholmen and Borgenvika perform in a large anticline. Figure 6.8 displays a stereoplot projection of the strike and dip measurements taken from this section. The π-axis was calculated and gives a trend of N065E and a plunge of 10° towards the ENE.

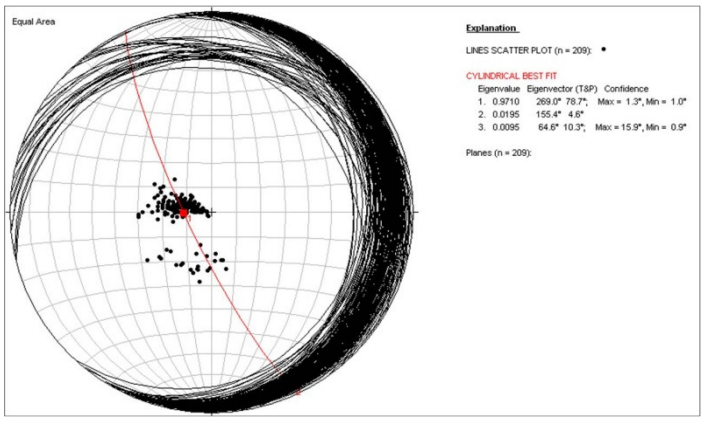

Figure 6.8: Stereoplot projection of strike and dip measurements (n=209) of bedding planes from Rolighet to Borgen (Borgenvika). The calculated π-axis gives a trend of N065E and a plunge of 10° towards ENE.

6.2.1 Subarea I

Subarea I comprises the southwestern part of Subarea 3 which stretches from Borgenvika in the north, along the shoreline towards the south-southwest including Limovnstangen (Figure 6.4c). In general, subarea I is characterized by gentle deformation in the form of gentle large scale folds in which dispersed zones of more intense deformation are displayed. Subarea I is defined on the basis of the occurrence of S- to SE-dipping contractional faults and folds associated with back-thrusting, displaying an opposite direction of transport compared to the regional direction. Three localities denoted Ia, Ib and Ic (From north to south respectively) will be presented from subarea I. Figure 6.11 displays two N-S oriented cross-sections denoted A-A' and C-C', whilst Figure 6.12 displays a NE-SW oriented cross-section denoted B-B', all of which include parts of subarea I.

From Borgenvika towards Haugertangen the sedimentary sequence comprises the Sælabonn- and Rytteråker formations (Figure 6.11b and Figure 6.12). The border between the Sælabonn- and Rytteråker formations is as mentioned a gradual transition, therefore the border between the two formations in cross-section B-B' is meant to illustrate where there is a dominance of limestone or sandstone beds.

Bedding planes in the northeastern part of Borgenvika (Borgen) strike NNE-SSW, shifting gradually towards NE-SW to ENE-WSW at Haugertangen which is situated approximately 900 m southwest of Borgen. Bedding planes in the northern part obtain rather gentle dips ranging between 08° and 20° towards ESE. Towards Haugertangen bedding planes display steeper dips in the order of 20° towards SE. Figure 6.9 displays the strike and dip measurements from bedding planes measured from Borgen to Verkensvika.

Steep faults with normal displacement were identified in the southern section of Borgenvika. In the same section the Rytteråker Formation becomes more dominant, whilst the Sælabonn Formation is absent after crossing a ravine from NW to SE, believed to be a normal fault. Here, several contractional structures in the form of folds and faults were documented. Towards southeast the steep cliffs present in Borgenvika disappear and the relief gradually

becomes more flat with limestone beds forming the shoreline towards Haugertangen. Both contractional faults and folds and extensional faults were identified along this section (Figure 6.12).

A large scale fold between Borgen (Borgenvika) and Haugertangen was not observed in the field. However, the calculated poles to the bedding planes display a systematic trend, which indicate the presence of what appears to be large gentle fold. The calculated statistical π-axis gives a trend towards N065E and a plunge of 09° towards ENE.

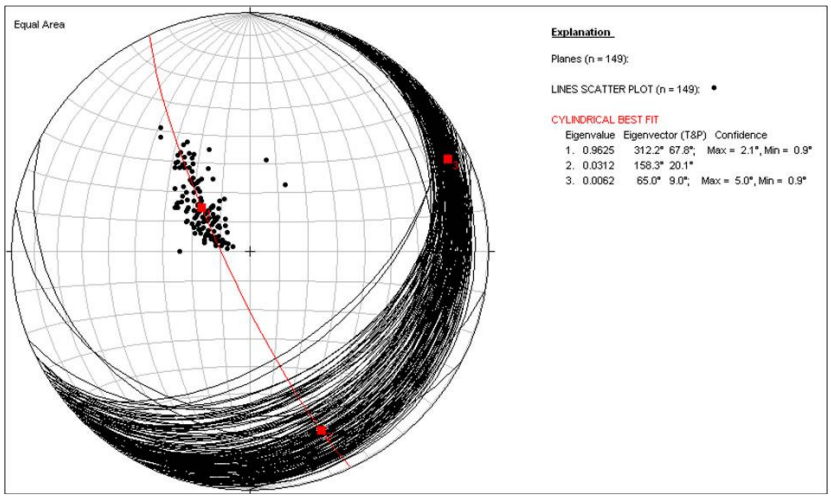

Figure 6.9: Stereoplot projection of strike and dip measurements (n=149) of bedding planes, obtained from Borgenvika (Borgen) to the southern tip of Haugertangen/northern Verkensvika. The calculated π-axis gives a trend of N065E and a plunge of 09° towards ENE.

The stretch from Haugertangen in the north to Limovnstangen in the south (approximately 800 m) is characterized by two large folds, denoted the Verkensvika syncline and the Limovnstangen anticline in this thesis (Figure 6.11b). On the northern side of Verkensvika, the transition between the Rytteråker Formation and overlying Vik Formation was identified based on the occurrence of red shales belonging to lower part of the Vik Formation. Here the bedding planes strike (E)NE-(W)SW, with an average dip of 41° towards (S)SE. Vegetation and loose material covers the central part of Verkensvika, concealing the rocks. On the south side, limestone beds and red shales of the Vik Formation reappear, striking E-W, with an average dip of 23° towards N. The distance between the occurrences of the red shale layers on the northern and southern side is approximately 420 m. Based on strike and dip

measurements of bedding planes situated on the northern and southern side of Verkensvika the π-axis was calculated, displaying a trend of N066E and plunge of 09° towards ENE which represents the fold axis of the syncline (Figure 6.10a).

Bedding planes constituting the southern limb of the Verkensvika syncline also forms/ or continues as the northern limb of the Limovnstangen anticline (Figure 6.13). From north to south across the middle, the Limovnstangen peninsula is about 320 m long. Strata on the northern side of Limovnstangen comprise the uppermost part of the Rytteråker Formation and exhibit an average strike of N265E with a mean dip of 24° towards N. Towards the middle section on the western side the strike of the bedding planes shifts towards NNW-SSE, dipping more gently towards ENE, comprising the Sælabonn Formation. This location represents the hinge zone of the anticline and is characterized contractional deformation, described in detail below. Further south on the western side a NNE-SSW strike (average N012E) is displayed, with a mean dip of 14° towards ESE. Bedding planes on the southeast and east side of the peninsula represents the lower and middle section of the Rytteråker Formation, respectively. On average the strata strike NNE-SSW (average N019E) with an average dip of 17° towards ESE, ranging between 08°-36°. Towards the northeastern side of Limovnstangen the strike of the bedding planes shift gradually towards N-S (averaging N360E), with an average dip of 13° towards E. Here is the uppermost part of the Rytteråker Formation displayed. Based on these measurements the statistical fold axis (π-axis) trending N057E, plunging 12° towards ENE was calculated for the Limovnstangen anticline (Figure 6.10b).

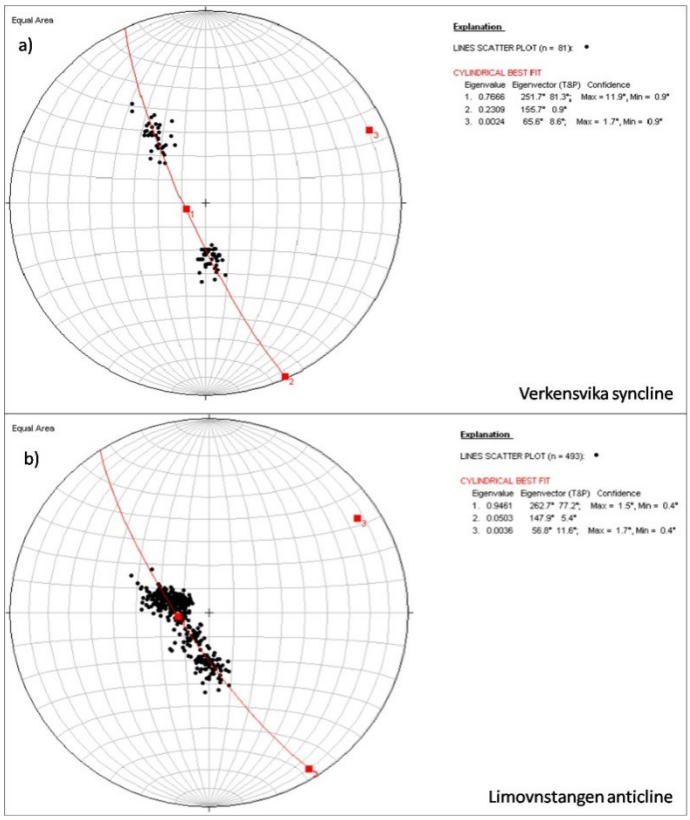

Figure 6.10: a) Stereoplot projection displaying the calculated fold axis (π-axis) of the Verkensvika syncline based on strike and dip measurements (n=81) of bedding planes. The trend of the fold axis is N066E and a plunge of 09° towards ENE b) Strike and dip measurements (n=493) of bedding planes at Limovnstangen. Calculated fold axis (π-axis) of the Limovnstangen anticline based on strike and dip measurements. A trend of N057E and plunge of 12° towards ENE was obtained.

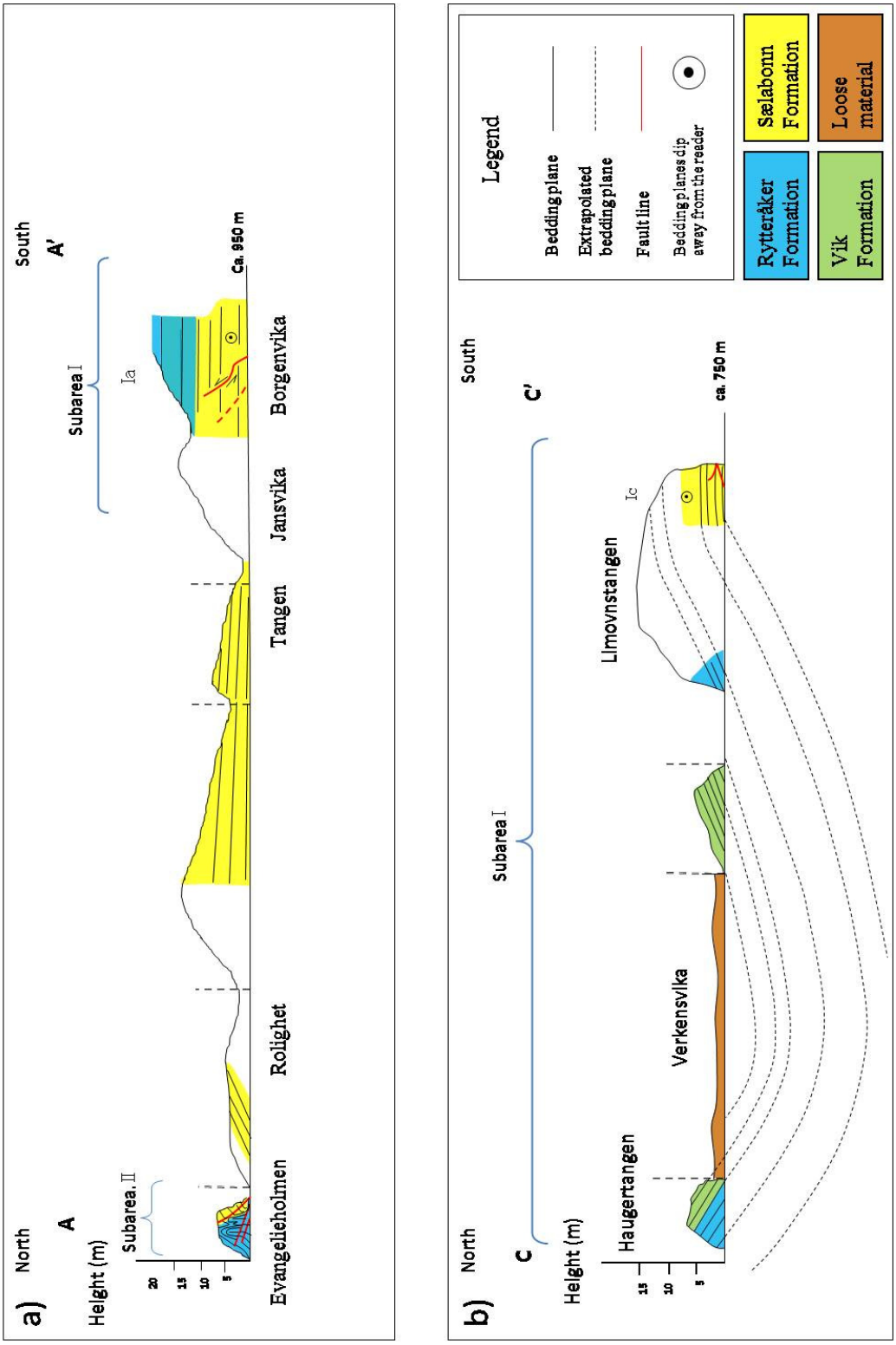

Figure 6.11: a) N-S cross-section from Evangelieholmen to Borgen, respectively. Vertical exaggeration = 5x. b) N-S cross-section from Haugertangen in the north to Limovnstangen in the south. Vertical exaggeration = 5x. Vertical stippled lines illustrate the positions where the cross-sections have been extrapolated.

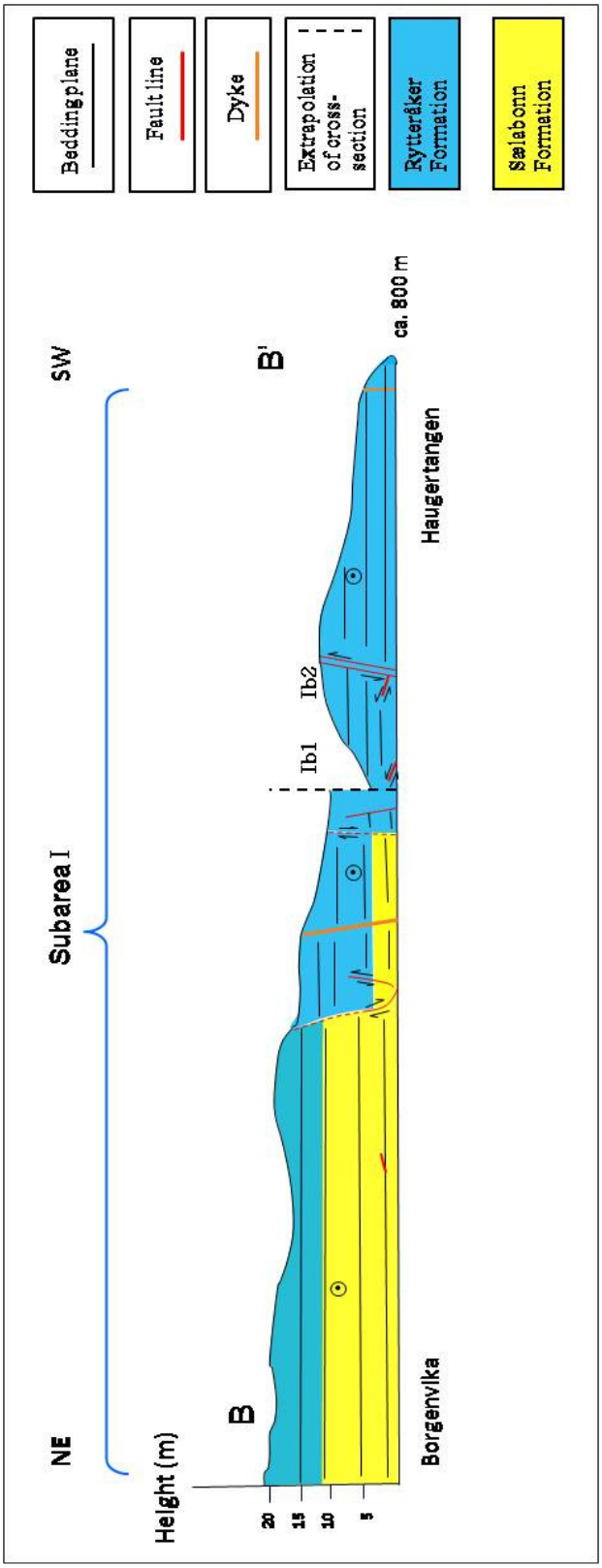

Figure 6.12: NE-SW oriented cross-section from Borgenvika to Haugertangen. Vertical scale is exaggerated 5x.

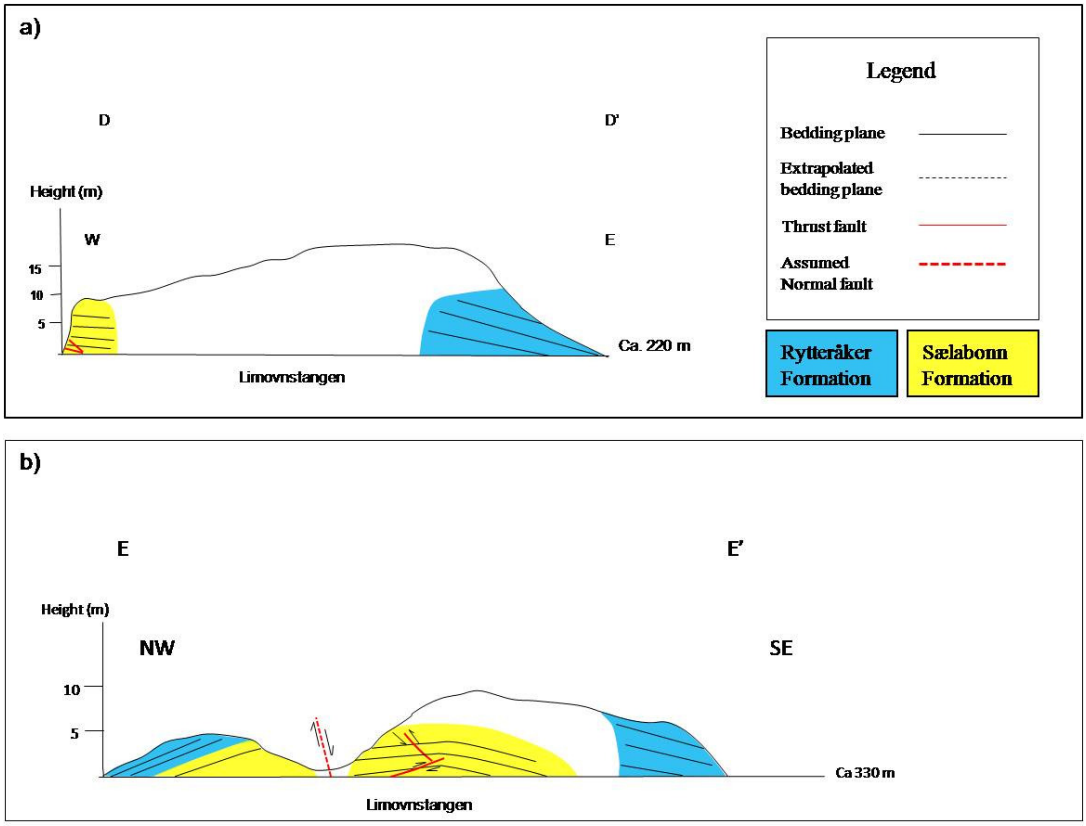

Figure 6.13: a) Profile D-D' is a E-W oriented cross-section of Limovnstangen. Vertical scale exaggerated 2x. b) Profile E-E' is a NW-SE oriented cross-section. Vertical scale exaggerated 5x.

Locality Ia. Borgenvika

The locality displays an approximately 40 m long and 10-15 m high vertical cliff situated at the shoreline in Borgenvika, about 150 m northwest of the Borgen farm (map sheet 1815 III Hønefoss, UTM 699 602).

The Borgenvika locality is characterized by a steep angle fault (Fault 1) and shallowly NE-ENE plunging asymmetrical anticline folds, together dominating the entire height of the exposed cliff, which is about 4 m. The folds are fault-propagation-folds (Figure 6.15). Additionally, a second set of folds and faults where identified, described below.

The sedimentary sequence comprises the transition between the Sælabonn and Rytteråker formations. The lower part is dominated by approximately 3-8 cm thick sandstone beds, interbedded with silt beds. Limestone beds appear more frequent towards the top of the cliff, dominating the uppermost part as the Rytteråker Formation. Bedding planes at Borgenvika strikes NNE-SSW, dipping on average 12° towards ESE (Figure 6.14).

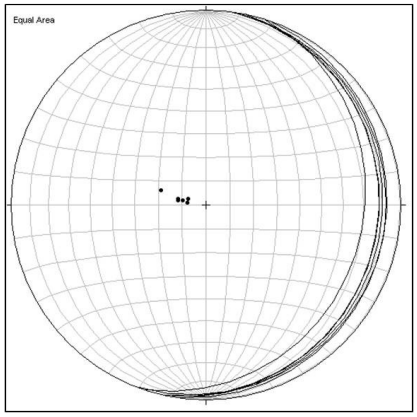

Figure 6.14: Strike and dip (n=7) of bedding planes at the Borgenvika locality.

A total of 16 fold axes were measured at Borgenvika (Figure 6.15d). The average trend of the fold axes is N052E, with an average plunge of 09° towards NE.

Fault-propagation-folds

The folded bedding planes in the uppermost 3 m of cliff display a tilted fold limb, constituting the footwall of Fault 1 (Figure 6.15). The overall geometry of the section is a fault-propagation-fold, forming an S-shaped monocline, which has been cut by the main fault. The axial plane strikes NE-SW, dipping approximately 50° towards SE. Bedding in the hanging wall, which terminates along the fault trace, displays drag folds with axial planes dipping towards SE, (convex towards NW). The fold axes measured plunges towards the NE and ENE. The footwall beds are in some places dragged downwards along the fault trace, reflecting the relative movement along the fault. The footwall bedding displays an average strike of N247E (WSW), with an average dip of 60° towards NNW. The dips range between 50°-70°.

The lower part of the structure appears to be an asymmetrical anticline fold which has been cut by Fault 1, forming a "snakehead" fold in the hanging wall of Fault 1, with an axial plane measured to N254E, dipping 47° towards NNW. Beds in the lowermost core, situated in the footwall of Fault 1, are strongly deformed and tight. It is not possible to correlate the bedding plane across the fault down-section with certainty. However, the beds down-section are thicker and more massive, both in the hanging wall and the footwall, displaying a coherence in lithology across the fault.

Description of faults

Fault 1 displays a planar geometry with reverse displacement. Calcite cement was observed on the fault plane in some places. The fault line can be traced from about 10 cm above the ground up to the top of the cliff. Measurements on the fault plane of Fault 1 gave an average strike towards N040E, with an average dip of 50° towards SE (Figure 6.15c). Slickenlines on the calcite cement could be observed along the fault plane in the lower part of the section. The slickenlines measured an average trend of N119E, plunging 50° towards ESE. The amount of displacement across the fault was not possible to deduce due to the orientation of

the fault plane in relation to the bedding. However, the lithology in the footwall and hanging wall are very similar.

The trend of the fold axes and strike and dip of the fault plane indicate a transport direction towards NW. The slickenlines on the calcite cement indicate a transport direction towards WNW (N299E).

Fault 2 is a low-angle fault which, where the fault line can be traced from ground level and for about 1 m towards north before it dies out (Figure 6.17). The strike of the fault plane was measured to N016E, dipping 04° towards ESE. Only one measurement was taken due to the short exposed distance of the fault plane. However, the orientation of the fault plane suggests a transport direction towards WNW which is fairly consistent with Fault 1. Beds situated in the footwall are flat lying, displaying the general strike and dip at Borgenvika (Figure 6.14), whilst the beds in the hanging wall display steep dips with a strike measured to N240E, dipping 60° towards NNW a few cm above the fault plane.

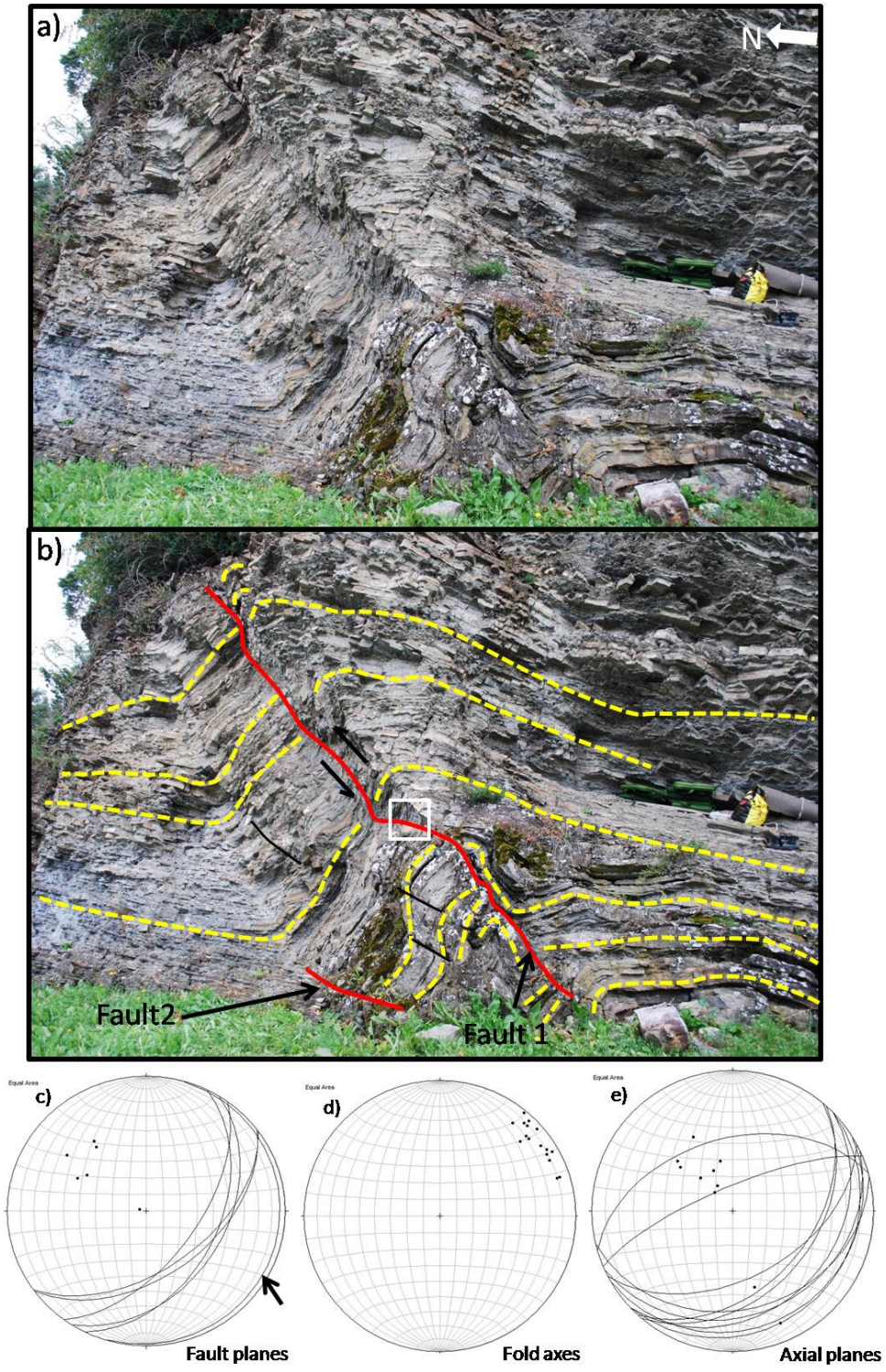

F

Figure 6.15: a) Photo of the exposed cliff at Borgenvika. (Bag of charcoal (middle right) as scale). b) Same photo as in a. with faults 1 and 2 marked with red lines. Yellow stippled lines follow a few selected beds to emphasize the folding. These are not meant to illustrate any displacement across the fault. Black solid lines mark fractures. Lineations were observed in the area within the white square (See Figure 6.16 for detail). c) Stereoplot displaying the fault plane orientation of Fault 1 (n=5) and Fault 2 (n=1), marked with black arrow). d) Stereoplot displaying fold axes (n=12). e) Stereoplot showing axial planes (n=11) of folds.

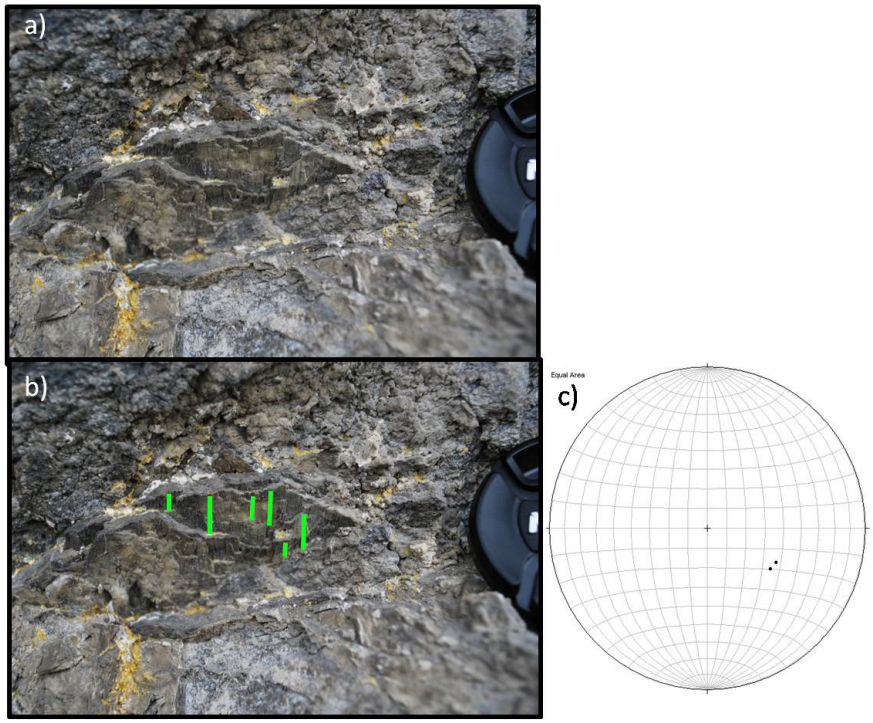

Figure 6.16: a) Photo of the area enclosed within the white square in Figure 6.15b (Lens cap as scale). b) Same photo as a. with slickenlines on calcite cement marked with green lines situated on the fault plane of Fault 1. c) Measurements of slickenlines (n=2) on calcite cement in the fault plane of Fault 1 projected in a stereoplot.

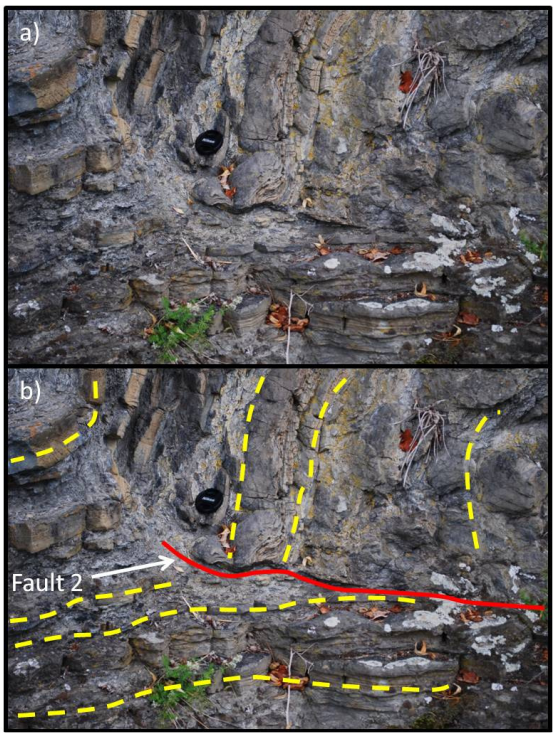

Figure 6.17: a) Detailed photo of Fault 2 (Lens cap as scale). b) Same photo as in a. Fault 2 is marked by a red line. Bedding is marked by stippled yellow lines.

Structures associated with bedding parallel shortening

Fold population 2

A second fold population was observed in the footwall of Fault 1 (Figure 6.18) and comprises open, symmetric folds with mainly shallowly NE to ENE-plunging fold axes. The average trend of the fold axes measured in the footwall of Fault 1 is N056E and an average plunge of 10° was obtained. Five axial planes were measured in the footwall of Fault 1, which gave an average strike of the axial planes of N060E, with an average dip of 25° towards SSE. The wavelength and the amplitude of the folds vary a bit. The folds with most curvature display wavelengths in the order of 30 cm and amplitude about 8 cm. Some of the beds display very gentle folding with amplitudes of about 1-3 cm. The folds are most evident in the sandstone beds. The folds are concentric and can be described as Class-1B folds, after Ramsay's (1967) fold classification. The folds appear to be buckle folds, formed by active folding.

The orientation of fold axes indicate that these folds were developed during a compressional event with the maximum stress axis (σ_1) directed approximately NNW-NW to SE-SSE.

Fault population 2

Associated with fold population 2 is a set of thrust faults, which cut and displace the sandstone beds at a low angle relative to the bedding plane. Figure 6.18c displays the down-section footwall of Fault 1. In one folded sandstone layer, approximately 4-5 cm thick, three faults (A1 to A3), cutting the bed, where identified. In the neighboring layer, about 2-3 cm thick, one fault (B1) was documented (Table 1 and Figure 6.18b). The faults are confined to the individual folded beds and cannot be traced into neighboring beds. Faults A1 and A2 cuts the bed in near inflection points on each side of the anticline and display opposite directions of transport, in which the footwall of both faults converge. Fault A3 and B1 cuts

the bed through the near the hinge zones of two separate small anticline folds. The displacement across fault A1 was measured to 7, 5 cm. On average the fault planes A1-A3 strike N265E, dipping towards N. Fault plane A1 exhibits the largest dip and A3 the smallest. Fault plane B1 strike N280E, dipping 46° towards N. Regarding the direction of transport connected to the thrust faults, this will be discussed further in chapter 7.

It should be noted that these structures where only observed in the footwall of Fault 1 at this locality, which might just be a coincidence. Further towards the north the cliff was inaccessible and therefore not investigated.

Fault plane	**Strike**	**Dip**
A1	260	64
A2	266	54
A3	268	24
B1	280	46

Table 1: Strike and dip measurements of fault planes A1 to A3 and B1.

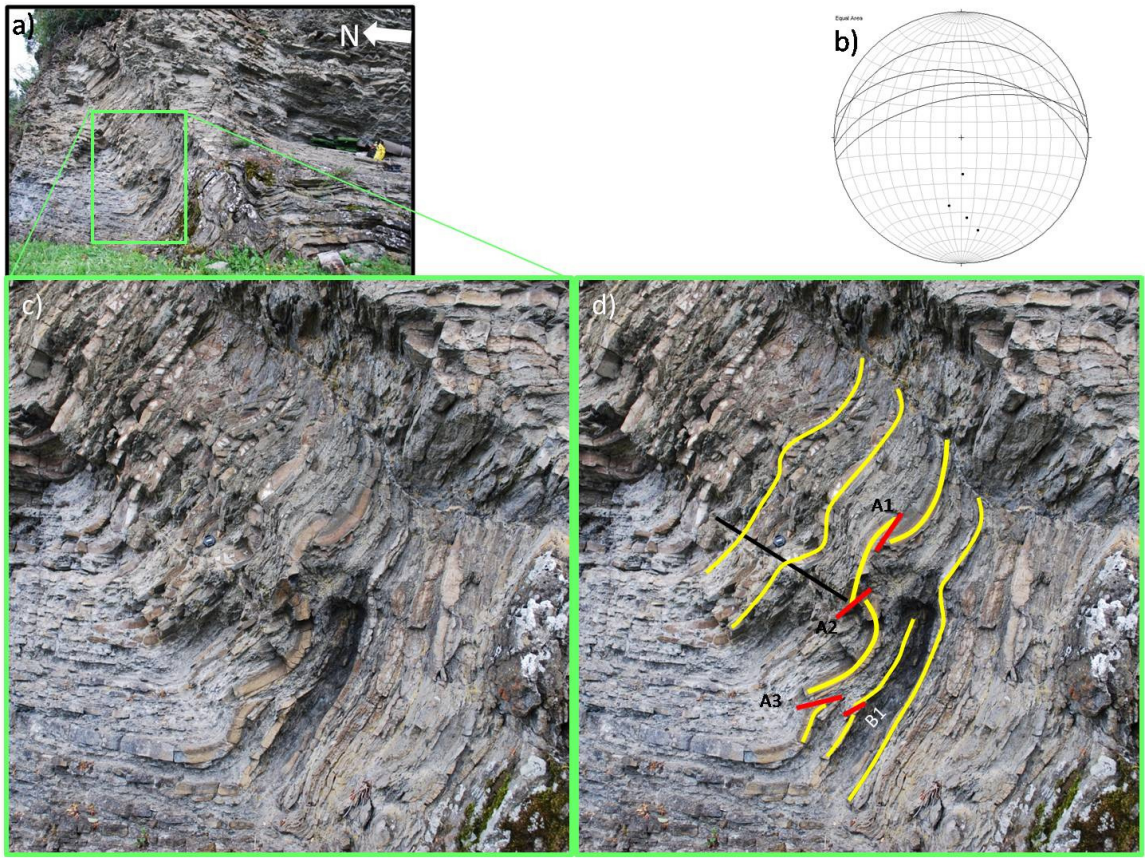

Figure 6.18: a) Overview photo of the Borgenvika locality (Lens cap as scale). b) Strike and dip measurements of fault planes (n=4) A1 to A3 and B1 projected in a stereoplot. c) Detail photo displaying tilted bedding planes situated in the footwall of Fault 1. d) A selected number of folded bedding planes are marked by yellow lines to illustrate the folding belonging to fold population 2. Red lines mark faults belonging to fault population 2. The black line marks a fracture.

Additionally, a set of fractures striking approximately sub-parallel to Fault 1 were recognized (Figure 6.15 and Figure 6.18).

Figure 6.19 displays a sketch of the Borgenvika locality. From the sketch it appears that there is a correlation across the fault, but this is difficult to say. From the sketch it the thicker beds dominate the lower part of the structure, decreasing in thickness upwards. Bedding-parallel shortening structures can be seen in the footwall of Fault 1 as well as smaller fractures.

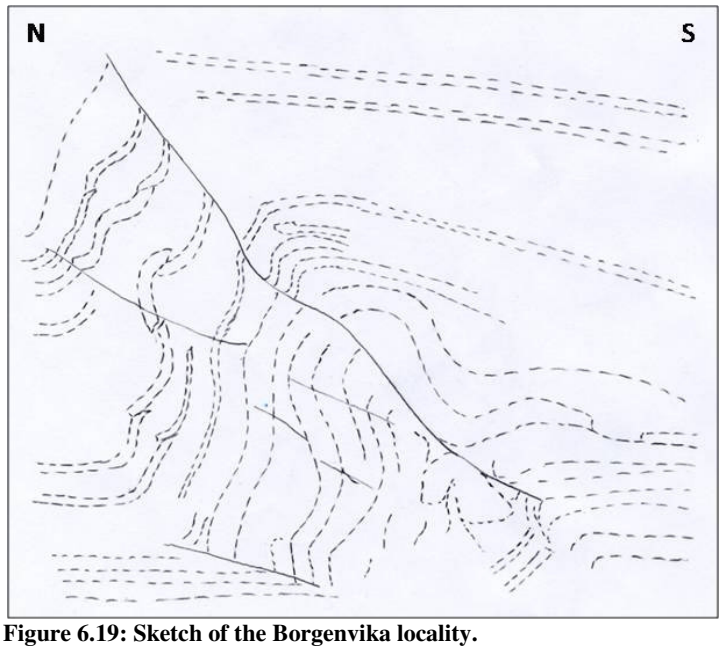

Figure 6.19: Sketch of the Borgenvika locality.

Summary

Based on the structures described above an assumed time line regarding the deformational history can be proposed, illustrated in Figure 6.20.

1. First a horizontal compressional phase resulting in development of low-angle (relative to the bedding planes) thrust faults (Fault population 2). The thrust faults display two separate directions relative to the bedding plane.
2. Secondly the buckle folds (Fold population 2) developed, folding the sandstone beds and the associated thrust faults. This is because the thrust faults (especially A3 and B1) dip at a low-angle to the bedding planes which indicate that these were formed prior to the folding, as the beds were approximately horizontal. However, regarding Fault A2 the faults appear to cut the bedding at a steeper angle compared to Faults A3 and B1.
3. Both Fold and Fault population 2 have subsequently been rotated, which is attributed to the development of the fault-propagation-folding (Fault 1). Down-section, the beds displays the most intense deformation in the form of tight folds, formed in front of the propagating fault, and subsequently cut by Fault 1. Fault 1 displays an

approximate direction of transport towards NW. Fault 2 (situated in the footwall of Fault 1) is horizontal, separating the steeply dipping beds in the hanging wall from horizontal beds in the footwall, indicating a relation to the fault-propagation-folding.

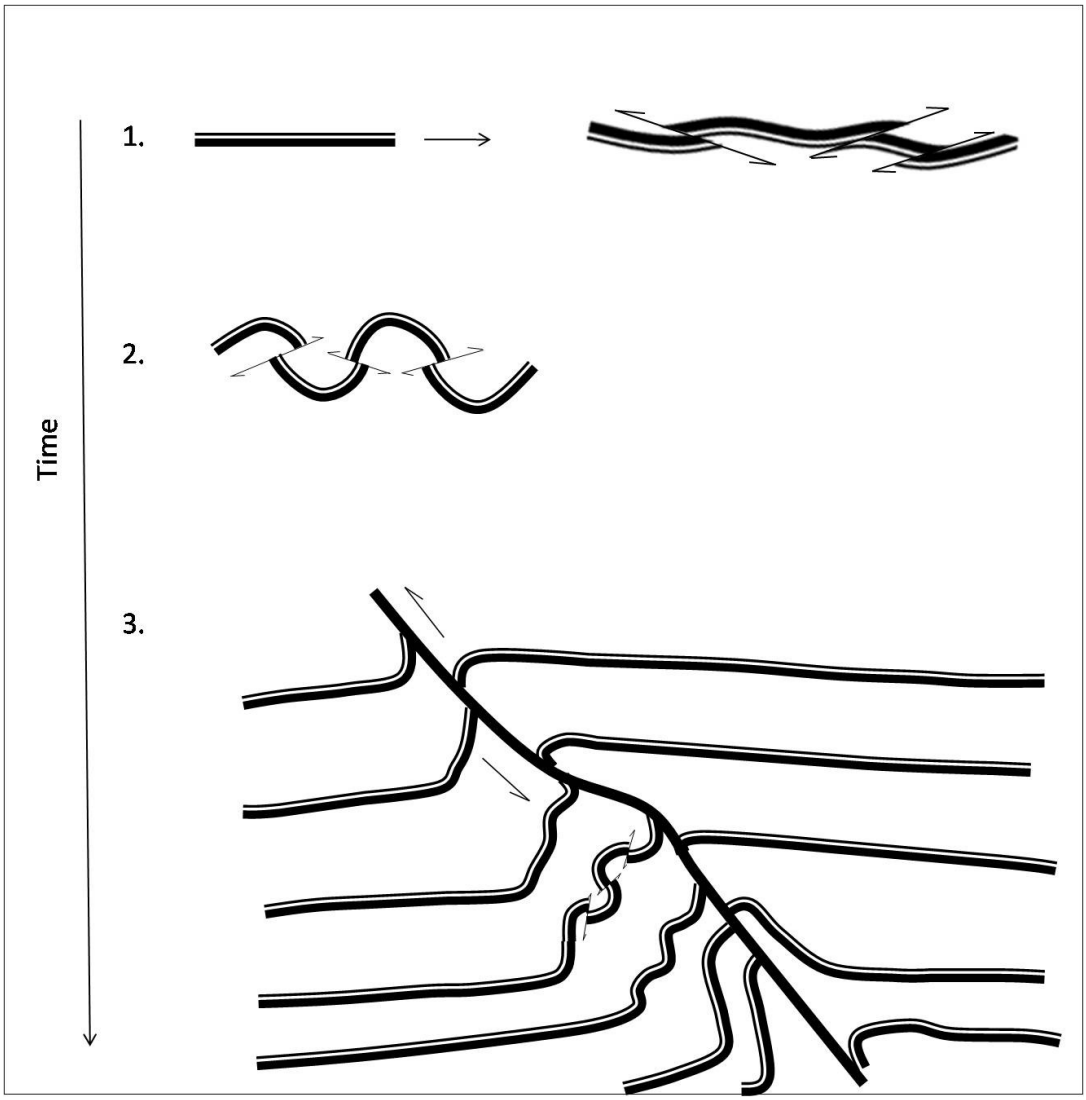

Figure 6.20: Schematic sketch illustrating the different structural elements and the possible deformational timing relative to each other at the Borgenvika locality.

Subarea Ib. Borgenvika-Haugertangen

Locality Ib comprises two localities, situated approximately 90 m apart. Both localities are located on the shoreline southwest of Borgenvika and 200-275 m NE of Haugertangen on the eastern shore of Tyrifjorden. From northeast to southwest the localities have been denoted Ib1 and Ib2, respectively (map sheet 1815 III Hønefoss, Ib1: UTM 694 596, Ib2: UTM 695 596). Low-angle contractional faults are displayed in both localities. Cross-section B-B' (Figure 6.12) displays the positions of the localities.

The ?middle Rytteråker Formation comprises the sedimentary succession at both localities. In the northeastern part the bedding planes display an average strike towards N031E ranging between N014E and N041E. The dip of the beds range between 13°-30°, averaging 18° towards ESE (Figure 6.21a). Southwest of locality Ib2 towards Haugertangen the strike of the bedding planes shifts towards an average of N042E, ranging between N031E and N064E. The average dip is 23° towards SE, ranging between 16° and 34°.

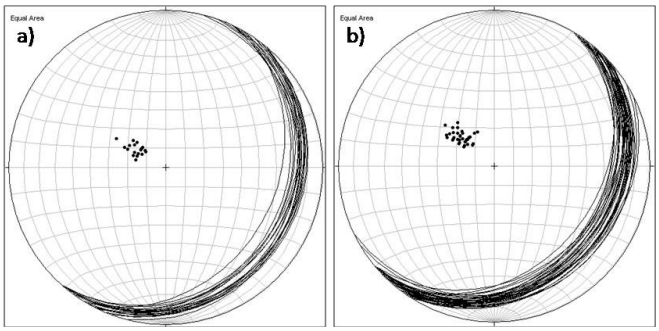

Figure 6.21: a) Stereoplot projection displaying the strike and dip of bedding planes (n=19) belonging to the Rytteråker Formation in the SW part of Borgenvika and SE towards locality Ib2. b) Strike and dip of bedding planes (n=39) of the Rytteråker Formation in the SW part of the section, SW from locality Ib2 towards Haugertangen.

Locality Ib1

Locality Ib1 is located on the southwestern tip of Borgenvika and displays a 6 m high slope which continues to Haugertangen towards the SE. The locality is characterized by two contractional faults denoted F1 and F2. Both fault lines display low angles and a ramp-flat-ramp geometry and cuts the bedding clean with no associated folding (Figure 6.22a, b).

Fault F1 is most evident of these two and can be followed from the water surface and up-section towards NE for about eight meters before it appears to die out (Figure 6.11b). Fault F1 displays reverse displacement of about 8-10 cm down-section which is displayed in Figure 6.11e where a quite dark pentamerid rich, possibly oil stained (Bjørn T. Larsen, 2009, pers. comm.) limestone bed can be correlated across the fault trace. Up-section a displacement of 4-5 cm is displayed. The average strike of the fault plane is N095E, with an average dip of 15° towards S (Figure 6.11g).

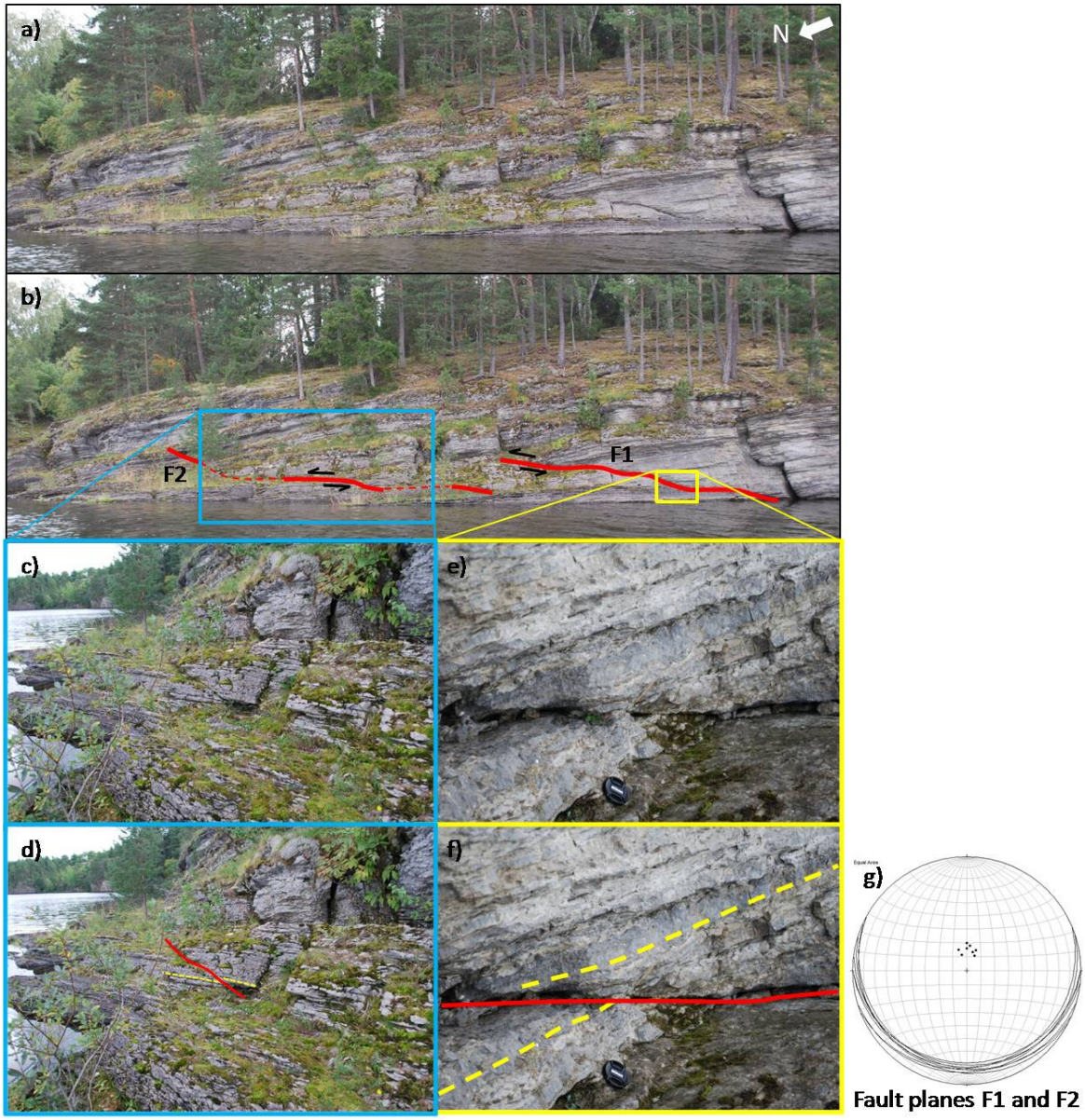

Figure 6.22: a) Photo of the southwestern part of Borgenvika. b) Two faults F1 and F2 are marked with red lines. Red stippled line indicates extrapolation of the fault traces. c) Detail of a section of fault F2 (Lens cap as scale). d) Same photo as c. with fault F2 marked with a red line. Yellow lines mark a displaced bedding plane. e) Detail of fault F1 (Lens cap as scale, placed about 20 cm above the fault line). f) Same photo as e. with fault F1 marked with a red line and bedding plane marked with a yellow line. g) Stereoplot projection of strike and dip of bedding planes obtained in the area in vicinity of the locality. h) Stereoplot projection of strike and dip measurements taken on fault plane F1 (n=7) and F2 (n=1).

Fault F2 is situated sub-parallel, about one meter down-section, in the footwall of fault F1. A reverse displacement of approximately 2-3 cm was identified down-section. Up-section an offset of about 1 cm is displayed. One measurement was obtained on the fault plane of fault F2. A strike towards N090E, with a dip of 20° towards S was obtained.

Locality Ib2

An approximately 8-10 m high cliff represents this locality. A low-angle thrust fault (Fault 1) cutting up-section towards north was documented (Figure 6.23a and b). The fault trace can be followed for about 6 m. The fault has been identified as a thrust fault because of the low angle and down-section the fault forms a lens, approximately 1,5 m long and 10-15 cm thick. Up-section the beds are folded. The folds are open, appearing to be fault-related folds due to the asymmetry of the folds. The fold axis measured trend N247E, plunging 08° towards WSW.

Three measurements were taken on the fault plane. The strike shifted between ENE-WSW and NE-SW, giving an average strike of N061E. The dip ranges between 30° and 42° towards the SSE and SE. Two of the measurements were taken on the fault lens. The third was taken up-section. Based on these measurements (Figure 6.23e) the fault displays an approximate direction of transport towards NNW.

The cliff that Fault 1 is situated in comprises the hanging wall of a fault with normal displacement. Bedding planes in the cliff displays an upwards drag, indicating that the cliff constitutes the hanging wall. Two measurements were taken on the fault plane. In the middle-section a strike of N002E and dip of 80° towards was obtained and up-section a strike of N006E with a dip of 86° towards the E was measured. Figure 6.23c display a detail of the folded beds situated up-section. The fault plane (belonging to the footwall) of the normal fault can be observed where the fault has cut the folded bedding. Slickenlines indicate the direction of slip on the fault, however, the slickenlines were not measured, but they are straight across the folded beds and consistent with movement across the fault seen on the surface of the hanging wall. This implies that the extensional fault post-date the fold.

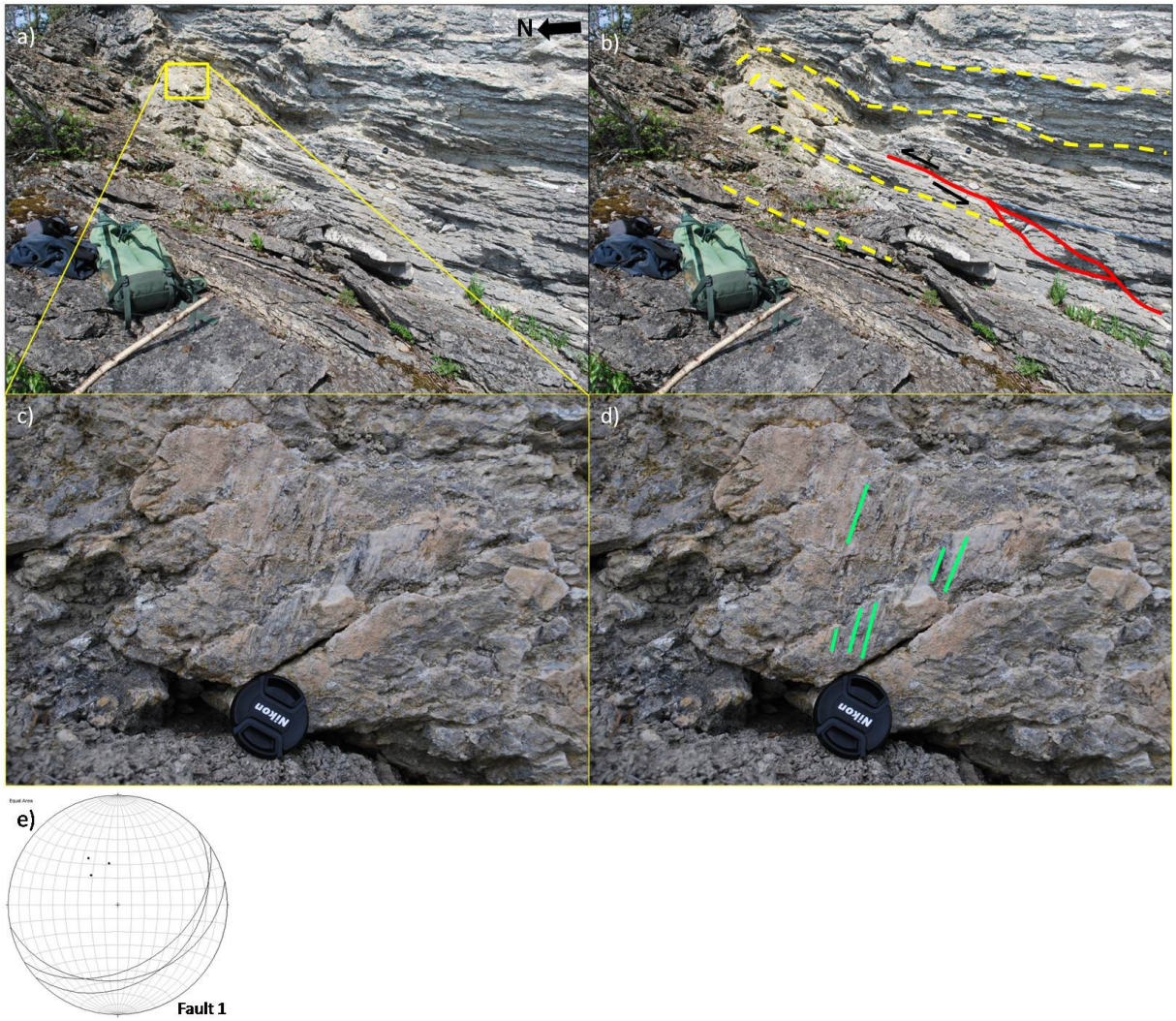

Figure 6.23: a) Photo from locality Ib2 displaying a thrust fault and a normal fault (Backpack as scale). b) Same photo as a. The thrust fault trace is marked with a red line. Bedding planes are marked with yellow lines. c) Detail from the upper part in figure a. (Lens cap as scale). d) Same photo as c., with slickenlines have been marked with green lines. e) Stereoplot projection displaying strike and dip measurements (n=3) taken on the fault plane of the thrust fault.

Locality Ic. Limovnstangen

The locality is located in the middle section on the western shoreline of Limovnstangen (Figure 6.4c) (map sheet 1815 III Hønefoss, UTM 692 586). An approximately 5 m high and 15 m long vertical cliff represents the locality. The exposed sedimentary sequence comprises the uppermost part of the Sælabonn Formation (Figure 6.13).

Structurally, the locality is situated in the hinge zone of the Limovnstangen anticline (Figure 6.11b and Figure 6.13) and is dominated by contractional deformational structures.

Figure 6.25 displays the deformed section at Limovnstangen. The locality is characterized by a lower main fault (denoted Fault 1) that cuts the bedding up-section towards the SE. Up-section a second fault (denoted Fault 2) with reverse displacement was identified, with the fault line cutting up-section towards NW in the cliff. Fault 2 splits in two faults, one low angle (2b) and one high angle (2a). Associated with Fault 2 is fault-propagation-folding, which is displayed in the up-section of Fault 2, similar to the structure described at the Borgenvika locality.

Figure 6.24 display three stereoplot projections illustrating strike and dip measurements from the Limovnstangen locality. In the northwestern part of the locality the bedding planes strike NNW-SSE (average N344E), dips range between 09°-16°, averaging 13° towards ENE. Beds in the central part of the locality display an average strike towards N303E. The dip ranges between 06°-24°, averaging 14° towards NNE. On the southeastern side of the locality the strike of the bedding shifts towards NNE-SSW (averaging N012E), with a mean dip of 14° towards ESE. Minimum and maximum dips measured are 07° and 18°.

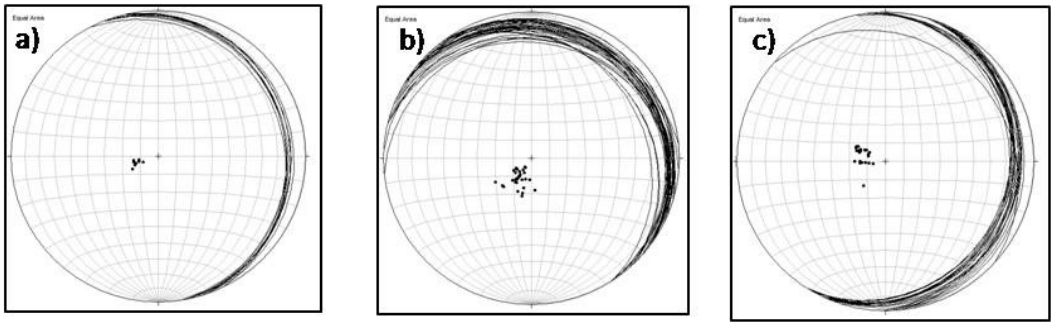

Figure 6.24: a) Stereoplot displaying strike and dip measured (n=9) on bedding planes in the northern part of the locality. b) Strike and dip on bedding planes (n=32) situated in the middle part. c) Strike and dip on bedding planes (n=22) in the southern part of the locality.

Fault-propagation-folds

The fault-propagation-folds are open and asymmetrically S-shaped monocline. The folds first appear at the point in the cliff where the fault trace of Fault 2 is getting steeper. This corresponds to the point where Fault 2b branches out from Fault 2.

Folds 1 and 2 are separate sandstone layers within this sequence and are open folds with horizontal to shallowly plunging to the east fold axes (Figure 6.25c). Fold 1 is situated up-section of Fold 2. Two axial planes on Fold 2 were measured and both strike ENE-WSW. The axial plane in the trough display a dip of 34° towards SSE, whilst the axial plane at the crest dips 60° towards SSE (Figure 6.25d). This is in contrast to the measured fold axes and indicates an error.

Fold 3 affects an isolated sandstone layer about three meters down-section to the NW in the cliff in relation to the fault-propagation-folds (Figure 6.26). The fold is associated with a small reverse fault (Fault 3), which nucleates a few cm below the folded bedding, then cutting the bedding up-section. The fold is asymmetric and open with wavelength and amplitude on the cm scale. The fold axis trend N060E, plunging 08° towards ENE (Figure 6.25c). The axial plane displayed a strike towards N058E (ENE) and dip of 80° towards SSE.

Fold nr.	Trend	Plunge
Fold 1	093	02
Fold 2 (trough)	090	07
Fold 2 (crest)	087	10
Fold 3	060	08

Table 2: Trend and plunge of fold axes at Limovnstangen.

Faults

Four faults denoted Fault 1, 2, 2b and 3 were identified at the Limovnstangen locality (Figure 6.25).

The fault trace of Fault 1 displays a planar geometry and from ground level towards SE, the fault cut up-section for approximately 4 m where it dies out. Five strike and dip measurements were obtained on the fault plane. The average strike of the fault plane is N283E, with an average dip of 21° towards NNE (Figure 6.25e). Groove lineations on a sandstone surface were observed on the footwall fault plane situated on top of a sandstone bed up-section. A trend towards N358E and plunge of 20° were measured (Figure 6.27). The fault line is parallel with the footwall bedding, whilst the hanging wall bedding is cut by the fault. Additionally, the angle of the fault suggests that Fault 1 is a reverse fault. The amount of displacement across the fault was not possible to measure. The strike and dip of the fault plane as well as the groove lineations indicate a transport direction towards S.

Fault 2 cuts up-section towards northwest from where Fault 1 dies out in the southeastern part of the cliff (Figure 6.25). Fault 2 displays listric geometry and reverse displacement. Down section the bedding is cut and displaced by the fault, but the displacement is difficult to measure accurately, but is in the order of cm. Up-section the fault dies out and the bedding across the fault line are not displaced, only folded. Three measurements on the fault plane

were obtained and gave an average strike of N061E, dipping in the direction of SSE. The dip of the fault plane was measured to 20° down-section and 62° up-section displaying a transport direction towards NNW. It was not possible to infer whether or not Fault 1 and Fault 2 cut each other, but Fault 2 flattens out towards SSE and appears to die out above or along Fault 1.

Fault 2b (Figure 6.25) is a low angle fault with reverse displacement which branches out from Fault 2 and can be traced up-section towards NW. The fault can be seen to cut and displace the sandstone bed comprising Fold 2 just beneath the trough of the fold. The amount of offset is estimated to be in the order of 10 cm.

Two strike and dip measurements of the fault plane were obtained. Down-section a strike of N359E and dip of 10° towards E was measured, whilst about 20 cm up-section a strike of N022E and dip of 06° towards ESE was measured (Figure 6.25g).

Fault 3 (Figure 6.25) is situated in the footwall of Fault 2b and is exposed over a distance of about one meter, displaying planar geometry. The fault is associated with Fold 3 (Figure 6.26), where the fault appears to nucleate a few cm beneath the folded bed. The fault displays reverse displacement, cutting the folded sandstone bed, displaying a displacement of approximately 1 cm. The fault line of Fault 3 is oriented approximately parallel to the fault line of Fault 2. Two strike and dip measurements, one down-section and one up-section, were taken on the fault plane giving an average strike of N023E, and average dip of 29° towards ESE.

Approximately 10 m towards the SSE, along the shoreline, the continuation of the cliff or the "back side" of it could be observed. Neither of the faults described above could be observed at this location, suggesting that Fault 1 has continued up-section with a steeper dip or that it has died out.

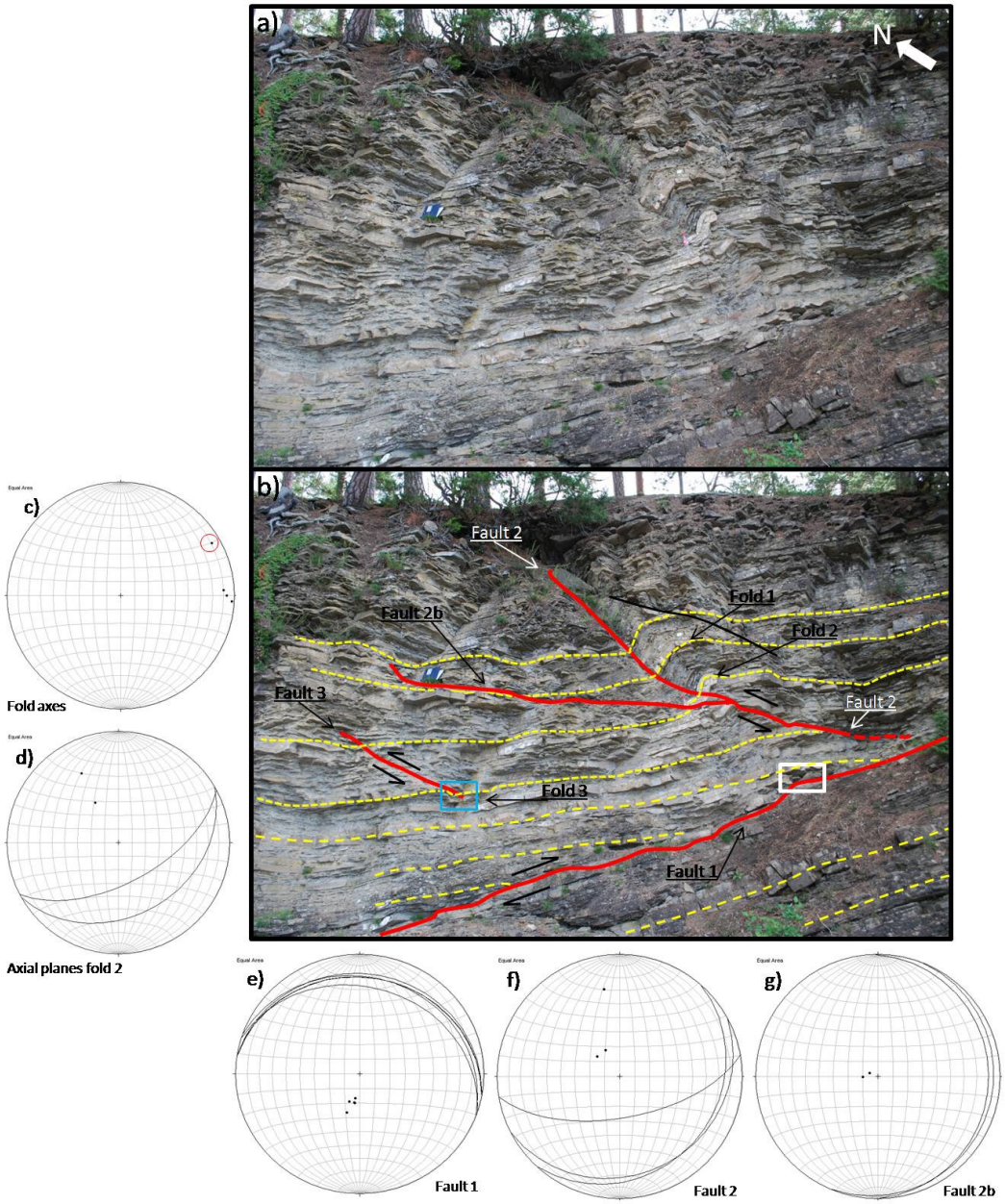

Figure 6.25: a) Section of the cliff at Limovnstangen (Logbook as scale). b) Same photo as in a. with faults and folds marked. Faults are marked with red lines, bedding with stippled yellow lines and a fracture with a black line. c) Fold axes (n=4) from the three folds. Fold axis of Fold 3 is marked with a red circle. d) Two axial planes on Fold 2. e) Stereoplot projection displaying the orientation of Fault 1 based on strike and dip measurements (n=5) of the fault plane. f) Orientation of Fault 2 (n=3) g) Orientation Fault 2b (n=2). Detail photos from the areas within the blue and white square can be seen in Figure 6.26 and Figure 6.27, respectively.

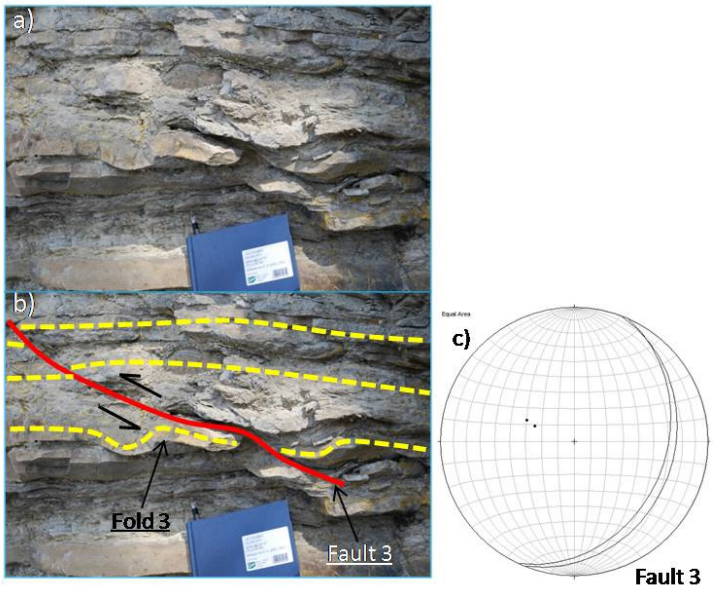

Figure 6.26: a) Detail photo of Fold 3 and Fault 3. b) Same photo as a. Fault 3 is marked with a red line, whilst bedding is marked with yellow lines. c) Stereoplot projection of strike and dip measurements (n=2) obtained on the fault plane of Fault 3.

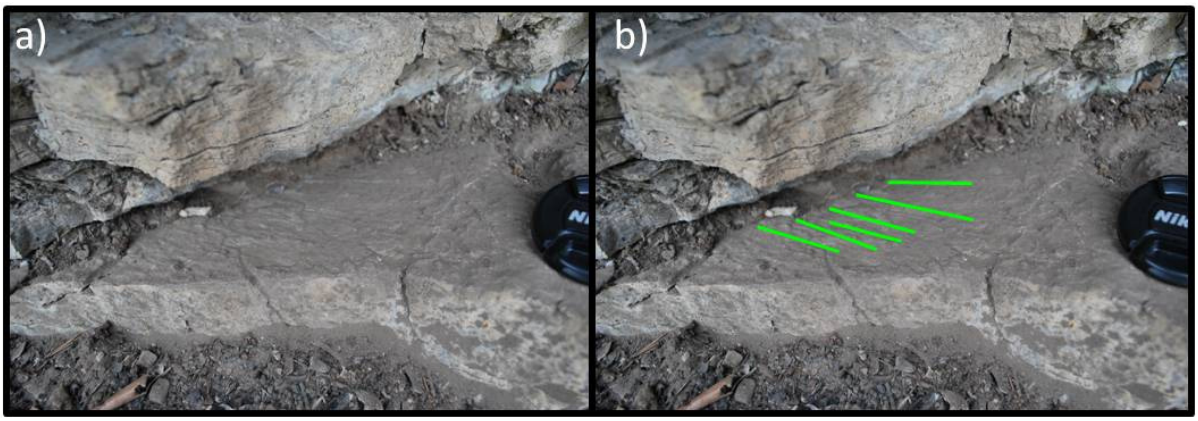

Figure 6.27: a) Detail from a part of the fault plane of Fault 1 with groove lineations. From the area within the white square in Figure 6.25b (Lens cap as scale). b) Same photo with the groove lineations marked with green lines with an orientation of N358E, plunging 20° towards N.

Summary

The main fault (Fault 1) is a low angle planar, reverse fault, displaying an approximate direction of transport towards S(SW). Three other contractional faults (2, 2b and 3) were identified, all of them displaying a contrasting direction of transport compared to Fault 1. Of these, Fault 2 is the most pronounced, displaying a listric fault trace indicating a transport direction towards NNW. Associated with Fault 2 is the development of fault-propagation-folds, which display shallowly plunging fold axes trending towards E. The axial planes measured display dips towards SSE, which indicating a transport direction towards N(NW) and represents an error in the measurements. However, both are fairly consistent with Fault 2. Fold 3 developed prior to Fault 3, which cuts and displaces the folded bedding planes.

6.2.2 Subarea II

Subarea II encompasses the islet Evangelieholmen (map sheet 1815 III Hønefoss, UTM 693 610). This section of the study area is defined as a separate subarea due to a structural style not present elsewhere in the study area.

Strike and dip measurements of bedding planes situated to the north-northeast and northeast of Evangelieholmen were obtained from the northeastern Sælabonn (map sheet 1815 III Hønefoss, UTM 695 613) and Kjelleberget (map sheet 1815 III Hønefoss, UTM 698 615). Northeastern Sælabonn displays an average strike of N043E and an average dip of 15° towards SE. At Kjelleberget an average strike of N040E and average dip of 23° towards the SE were obtained (Figure 6.28a).

Measurements of bedding planes obtained from Rolighet (map sheet 1815 III Hønefoss, UTM 694 608), which is situated approximately 100-120 m south-southeast of Evangelieholmen (Figure 6.11a), exhibit an average strike of N287E, with an average dip of 23° towards NNE (Figure 6.28b).

At Pålerud (map sheet 1815 III Hønefoss, UTM 695 611) E-ENE of Evangelieholmen, bedding planes display contrasting strike and dip. The majority of the bedding planes measured display an average strike of N282E (ranging between ENE-WSW and N-S), with an average dip of 24° towards NNE (ranging between 04°-46°). However, bedding planes with an average strike of N047E (ranging between NNE-SSW and ENE-WSW) and average dip of 52° towards SE (ranging between 28° -72°) were also documented (Figure 6.28c).

These measurements indicate that Evangelieholmen is situated in a syncline. The calculated fold axis (π-axis) displays a trend of N061E and a plunge of 12° towards ENE (Figure 6.28d). However, there were few measurements obtained from the area north and northeast of Evangelieholmen. The northern part of Sælabonn exhibits mostly of low relief terrain with few exposed rocks.

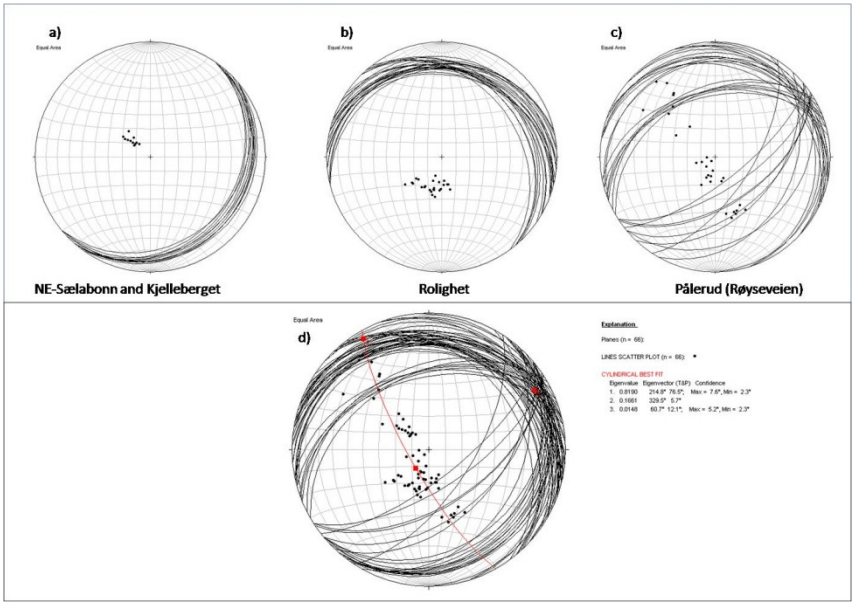

Figure 6.28: a) Stereoplot projection of strike and dip measurements of bedding planes obtained from northeastern Sælabonn and Kjelleberget (n=11). b) Strike and dip measurements of bedding planes situated at Rolighet (n=26). c) Strike and dip of bedding planes (n=29) measured around Pålerud d) Data from a, b and c plotted together (n=66). Calculated π-axis gives a trend of N061E and a plunge of 12° towards ENE.

Locality Evangelieholmen

The islet is for the most part covered with vegetation, except for the western and southern sides which are exposed. Evangelieholmen is located in the northeastern part of Sælabonn and is 60-70 m in length from north to south and about the same from east to west. On its highest point Evangelieholmen is approximately 10 m and is connected to Pålerud to the east by a thin strip of land. The western side displays a near vertical cliff, whilst the southern side is more accessible (Figure 6.29a).

Evangelieholmen is characterized by contractional deformation, both ductile and brittle in the form of upright folds, low-angle thrusts and high-angle reverse faults. The different structural elements are described below.

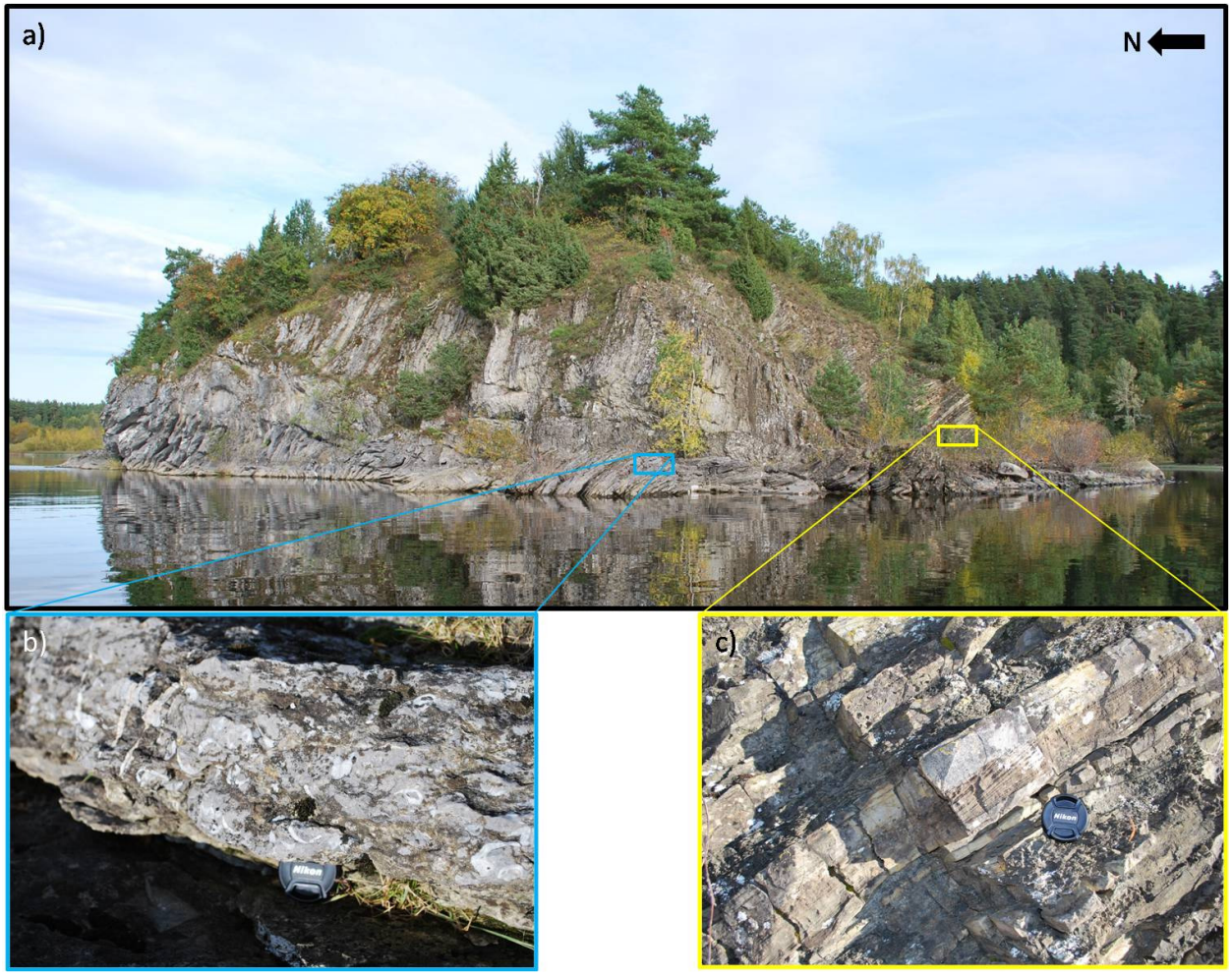

Figure 6.29: a) Photo of Evangelieholmen. b) Photo of pentamerids within a limestone bed of the Rytteråker Formation (Lens cap as scale). c) Sandstone and shale beds comprising the Sælabonn Formation (Lens cap as scale).

The rocks on Evangelieholmen comprise the Sælabonn- and Rytteråker formations. Most dominant is the Rytteråker Formation, whilst the Sælabonn Formation is present only on the southern side (Figure 6.29c). On the lower southwestern side, pentamerids limestone of the Rytteråker Formation can be observed (Figure 6.29b). Towards north the limestone becomes more massive, displaying a bluish coloration and the differentiation between bedding planes is more difficult. This represents a higher stratigraphic level within the Rytteråker Formation.

Folds

A total of 32 fold axes were measured and they display an average trend towards N058E, ranging between N035E and N086E, with a mean plunge of 14°, ranging between 08° and 24° (Figure 6.30).

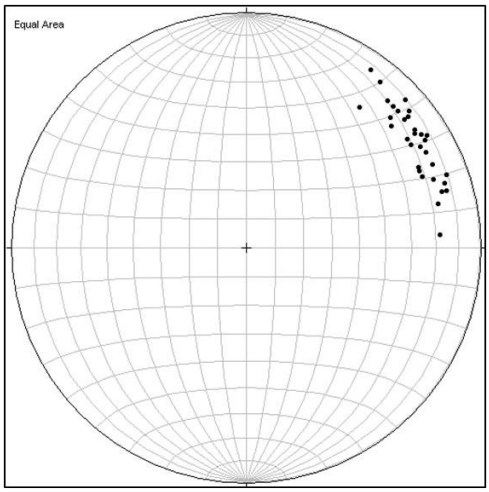

Figure 6.30: Stereoplot projection of fold axes (n=32) measured at Evangelieholmen.

Fold population 1.

In the cliff on the southwestern side of Evangelieholmen the strata comprises thin, 2-5 cm thick alternating limestone and siltstone beds. Fold population 1 was identified on the basis of the folds displaying tight to isoclinal fold limbs and upright axial planes (Figure 6.31b and c).

Fold 1 is a disharmonic anticline fold with an upright axial surface dipping steeply towards SSE. The wavelength can be estimated to be around 2 m. The amplitude of fold was difficult to determine due to erosion, but the exposed part displays a fold height of about 3 m. Due to erosion and faulting of the southern fold limb the geometry of the southern limb is difficult to deduce. The northern limb is well exposed and the hinge zone can be seen in the

uppermost section and the axial plane appears upright. In the lower core the folds are isoclinal also with upright axial planes.

The average trend of the fold axes measured in the fold is N059E, with an average plunge of 16° towards ENE. Individual bedding planes within the fold display gentle folding, which will be described later. Two bedding plane measurements were taken on the northern-fold limb and it gave an average strike of N256E. Both measurements recorded a dip of 46° towards NNW.

Bedding planes in the lower part of the southern-limb of Fold 1 is cut by a steep angle fault, denoted Fault G. Two measurements were performed on the fault plane which gave the following strike and dip: N044E, dipping 72° towards SE and N050E, dipping 84° towards the SE. Up-section the fault line is less clear, but it appears to cut the SSE-limb of Fold 1 in the uppermost part of the cliff as well.

Whether or not the bedding planes of FolD1 continue into a new fold to the SSE is difficult to determine with certainty due to the presence of Fault G and erosion. Additionally, the orientations of the bedding planes up-section indicate the presence of a synform with a wavelength of about 30-40 cm south-southeast of Fold 1 (Figure 6.31d).

The bedding is tightly compressed with bedding comprising what appears to be the northern limb of the neighboring fold (described later). Bedding planes to the south-southeast of Fold 1 and Fault G, display steep dips averaging 77° dipping towards NW and (S)SE. The contrasting dips are attributed to gentle folding of the bedding (described later). Bedding planes down section in the SSE-limb of Fold 1 are bordered by two faults, forming a triangular zone. Here the beds flatten out, displaying an average strike of N046E and mean dip of 37° towards SE, based on two measurements.

Parasitic folds

Fold 1b is a parasitic anticline fold with shallowly NE-plunging fold axis situated in the northern limb of Fold 1. The trend of the fold axis was measured to N050E, plunging 10° towards NE. Fold 1b is also a disharmonic fold with an upright axial surface, which displays a listric shape, with an approximate fold width of 30 cm and fold height of 15cm. Due to vegetation, beds higher up in the cliff are concealed.

On the south side of Fold 1the bedding is in general characterized by steep dips and gentle folding which is especially evident on the southern side of the islet (Figure 6.32). The folds are asymmetric and open, displaying fold axes with trends ranging between NE-ENE, with an average trend of N050E and average plunge of 15°. A wavelength of about 10-20 cm and approximate amplitudes in the order 1-3 cm characterize the folds. The axial planes were not measured, but from photographs, it can be seen that these are inclined dipping towards the NW. Due to the increase of the age of the strata towards the south on the islet, these folds display a vergence towards (N)NW. The folds in Figure 6.32 are assumed to be parasitic folds situated on the northern-fold limb of a larger anticline fold (described later), which may also form the southern-limb of the neighboring syncline. However, due to faults and erosion it is not possible to work out the precise geometry.

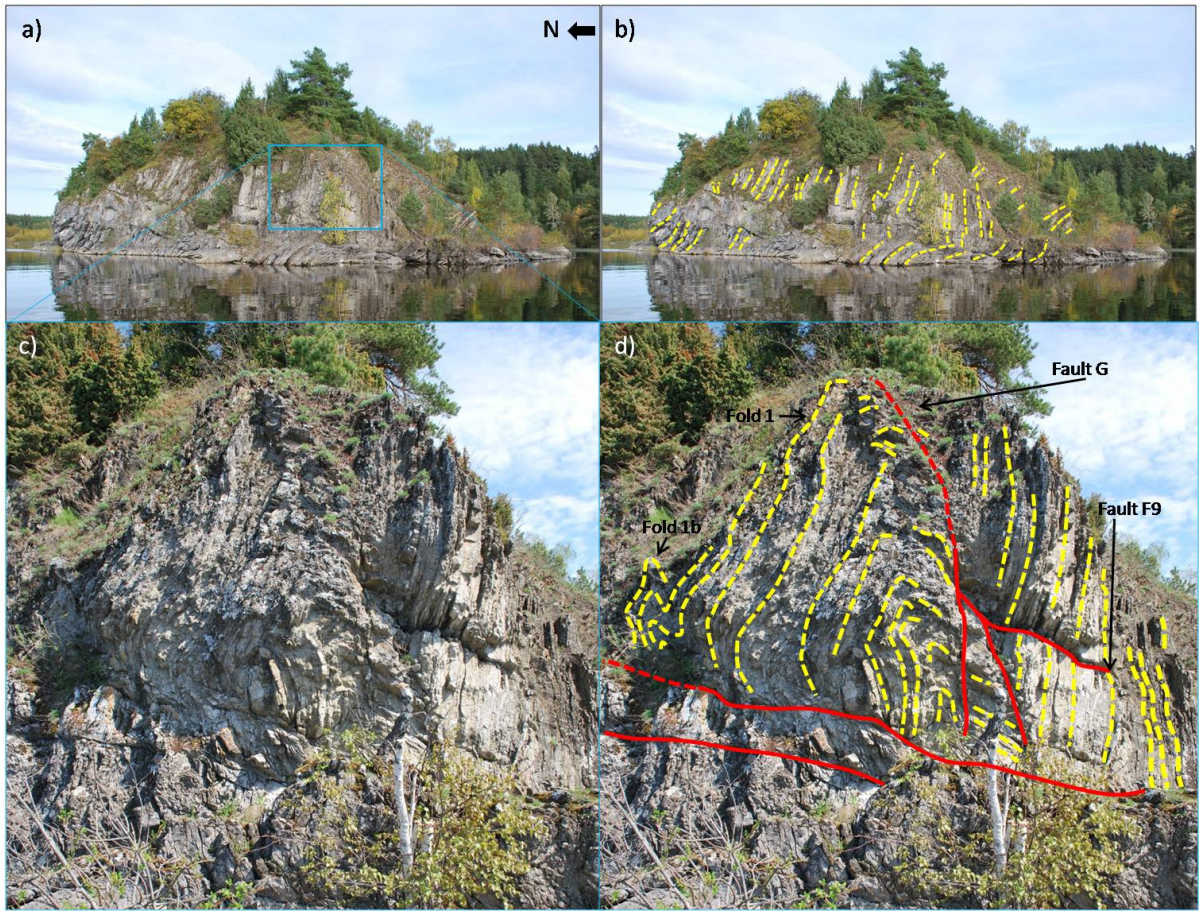

Figure 6.31: a) Overview photo of Evangelieholmen. b) Same photo as in a. Bedding planes are marked with yellow lines. c) Detail of upright folds on the southwestern side of Evangelieholmen. The height from ground up is approximately 3 m. d) Same photo as in c. with bedding planes marked with yellow stippled lines. Fault lines are marked with red lines. Stippled red line represents extrapolation of the fault line.

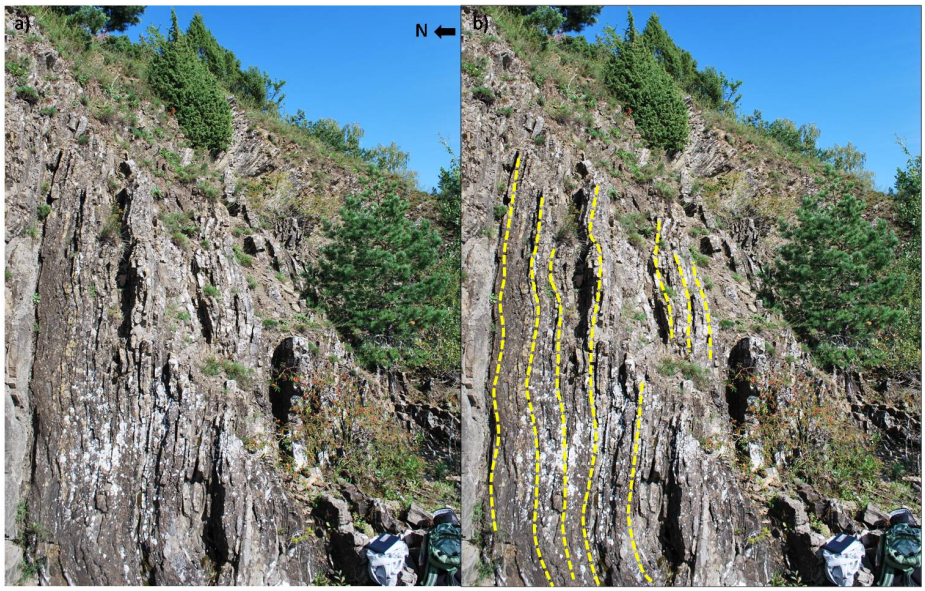

Figure 6.32: a) Photo of the southern side of Evangelieholmen (Logbook as scale). b) Same photo as a. Yellow stippled lines marks bedding planes.

Western side of Evangelieholmen

Bedding planes situated north of the folds described above display steep dips (Figure 6.33). In the upper middle part of the western cliff the beds exhibits the same overall strike and dip as the beds associated with folding. The bedding planes strike mainly ENE-WSW to NE-SW, dipping towards NW-NNW. However, in the middle section, steep dipping beds (up to 84°) towards SE were documented. Bedding planes situated in the lower northwestern side of Evangelieholmen display more gentle dips, with an average dip of 47° towards NW. Due to vegetation cover and erosion it is not possible to infer whether the beds are part of larger folds, similar to Fold 1, or just tilted.

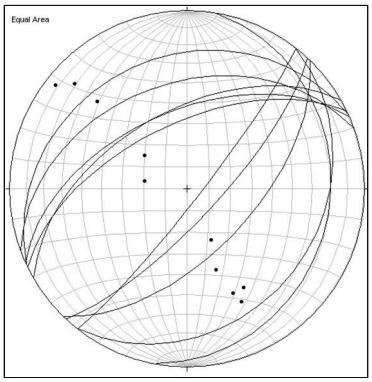

Figure 6.33: Strike and dip of bedding planes (n=10) on the northwestern side of Evangelieholmen.

Southwest side of Evangelieholmen

Bedding planes on the lowermost southwest side of Evangelieholmen display much less intense deformation compared to the upright folds (Figure 6.31b). The beds strike NE-SW to E-W dipping towards NE and N performing in a gentle anticline-syncline pair. In the northern section the beds dip about 42°-45° towards the NE before flattening out in the middle section where the beds are almost horizontal, dipping 08°-10° towards N. Towards the south the beds become steeper, striking NE-SW, with a measured dip of 60° towards NW on the southernmost side.

Thrust faults (Fault population 1)

Low-angle thrust faults are a dominant feature on the western side of Evangelieholmen. All the fault lines cut up-section towards NNE, with fault F5-F7 obtaining the steepest gradient in the order of 20° (Figure 6.36b). The fault lines of faults F1-F4 lie sub-parallel to each other. All the faults cut the tilted and folded limestone bedding of the Rytteråker Formation. A detailed photo of faults F1-F4 is displayed in Figure 6.37.

Fault F1

Fault F1 is the best exposed fault plane on the southwestern side of the islet. The average strike (Figure 6.36f) of the fault plane is N354E, with a mean dip of 19° towards E, ranging between 4°-30°. The fault trace can be followed along the western cliff, where it cuts Fold 1, farther towards north towards a bush where it appears to die out.

Cylindrical drag folds are present in the hanging wall of fault F1 on the southwestern side of the islet, displaying the relative reverse movement across the fault as indicated in Figure 6.37e. These are fault-related folds. The drag folds in the hanging wall are convex towards NW-NNW. The drag folds obtain shallowly plunging fold axes towards NE-ENE. In the same location a set of N111E trending slickenlines were identified on the fault plane. These displayed a plunge of 06° towards ESE, which indicate a WNW (N291E) directed transport across the fault plane. This correlates well with the strike and dip of the fault plane.

On the southwest side the pentamerid limestone of the Rytteråker Formation is visible (Figure 6.29b). In the footwall of fault F1, limestone beds of the Rytteråker Formation are evident. These appear to be mostly composed of pure limestone. In the hanging wall of fault F1 the gradual transition between the Rytteråker and the Sælabonn formations was identified based on the increasing amount of sandstone beds. This shows that the displacement across fault F1 must have been several meters.

Fault F2

Two measurements were obtained from the fault plane of fault F2 which gave an average strike of N033E and a mean dip of 9° towards ESE-SE (Figure 6.36e). Fault F2 becomes concealed down-section beneath Fold 1 towards the southern part of Evangelieholmen. To the north a fault lens approximately 1 m long and 10 cm thick, consisting of several smaller horses, forming a duplex, was documented (Figure 6.37c). Two measurements were taken on the thrust faults defining the horses. These exhibits an ENE-WSW oriented strike (N058E and N066E) and dip towards SSE (34° and 44°, respectively).

Approximately two meters to the north, the fault disappears behind vegetation. Above the lens, in the hanging wall of the fault, bedding planes display drag folds which show the relative reverse movement across the fault, similar to that of fault F1.

Fault F3

An average strike of N030E and a mean dip of 21° towards ESE were attained from four strike and dip measurements (Figure 6.36d). Fault 3 is exposed over the same distance as fault F2, but do not display lenses. The fault trace cuts the tilted and folded limestone beds and the beds are displaced approximately 10 cm with the same relative movement as fault F1 and F2. Fault F2 and F3 approach each other both towards the north and to the south, possibly forming a lens.

Fault F4

Based on four measurements, an average strike of N011E and dips ranging between 14°-22°, averaging 18° towards E-ESE were recorded (Figure 6.36c). The average strike is influenced by one measurement which exhibits a strike of N296E, dipping 22° towards NNE. This is in contrast to the three other measurements which alone obtain an average strike of N036E, with an average dip of 17° towards SE. Fault 4 splits and develops a lens, approximately 1 m in length and a maximum vertical thickness of approximately 20 cm. Within the lens, two smaller, high-angle thrust faults, forming a duplex structure, similar to the one mentioned in

the description of Fault F2. A strike of N046E and dip of 62° towards SE was measured on a fault bordering the southernmost horse.

Fault F5

One measurement was obtained from the fault plane of Fault F5, which gave a strike of N030E and a dip of 36° towards ESE (Figure 6.36c). The fault trace travels up-section for about 3 m from ground level, where it dies out or becomes concealed due to weathering and erosion.

Fault F6

The strike of the F6 fault plane was measured to N029E with a dip of 19° towards ESE based on one measurement. The fault trace lies parallel to the underlying Fault F5 and can be followed from the centre to the top of the islet on the northwestern side.

Fault F7

No measurements were taken of the F7 fault, due to inaccessibility and poor exposure of the fault plane. The fault trace propagates parallel, approximately half a meter above Fault F6 and can be observed over the same distance (Figure 6.36b).

Faults F2, F3 and F4 could not be correlated with faults F5, F6 and F7 with certainty due to vegetation and as mentioned poor exposure in the central upper part of the cliff. However, it is possible that the latter faults are a continuation of the former.

Fault F8

On the north-westernmost side of Evangelieholmen the bedding planes (Rytteråker Formation) are almost horizontal, displaying an average strike of N349E and average dip of 6° towards ENE-E on this surface. Two-three meters to the south there is an abrupt change in the strike and dip of the bedding planes. Here the beds strike ENE-WSW, dipping approximately 50° towards NNW (Figure 6.34).

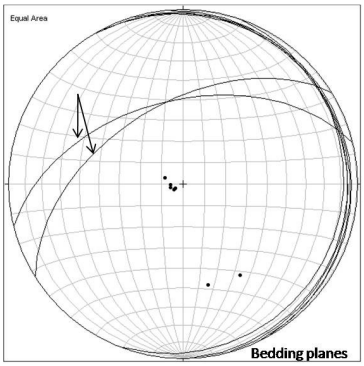

Figure 6.34: Stereoplot displaying the orientation of bedding planes (n=7) situated on the NW-side of Evangelieholmen. The black arrows points to the measurements taken on the first occurring steep dipping bedding planes to the south of the flat lying beds on the northwest side of Evangelieholmen.

In connection to the change in strike and dip of the bedding planes on the northwest-side, a flat surface (denoted F8) was identified (Figure 6.36b), separating the steeply dipping beds from the more horizontal beds, indicating a possible fault plane. However, the lithology on the western and northwestern side of the islet display clear signs of weathering as well, which makes the determination more difficult. An average strike of N034E (NNE-NE) and a mean dip of 22° towards ESE-SE were obtained (Figure 6.35).

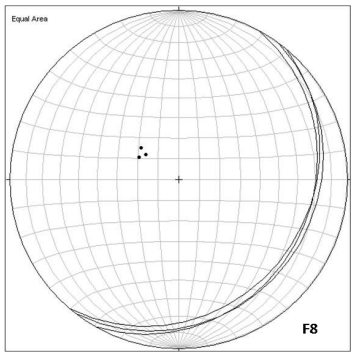

Figure 6.35: Stereoplot projection of measurements (n=4) obtained from the F8 fault plane surface.

Fault F9

Fault F9 is situated approximately 1,5 m up-section of Fault F1 on the southwestern side of Evangelieholmen (Figure 6.31d and Figure 6.37e). The fault is planar and cuts the steeply tilted limestone and siltstone beds of the Rytteråker Formation. The fault trace nucleates on the southwestern side and cannot be followed farther to the east in the cliff. To the north, the fault trace cuts Fold 1 and merges with Fault G (described above) after approximately 1,5 meters. Whether it terminates or propagates up-section as Fault G will be a matter of discussion. The fault displays a reverse displacement of 1-3 cm. Two measurements were taken on the fault plane, both displaying a N-S directed strike and dip towards E (N005E with a dip of 12° towards E and N353E with a dip of 20° towards E), which gives an average strike of N359E, and dip of 16° towards E.

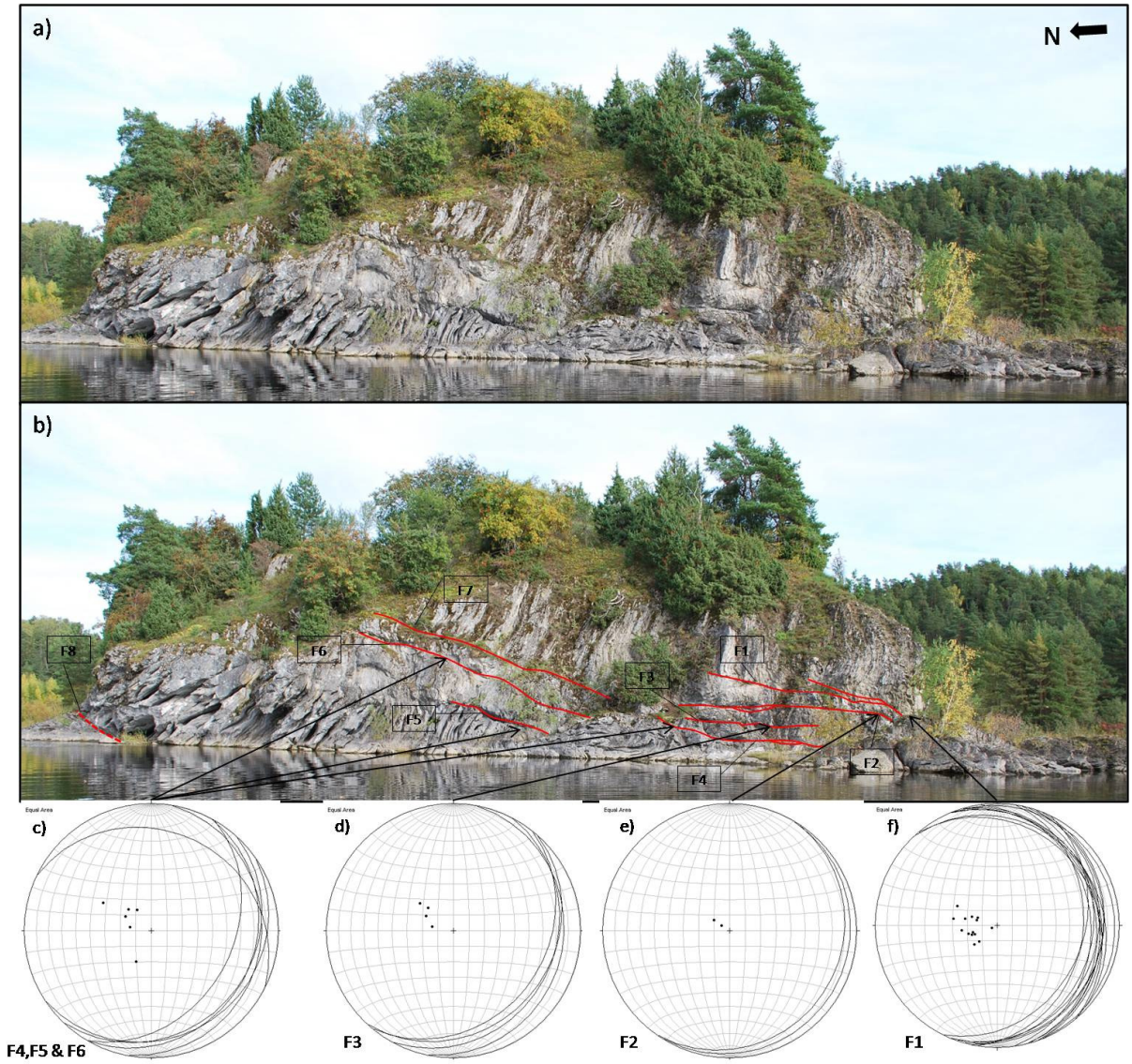

Figure 6.36: a) Photo of the western side of Evangelieholmen. b) Same photo as in a. Faults marked with red lines. c) Stereoplot projection of the Strike and dip measurements of fault planes F4 (n=4), F5 (n=1) and F6 (n=1). d) Strike and dip of fault plane F3 (n=4). e) Strike and dip measurements of fault plane F2 (n=2). f) Strike and dip measurements of fault plane F1 (n=14).

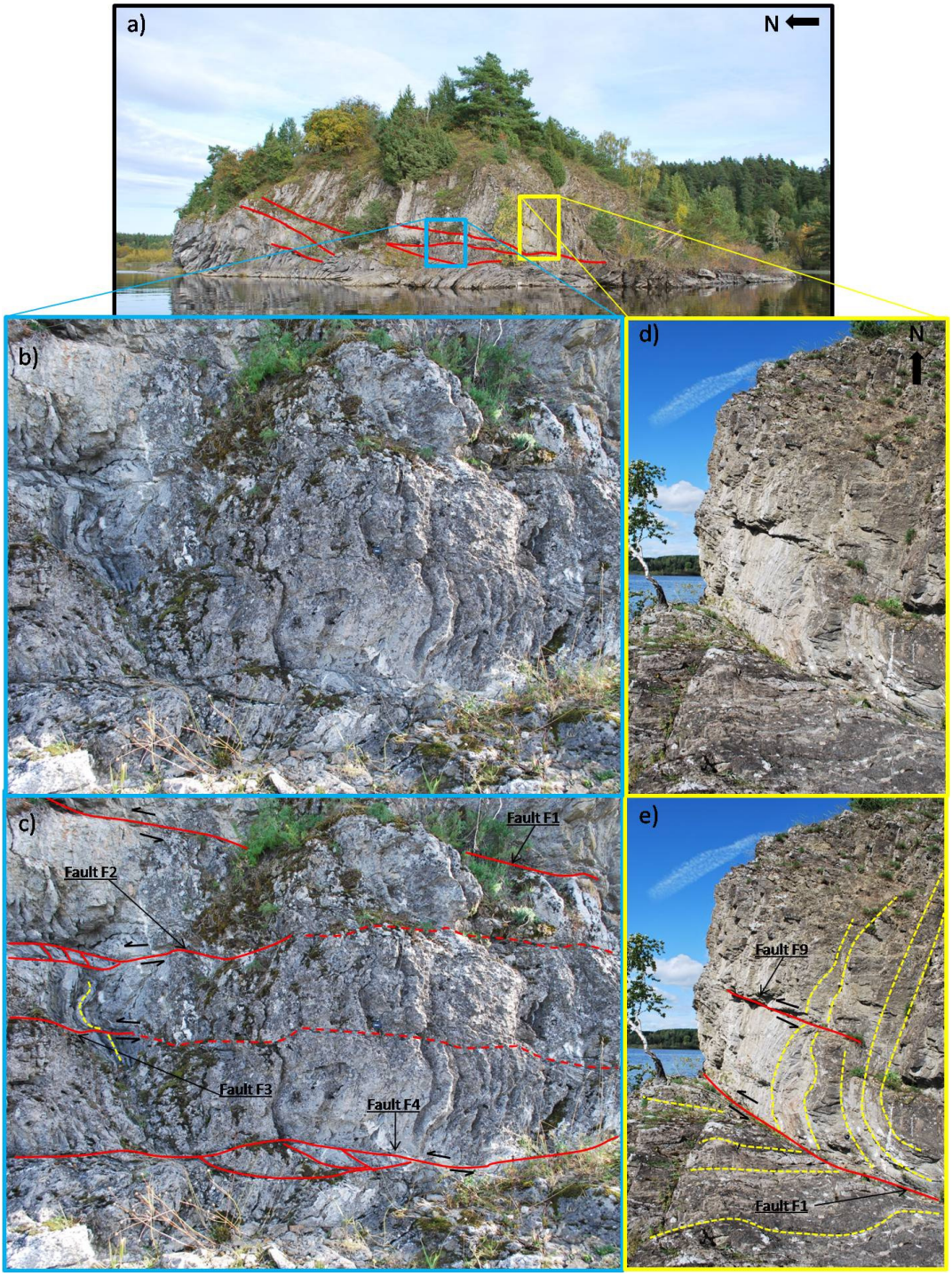

Figure 6.37: a) Overview photo of the west and south side of Evangelieholmen. Detail photos from the areas within the colored frames b) Detail photo of a section of tilted and faulted limestone beds of the Rytteråker Formation. c) Same photo as b. with faults F1, F2, F3 and F4 illustrated by red lines. d) Photo displaying steep and faulted alternating limestone and siltstone beds of the Rytteråker Formation on southwestern side of the islet. e) Same photo as d. with faults F1 and F9 marked with red lines.

Fault H1

On the southwestern side of Evangelieholmen a fault denoted H1, was identified (Figure 6.38a, b). Down-section the fault trace is planar with an approximate dip of 30°. Up-section the fault trace displays a steep, almost vertical dip. The fault plane was poorly exposed due to debris. Down-section two measurements were obtained. On a surface parallel to the fault plane, a strike of N026E and a dip of 28° towards ESE were obtained (Figure 6.38g). The second one was measured on a surface constituting the top of the footwall, appearing grinded by the fault movement displaying a strike of N015E, with a dip of 30° towards ESE. Up-section, two measurements with an average strike of N182E, and an average dip of 81° towards W were measured on a steep surface dividing the tilted bedding in the hanging wall from the steep, almost vertical beds on the southwestern side (Figure 6.38c and d). This might be an incorrectly interpreted fault plane surface, or it might be due to the fault dying out up-section.

Figure 6.39 displays the strike and dip of the bedding planes situated in the footwall and hanging wall of fault H1. Bedding planes comprising the footwall of Fault H1 dip for the most part towards NW, but also towards SE due to the beds being gently folded. Beds dipping towards NW display an average strike of N227E (SW) and average dip of 68°. Beds which dip towards SE display a mean strike of N051E (NE) with an average dip of 80°. Bedding planes situated in the hanging wall of fault H1display an average strike of N252E, with dips ranging between 26°-74° towards NNW.

The approximate border between the Rytteråker- and Sælabonn Formation has been marked in Figure 6.38b and is situated in the footwall of fault H1 on the south side of Evangelieholmen. There is a dominance of limestone towards north-northwest and sandstones towards south-southeast. Strata up-section in the hanging wall of fault H1 appears quite similar to those in the footwall. Down-section in the hanging wall the strata is dominated by sandstone beds, interbedded with shale belonging to the Sælabonn Formation. Footwall beds terminating against the fault line indicate a drag up-section.

South side of Evangelieholmen

The overall geometry of the south side of Evangelieholmen is that of an asymmetrical open, anticline with a with a steep, almost vertical NNW limb and a less steep SSE-limb also dipping towards NNW. The fold axis trends approximately NE-ENE with an inclined axial plane dipping ca 50° towards SSE.

Folded sandstone beds were documented down-section in the footwall of fault H1, about half a meter from the fault trace. The fold comprises two sandstone beds. Only the top of hinge zone of the fold was observed, but it appeared tight. Two fold axes were measured, displaying a trend of N039E, plunging 10° towards NE of the uppermost fold and a trend of N035E, plunging 08° towards NE was measured on the lowermost fold.

Down-section at ground level, in the hanging wall of fault H1, S-shaped folds can be observed (Figure 6.38e and f). Up-section only the upper crests of the S-shaped folds are visible, forming apparent drag folds. However, the S-shape indicates that these are not drag folds, at least not down-section (Figure 6.40a). The folds are open and display shallowly plunging ENE-trending fold axes, displaying an average trend of N072E, with a mean plunge of 14° and gently inclined axial planes dipping towards SSE. Down-section the wavelengths of the S-shaped folds are in the order of 20 cm with amplitudes of about 5-10 cm.

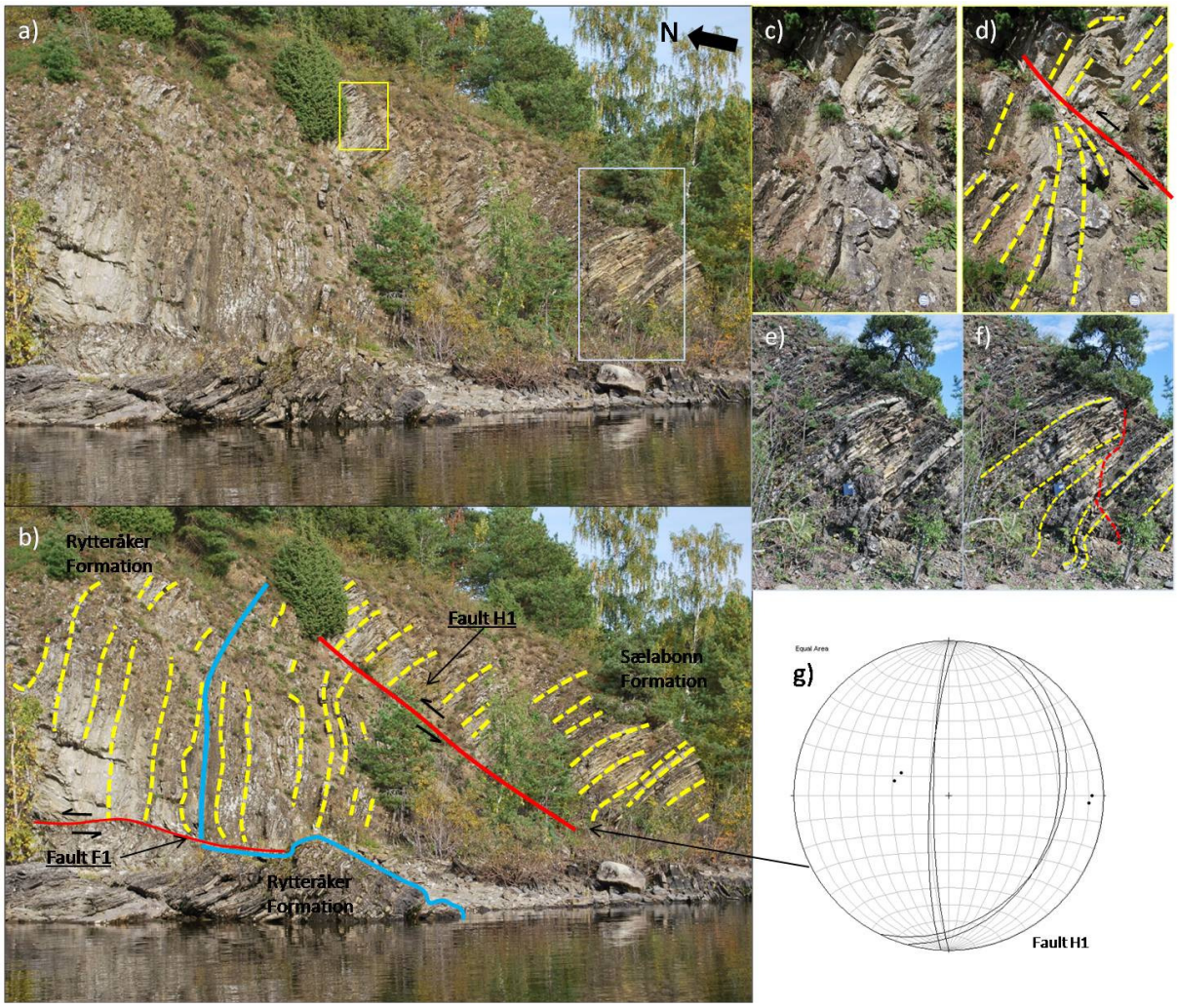

Figure 6.38: a) South side of Evangelieholmen. b) Same photo as a. with bedding marked with yellow lines. Faults F1 and H1 are marked with red lines. The vertical blue line marks the border between the Rytteråker- and Sælabonn Formations, where on the northern side limestone beds are dominant, whilst on the south side, sandstone beds are dominant. The horizontal blue line illustrates that the Rytteråker Formation is situated below Fault F1. c) Detail photo from the area enclosed in the yellow square in photo a. (Lens cap as scale). d) Same photo as c. but with bedding marked with yellow lines. e) Photo of southern tip of the islet, enclosed in the blue square in photo a. (Logbook as scale). f) Same photo as e. Bedding is marked by yellow lines. The red line marks a line where the bedding does not correlate across. g) Stereoplot projection of strike and dip measurements (n=4) taken on the fault plane of fault H1.

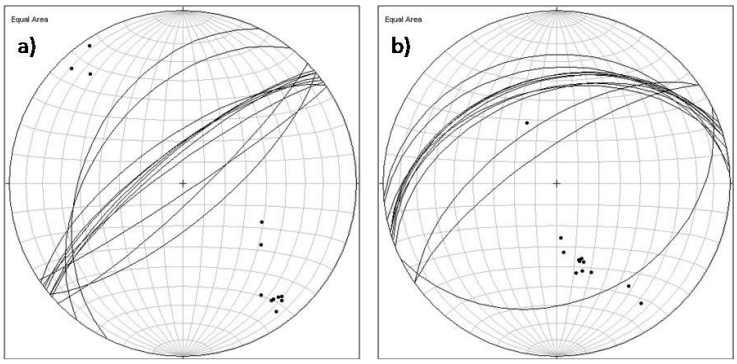

Figure 6.39: a) Bedding planes (n=12) constituting the footwall of fault H1. b) Bedding planes (n=13) situated in the hanging wall of fault H1.

Figure 6.40 displays two sketches of Evangelieholmen. Here the tight- to isoclinal folds and the extensive thrust faults are evident.

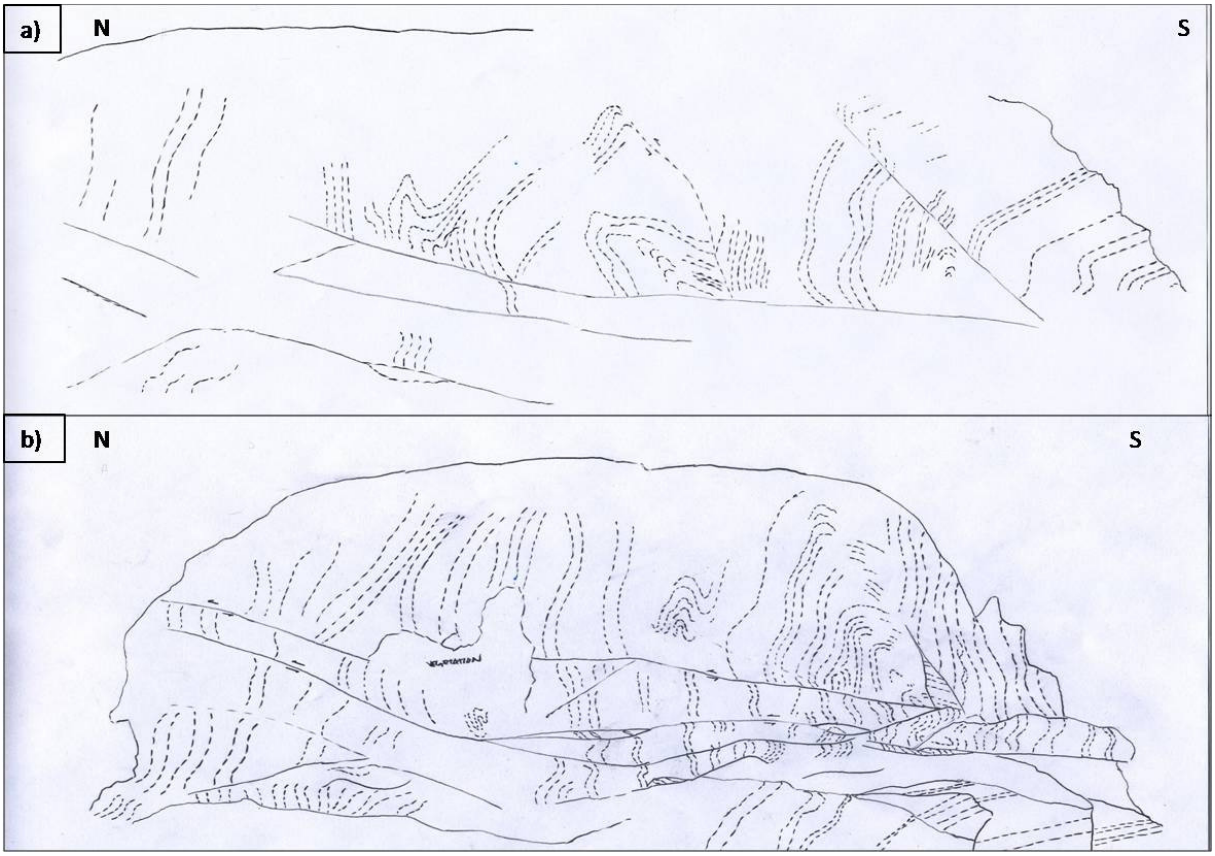

Figure 6.40: a) Sketch of the southwestern part of Evangelieholmen. b) Sketch of the middle section of Evangelieholmen.

Structures associated with bedding parallel shortening

A set of low-angle thrust faults associated with bedding-parallel shortening were also identified at Evangelieholmen. Similar to Borgenvika, associated folds will be described together. The faults and folds are denoted fault and fold populations 2. Population 2 has been subdivided into two groups owing to structural differences described below.

Fold and fault population 2a

Figure 6.41a displays the western and southwestern side of Evangelieholmen. Figure 6.41b comprises a detail photo of steep dipping and folded limestone beds of the Rytteråker Formation. Two folds (A and B) have been marked in the figure. These folds form an antiform-synform pair. The folds are open, symmetric folds with gently inclined axial planes obtained from the photo. The axial planes were measured, giving an N-S strike, indicating that a mistake was done obtaining these measurements. The folded bedding is limited up-section by fault F2 and down-section by fault F3 (described above). Fold A has a wavelength of about 15 cm and amplitude of 4-5 cm with a fold axis trending N062E and plunging 14° towards ENE. Fold B displays a shorter wavelength and a fold axis trending N051E, plunging 14° towards NE. The movement along the fault planes of thrust Fault 2 and 3 appears to have dragged the bedding and increased the curvature of the fold.

In connection to fold population 2a a contractional fault cutting the folded bed was observed. In Figure 6.41c a steep angle fault, can be seen to cut the limestone bed nearly parallel to the bedding plane. The thrust fault is only cutting the folded bed and cannot be traced up- or down-section into neighboring beds. The fault plane of Fault A strikes N244E and dip 70° towards NNW (Figure 6.41f). It was not possible to identify the orientation of the bedding in terms of base or top of the bedding plane. Therefore the direction of transport is not possible to infer.

Fold and Fault population 2b

Figure 6.41 d and e display another example of bedding-parallel shortening. Thin limestone beds exhibits asymmetric folds cut by thrust faults. The limestone beds are interbedded with thin siltstone beds. Faults B2 and B3 cut the same folded bed, where Fault B2 is situated in the footwall of fault B3. The structure seems to involve two neighboring limestone beds. Bedding planes situated between fault B2 and B3 display what appears to be tight folding, however, the exact geometry of the structure is difficult to elucidate. Fault B2 exhibits an offset of approximately 2 cm, whilst fault B3 displays a displacement across the fault of about 1 cm. The strike of the fault planes of B1-B3 ranges between NNE-SSW to ENE-WSW. Displaying steep dips towards NNW (B3), WNW (B2) and SE (B1) (Table 1). Additionally, what appears to be fault has been marked in Figure 6.41e. This might be a continuation of Fault B2, or a separate fault, but no measurements were taken. If this is a fault, then there are two separate directions of transport relative to the bedding plane. However, it is difficult to separate the different beds from each other. In chapter 7 (discussion), rotation of the data will be discussed in order to deduce the direction of transport prior to tilting.

Fault plane	**Strike**	**Dip**
Population 2a. Fault A	N244E	70
Population 2b. Fault B1	N053E	76
Population 2b. Fault B2	N206E	72
Population 2b. Fault B3	N245E	70

Table 3: Orientation of fault planes A, B1, B2 and B3.

In association with the fold population 2a and 2b described above, axial plane fractures were identified. The fractures are filled with a white material, presumably calcite, forming veins which are isolated to the bedding. In the bed comprising Fold A the veins dip approximately perpendicular to the bedding plane. The beds cut by faults B1-B3 also display fractures, but these do not dip perfectly orthogonal to the bedding plane. These fractures appear to be tensile fractures, probably formed during the folding of the beds. However, multiple sets of fractures were observed and this is beyond the scope of this thesis and will not be discussed further.

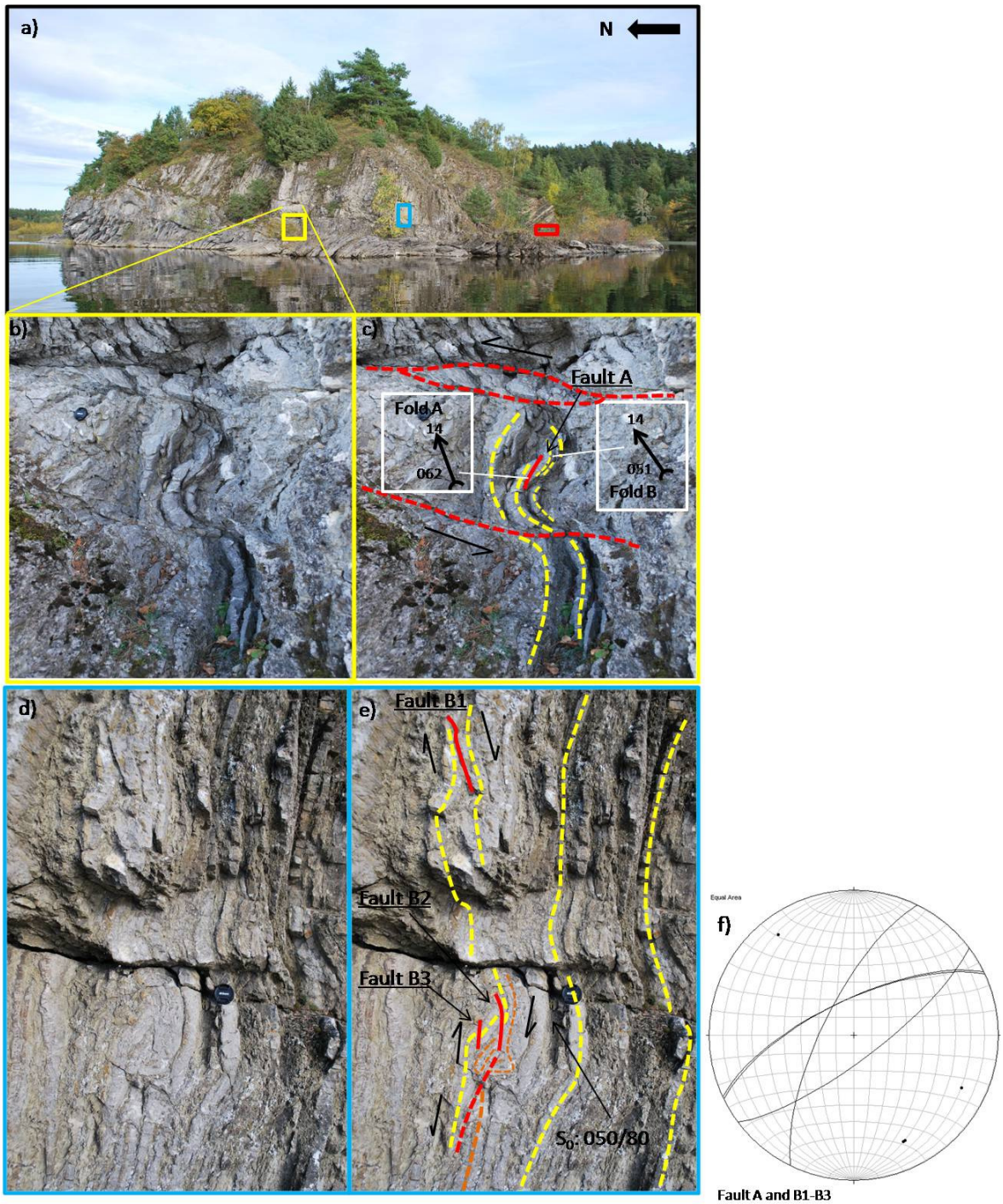

Figure 6.41: a) Overview photo of Evangelieholmen. Color of the squares is in concordance with the colors of the picture frames. Figure 6.42 displays the area enclosed in the red frame. b) Folded and faulted limestone bed belonging to fold and fault population 2a (Lens cap as scale). c) Same photo as in b, with yellow lines marking the bedding, whilst the red line marks the Fault A. Stippled red lines marks Fault 2 and 3. Trend and plunge of folds A and B are illustrated within the white frames. d) Folded and faulted limestone beds comprising fold and fault population 2b (Lens cap as scale). e) Same photo as in d., but with bedding marked with yellow and orange lines and faults with red lines. Stippled red line marks a possible fault f) Stereoplot projection displaying the orientation of faults A (n=1) and B1-B3 (n=3).

Fault population 3- Foreland-directed thrust fault

On the southernmost part of Evangelieholmen, comprising the Sælabonn Formation, an almost bedding parallel fault with reverse displacement of about 40 cm across the fault, here denoted Fault C was recognized (Figure 6.42a and b). Fault C is situated in the hanging wall of Fault H1 (described above). The fault plane display an average strike of N246E, obtained from three measurements, displaying a SSE-directed transport. The dip on the fault plane down-section is 52° towards NNW, with calcite cement in the fault trace. Up section the fault exhibits a dip of 45° towards NNW. Here, the fault has propagated within a shale bed (Figure 6.42b). Figure 6.42 c and d display the fault trace down-section. The fault trace is straight where the beds are folded and seems to cut through an underlying sandstone bed. This indicates that Fault C post-dates the folding of the beds. However, in the lowermost section, although difficult to say, it seems like the fault trace follows parallel to the bedding plane down below ground and therefore appears to be folded. Fault C was the only foreland-directed thrust identified at Evangelieholmen.

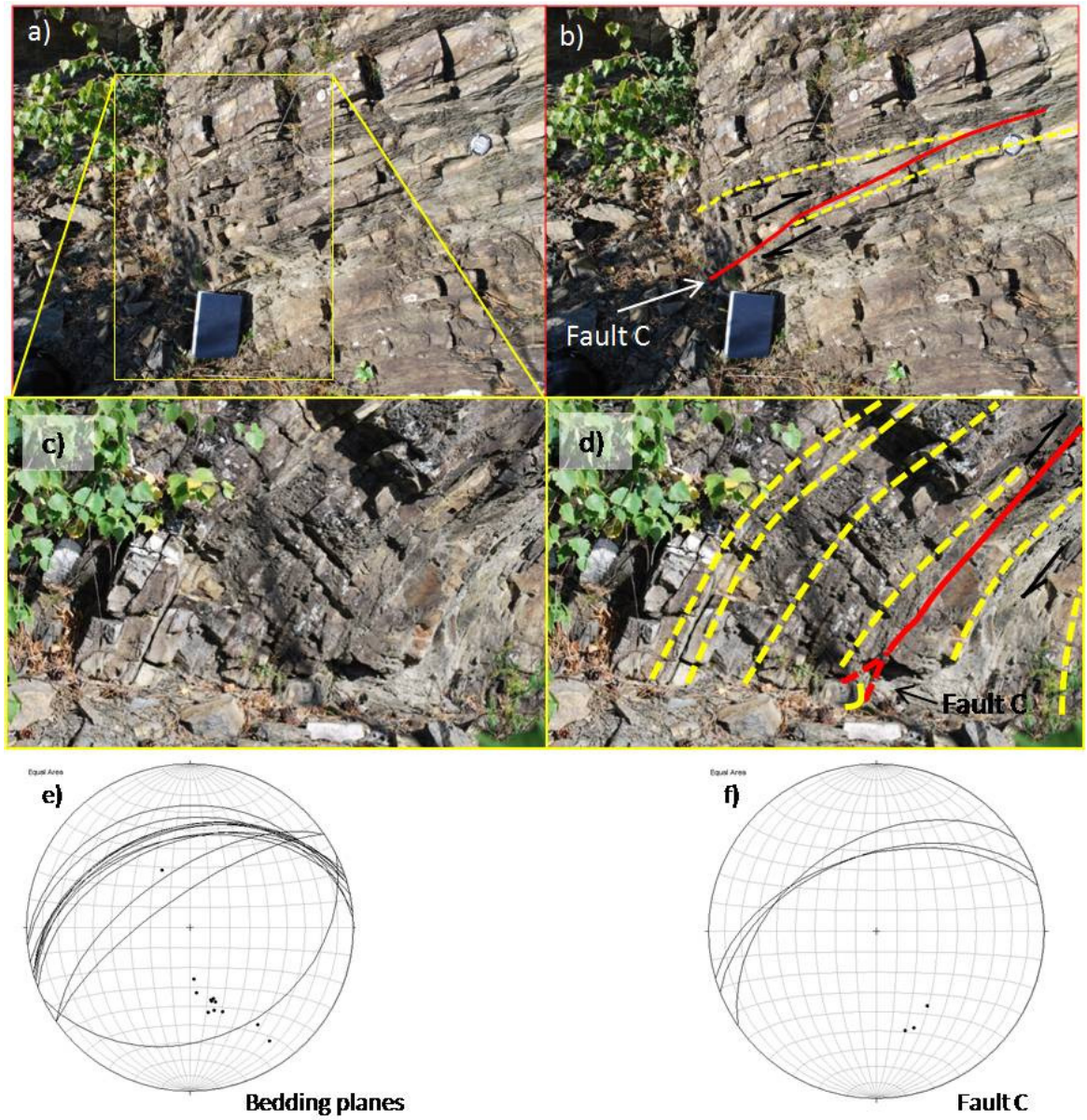

Figure 6.42: a) Detail photo from the southern tip of Evangelieholmen (within the red square in Figure 6.41a), displaying sandstone beds of the Sælabonn Formation (Logbook as scale). b) Same photo as a., but with two bedding planes marked with yellow lines to illustrate the displacement along fault C, which is marked by the red line. c) A down-section detail from the area within the yellow square in photo a. d) Same photo as in c., displaying Fault C marked with a red line. Stippled red lines are extrapolation of the fault plane in two possible directions down-section. Bedding planes marked with yellow lines e) Strike and dip of bedding planes (n=13) at the location illustrated in a Stereoplot. f) Strike and dip measurements (n=3) on the fault plane.

Extensional faults

Down-section on the southwestern tip of Evangelieholmen a near vertical N-S fault striking N355E, with a dip of 82° towards E was identified. The fault is calcite filled and cuts through the tilted limestone beds of Rytteråker Formation. A few meters towards north, close to the water edge, along the western side of the islet, a second steep fault was observed cutting the limestone of the Rytteråker Formation. The fault plane was cemented with calcite where a strike and dip measurement was performed, giving a strike of N334E and a dip of 76° towards ENE.

Summary

Evangelieholmen is characterized by moderate contractional deformation of both the Rytteråker- and Sælabonn formations. Based on the different structural elements described above a deformational time line can be proposed. Figure 6.43 displays a schematic sketch illustrating the development of the different structures described above in chronological order.

1. Low-angle thrust faults in connection to bedding-parallel shortening are assumed to be the oldest structures observed (Figure 6.41). Fault A (population 2a) has cut the limestone bed parallel to the bedding plane which subsequently has been folded (fold population 2a). The structure involving fault population 2b is complex. However, the thrust faults dip at a low-angle relative to the bedding planes and it appears that the beds have been compressed and tightly folded in the central part (faults B2 and B3) and cut by thrust faults. In Figure 6.43, stage 1, the thrust faults display two separate transport directions. This might not be the case regarding the associated thrust faults at Evangelieholmen.

2. The southwestern side is characterized by tight- to isoclinal folds with upright axial planes and shallowly NE-ENE trending fold axes (fold population 1). A vergence could not be identified based on the geometry of the folds. Situated in the steep fold limbs of the upright folds are the folds and faults associated with bedding-parallel shortening. This displays that the tight- to isoclinal, upright folds post-dates the bedding-parallel shortening structures.

3. Fault C (fault population 3), is situated on the south side of Evangelieholmen is a low-angle thrust fault (Figure 6.42). Down-section the fault cuts the folded sandstone and thin shale beds, whilst up-section the fault trace is situated within a shale bed. The fault plane exhibits an average strike of N246E, indicating a direction of transport towards SSE. The straight fold trace suggests that folding occurred before Fault C. No other foreland-directed thrust faults were observed on Evangelieholmen.

4. Both fold and fault population 2 and the upright folds are cut by extensive thrust faults (Fault 1-7, fault population 1). Hence, the thrust faults post-date both. Fault 1 is the best exposed, with a fault plane displaying an average strike of N354E. Slickenlines on the fault plane (limestone bed) indicate a transport direction towards WNW on the southwest side of Evangelieholmen. Strike and dip of Faults 2-5 (fault planes) deviate slightly from Fault 1. The former thrust faults display mainly a strike towards (N)NE, with dips toward (E)SE, indicating a transport direction towards (W)NW. Fault H1 cuts the folded bedding on the south side of Evangelieholmen, indicating a transport direction towards WNW.

5. The near vertical calcite filled extensional faults pre-dates the development of the upright folds because the faults are not involved in the folding and can be seen cutting the tilted bedding. It was not possible to see whether the normal faults pre- or post-dates the SSE-directed thrust (Fault C) or fault population 1 (F1-F9 and H1). However, due to the (NW)N-S(SE) strike and the dip of the faults, these are assumed to be Permian extensional faults (Sundvoll and Larsen 1994, Heeremans et al. 1996) and are therefore placed as the youngest structures. This stage will not be discussed further in this thesis.

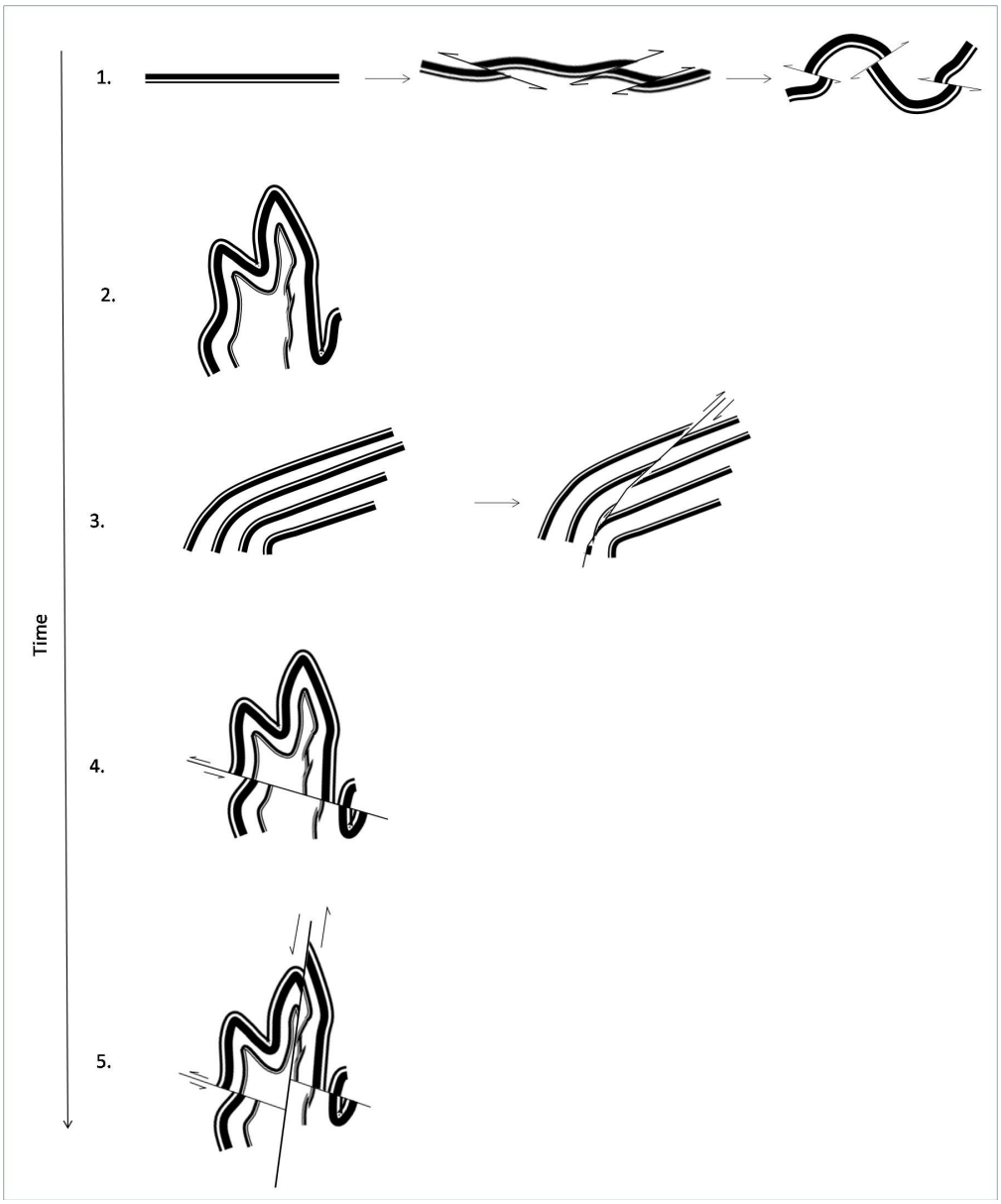

Figure 6.43: Schematic sketch illustrating the different compressional structures recognized at Evangelieholmen displayed in what is thought to be the chronological order of development. 1) Bedding-parallel shortening involving thrust fault and subsequent folding. 2) Development of isoclinal to tight upright folds. 3) Low-angle foreland-directed thrusts. 4) Low-angle hinterland-directed thrust faults. 5) Extensional faults.

6.3 Structural geological maps

Figure 6.44 and Figure 6.45 display two maps which display sections of the maps sheets N5-raster Ullern (1:5000) (Hole_municipality 2009b) and N5-raster Rytteråker (1:5000) (Hole_municipality 2009a) covering the study area. Added to the maps are the main thrust faults, normal faults, slickenlines and groove lines measured on fault planes, fold axes, dykes and strike and dip measurements taken on bedding planes. The different lithological units identified in the study area are also placed on the map.

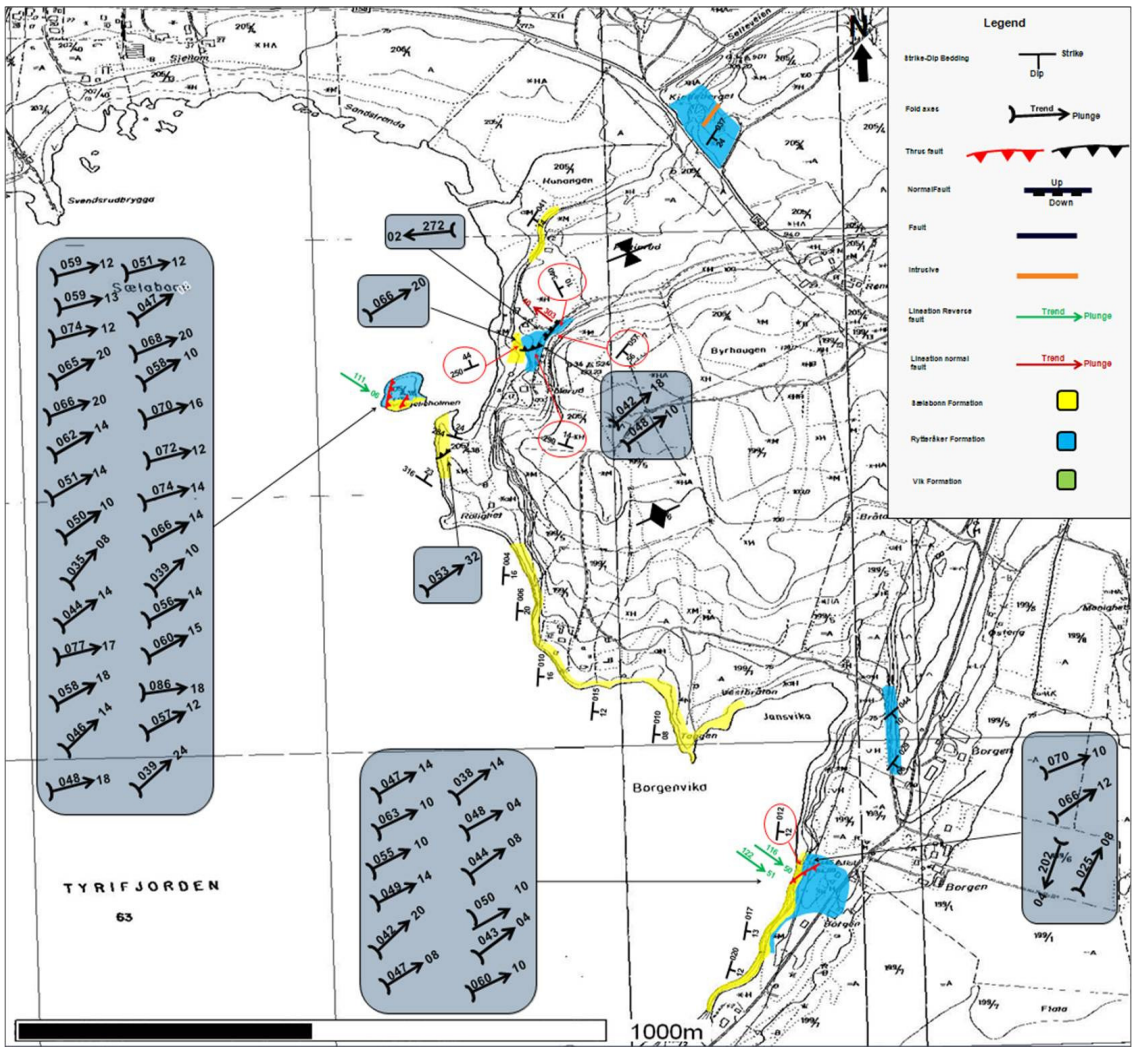

Figure 6.44: a) Section of the map sheet N5-raster Ullern 1:5000 (Hole_municipality 2009b) covering Sælabonn and Borgenvika in the northern part of the study area. Stratigraphy and structural data collected during the field work have been added to the map sheet.

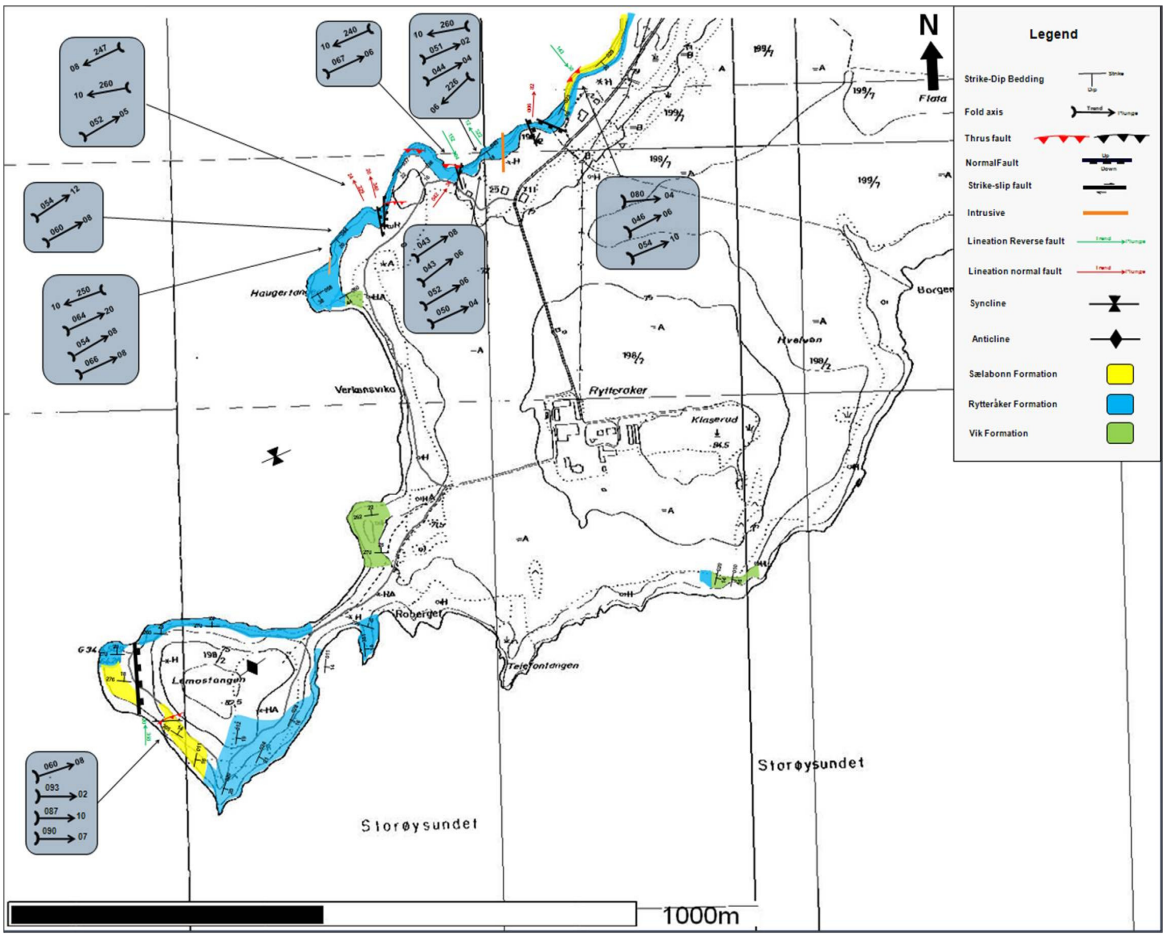

Figure 6.45: Section of the map sheet N5-raster Rytteråker (1:5000) (Hole_municipality 2009a) displaying Rytteråker and Limovnstangen which comprise the southern part of the study area. Added to the map are the structural geological data collected in the field and the stratigraphy.

7 Discussion

In the following, the structural elements described in chapter 6 will be discussed chronologically, focusing on the significance of each type of structure (phases of deformation) and the time relation between the phases. Accordingly structural features related to bedding-parallel shortening are discussed first, since the field analysis has shown that these are the oldest preserved structures in the study area. The second phase encompasses tight to isoclinal folds with upright axial planes, whereas phase three is dominated by foreland-directed low-angle thrust faults post-dating the development of the folds with upright axial planes (phase 2). Finally, the hinterland-directed thrusts will be discussed. Each of the phases are eventually compared with and correlated to the main stages of Caledonian structuring in the Oslo Region.

Structures identified as deformational phase 1 (oldest) are denoted D1 and structures belonging to deformational phase 2 will be denoted D2 and so forth. Associated thrust faults related to each of the phases are denoted with an S (Hence S1 encompass thrust faults related to D1). Regarding the associated folds these will be denoted with an F.

For convenience, the structural development is subdivided into ”phases”. It is stressed that these are valid for the study area, not implying that they be used in correlation to the main phases (Roberts 2003) of the Caledonides as seen on a regional scale.

7.1 Phase 1. Structures related to bedding-parallel shortening

As demonstrated in chapter 6, the earliest stage of deformation in the study area comprises bedding-parallel-shortening and structures affiliated with such shortening. These include low-angle thrust faults and associated folding confined to the competent beds typically seen at Borgenvika (Figure 6.18) and Evangelieholmen (Figure 6.41).

Beds oriented parallel to the main stress axis are likely to become shortened by the development of bedding-parallel thrusts and folds. Figure 7.1 displays a schematic illustration of how the bedding-parallel shortening structures presumably have developed in phase 1. Two directions of thrust faults relative to the bedding plane are displayed, as observed in the field.

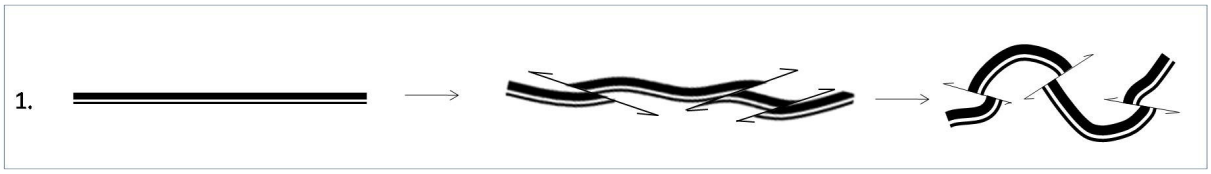

Figure 7.1: 1) Schematic illustration displaying the assumed evolution of structures related to deformational phase 1 associated with bedding-parallel shortening.

Tectonic transport direction

The measured thrust faults (A1-A3 and B1) that cut the folded beds at Borgenvika all strike E-W (average N265E), dipping towards the north, ranging between 24°-64° (Table 1).

To determine the pre-folding thrust direction, the strike and dip of the thrusts faults (A1-A3 and B1) at Borgenvika were rotated to their original (assumed horizontal) position by using a fold axis by fault A1 and A2 (Figure 6.18).

This fold axis was used because the fold is a part of the same bed as the thrust faults, and therefore obtaining a more correct rotation of the bedding plane. The trend and plunge of the fold axis are N072E and 08°. The trend of the fold axis is oriented slightly more to the E, compared to the average, but displays the same dominant trend. The bedding plane (before rotation) strikes N244E, and dips 60° towards NNW. Figure 7.2 displays the result. After rotation, two of the faults strike approximately N(NE)-S(SE), dipping towards E(SE), and NNW-SSE, dipping ENE and the fourth strike NE-SW, dipping SE. This indicates that the phase 1 shortening ($\sigma_1 = \sigma_H$) was oriented approximately NW-SE to ENE-WSW, which is generally consistent with what is known for the regional transport in the Oslo Region (Bockelie and Nystuen 1985, Hossack and Cooper 1986, Larsen and Olaussen 2005, Gabrielsen and Larsen in press).

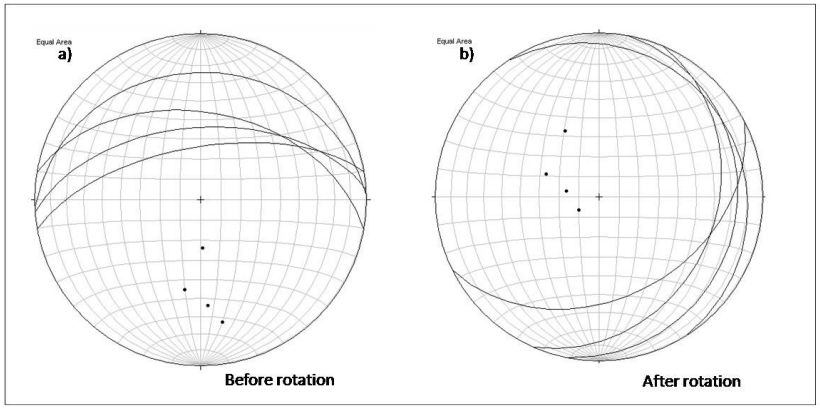

Figure 7.2: a) Stereoplot projection of the strike and dip of fault planes A1-A3 and B1 at Borgenvika (n=4). b) Same data as in a. The stereoplot displays the data after being rotated around a fold axis with a trend of N065E and plunge of 10° associated with the thrust faults, by an amount of 60° which was measured on a bedding plane close to the thrust faults.

The same approach was performed on fault plane measurements obtained from faults B1-B3 (fault population 2b) at Evangelieholmen (Table 3). The strike of Faults B1 and B3 correlate well, striking N053E and N245E. Whilst a strike of N206E was measured on Fault B2 (Figure 6.41f). A neighboring bed to the structure measured a strike of N050E with a dip of 80° towards SE (before rotation). A fold axis measured on a parasitic fold situated about 1.5 m to the SE was used as the rotational axis. This is because a fold axis related to the structure was not measured in the field. However, the fold axes measured on the south side

of Evangelieholmen display quite homogeneous trends. A trend of N055E and plunge of 13° were measured on the fold. Figure 7.3 displays the stereoplot projections before and after the rotation of the data. The three thrust faults now display very contrasting strike of N-S, E-W and NW-SE. This result makes it difficult to suggest a direction of transport.

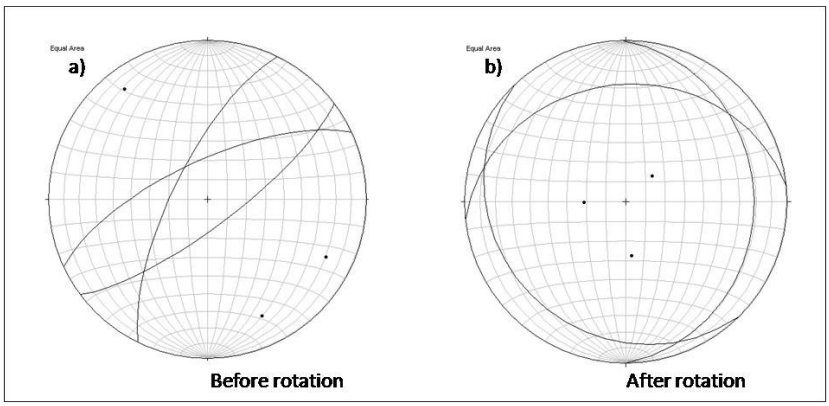

Figure 7.3: a) Stereoplot projection of the strike and dip measurements (n=3) of fault planes B1-B3 at Evangelieholmen. b) Same measurements rotated around a fold axis (situated approximately 1,5 m SE of the faults) with a trend of N055E and plunge of 13°. The strike and dip of the bedding plane neighboring the faults (to the SSE) measured a strike of N050E with a dip of 80° towards SE. The data was therefore rotated by a magnitude of 80°.

Buckle folds associated with the bedding-parallel shortening were documented at both Borgenvika (fold population 2, Figure 6.18) and Evangelieholmen (fold population 2a, Figure 6.41b). With continued compression the beds were folded (Figure 7.1). The buckle folds are mainly symmetric and open, which indicates a bedding-parallel shortening deformation. The NE-ENE to SW-WSW orientation of the fold axes indicate that σ_1 was oriented NW-SE to NNW-SSE at the time of deformation, which is in slight contrast to the D1 thrust faults. Fold population 2b Evangelieholmen was complicated and more deformed compared to the buckle folds (fold population 2). The structure resembles stage 2 in Figure 7.1. The more intense deformation may be due to the thinner limestone beds, compared to the thicker and more competent limestone and sandstone beds of fold population 2.

Age of phase 1 structures

The thrust faults and the associated folds have been identified as structures of the first deformational phase. This is because the beds which comprise these structures were documented to have taken part in several later deformational phases which are discussed below. The thrust faults developed prior to the buckle folds as seen on Borgenvika. The orientation of σ_1 in context to the buckle folds differ from that of the thrust faults, as indicated by the rotated measurements (Figure 7.2). However, there are too few measurements to draw a conclusion based on this, and as mentioned, both are consistent with the regional transport documented in the Oslo Region. Also, there was not observed structures which pre-date the bedding-parallel shortening structures.

7.2 Phase 2. Folds with upright axial planes

Fold population 1 at Evangelieholmen comprise tight-isoclinal disharmonic folds with upright axial planes, described in chapter 6 (Figure 6.31). This deformational style was not recognized elsewhere in the study area. A schematic illustration to how the folds were prior to erosion and thrusting has been illustrated in Figure 7.5. Based on the field data described in chapter 6, the upright folds constitute the second deformational phase in the study area.

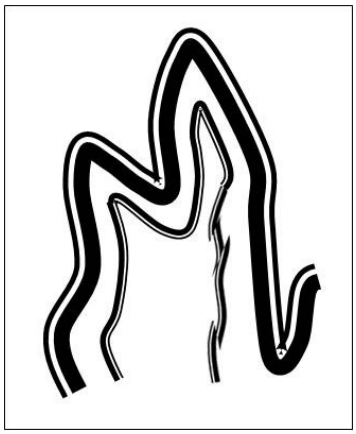

Figure 7.4: Principal sketch displaying of the tight- to isoclinal, upright folds at the southwest side of Evangelieholmen prior to thrusting and erosion. Additionally, bedding-parallel structure (D1) situated in the fold limb.

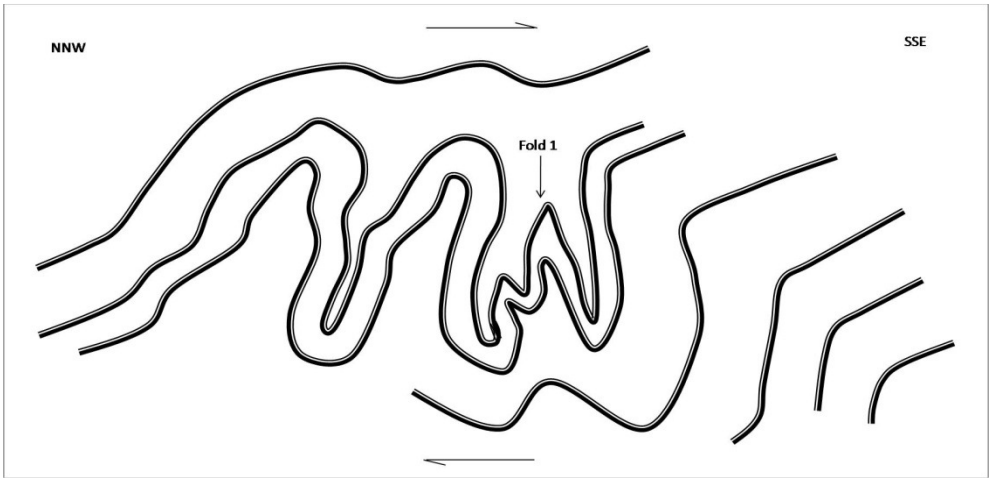

Figure 7.5: Schematic sketch illustrating the possible geometry of the folds prior to erosion and thrust faulting at Evangelieholmen.

Tectonic transport direction

Fold 1 is a tight-isoclinal fold with an upright axial plane with a steep dip towards SSE and a shallow plunging fold axis trending ENE. Fold 1b is a smaller parasitic fold situated on the NNW-limb of Fold 1, displaying a shallowly plunging fold axis trending NE. The geometry of the folds does not show a vergence indicating the direction of transport. The trend of the fold axes indicate that the maximum stress axis (σ1) was oriented approximately NW-SE to NNW-SSE at the time of deformation. This is also supported by the parasitic folds on the south side of Evangelieholmen (Figure 6.32). However, the geometry of Evangelieholmen exhibits a vergence towards SE-SSE, due to the steep beds on the south side and less steep on the northern side. This is schematically illustrated in Figure 7.5. Compared to the rotated data obtained from S1 at Borgenvika, the direction of transport has shifted towards south.

Fault G (Figure 6.31) is a steep angle reverse fault striking NE-SW, with a steep (72° and 84° were measured) dip towards the SE. The fault cuts the southern-limb of Fold 1 (Figure 6.31). The fault splays into two fault traces down-section, where both terminate against Fault F1 (discussed later). There is a possibility that Fault G developed during the development of the tight- to isoclinal folds. This is because the strike of Fault G is fairly parallel to the strike of the bedding planes (NE-SW to E-W) within the fold, which is in contrast to fault F1 (D4) situated beneath which strike N-S.

Age of phase 2 structures

The structures recognized as D1 are situated in steep to near vertical fold limbs of the upright folds. The buckle folds (F1) display gently inclined axial planes and the associated thrust faults (S1) exhibit very steep dips, thus displaying a rotation attributed to the development of the upright, tight- to isoclinal folds, which post-dates D1.

7.3 Phase 3. Foreland-directed thrust faults and folding

As described in chapter 6, a set of foreland-directed thrust faults were documented in the study area, at Evangelieholmen and Limovnstangen (Figure 6.25 and Figure 6.42). Figure 7.6 displays a schematic sketch illustrating a fault cutting through folded beds. Associated with the same deformational phase are the large open folds with wavelengths on the hundreds of meters scale which characterizes the study area (Figure 7.7).

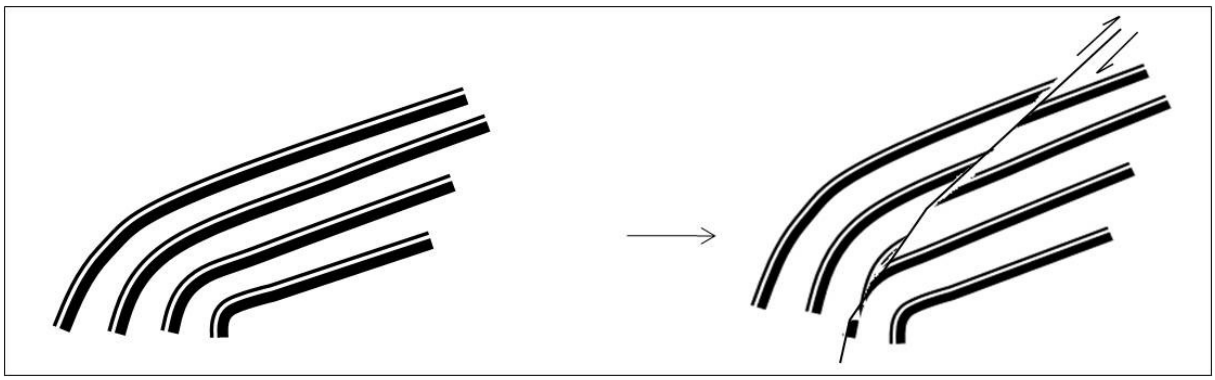

Figure 7.6: Schematic sketch illustrating a foreland-directed thrust fault (D3) cutting a fold associated with D2.

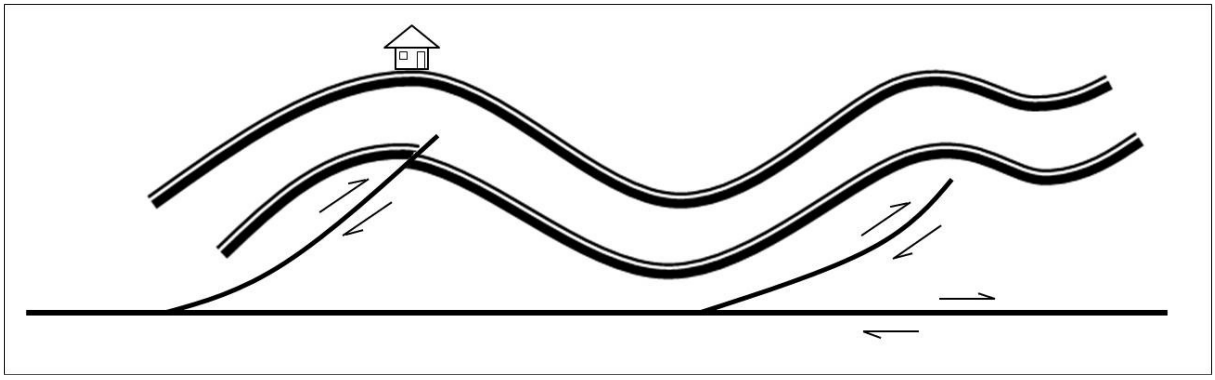

Figure 7.7: Principal illustration of large scale folds (D3) and foreland directed thrust faults (D3).

Tectonic transport direction

The fault plane of Fault C at Evangelieholmen strikes ENE-WSW and displays an average strike of N246E, with a dip ranging between 52° and 45° towards NNW, which gives an approximate transport direction towards SSE. An average strike of N283E and an average dip of 21° were calculated on the basis of strike and dip measured on the fault plane of Fault 1 at Limovnstangen (Figure 6.25). Additionally, groove lineations were measured which display an N-directed trend and a plunge of 20° (Figure 6.27). Hence an approximate direction of transport toward S can be inferred.

The large folds situated within the study area are open shallowly ENE-plunging folds (Figure 6.9, Figure 6.10 and Figure 6.28). Figure 6.11, Figure 6.12, Figure 6.13 displays the cross-sections through the study area illustrating the folds. The precise geometry of the folds situated between Evangelieholmen and Haugertangen was not obtained. The Limovnstangen anticline is fairly symmetric, whilst a vergence towards SSE is displayed by the Verkensvika syncline. The approximate SSE-directed transport displayed by majority of the structures encompassing D3 and is, as mentioned above, consistent with the main regional transport direction in the Oslo Region.

Age of phase 3 structures

On the southernmost side of Evangelieholmen Fault C can be seen to cut through and displace a fold (F2) (Figure 6.42). This indicates that the fold pre-dates the thrust fault. Further, foreland-directed thrust affected by D2 structures was not observed.

7.4 Phase 4. Back-thrusting

Hinterland-directed low-angle thrust faults and fault-propagation-folds were recognized in several places in the study area. These thrust faults and fault-propagation-fold structures have been identified as deformational phase 4, based on the direction of transport and the time relationship to other deformational phases as shown in chapter 6.

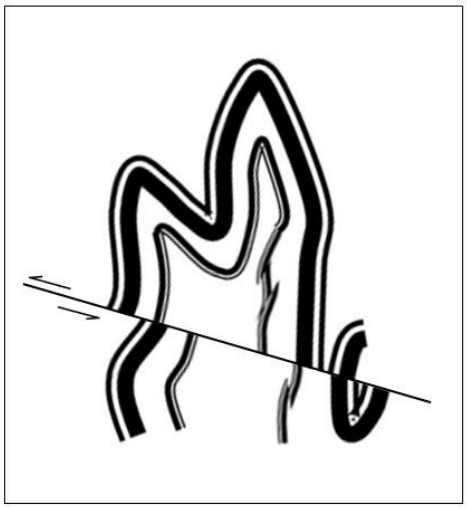

Figure 7.8: Schematic illustration displaying an upright fold and folded D1 structures which subsequently has been cut by a back-thrust.

Tectonic transport direction

Fault-propagation-folds were documented at both Borgenvika and Limovnstangen. The main reverse fault at Limovnstangen and the associated fault-propagation-folds displays an approximate direction of transport towards NNW (Figure 6.25), whilst the smaller associated thrust faults indicate a transport direction towards WNW (Figure 6.26).

The main reverse fault (Fault 1) at Borgenvika gave an average strike of N040E with a mean dip of 50° towards SE (Figure 6.15). Calcite cement on the fault plane exhibits lineated slickenlines trending N119E, plunging 50° towards ESE (Figure 6.16). The shallowly

plunging fold axes of the associated fault-propagation-folds trend mainly NE, but also to the ENE. It is indicated an approximate direction of transport towards NW. A smaller secondary fault (Fault 2) displayed a strike of NNE-SSW, which is fairly consistent with the direction of transport displayed by the main fault (Figure 6.17).

Locality Ib1, situated between Borgen and Haugertangen exhibits low-angle thrust faults striking E-W, dipping towards S (Figure 6.22), hence, an approximate transport direction towards the N is inferred. A similar low-angle thrust was documented at locality Ib2 (Figure 6.23). Based on the average of the measurements taken on the fault plane a transport direction towards NNW can be deduced.

Fault population 1 at Evangelieholmen comprises several low-angle thrust faults (Figure 6.36). The fault planes display an average strike ranging between N-S (Fault F1 and F9) and NNE-NE to -SW-SSW, displaying dips towards E and SE-ESE. The drag folds in the hanging wall of fault F1 are evident and display a drag towards NW-NNW (fold axes trend NE-ENE) (Figure 6.38d). The same relative displacement can be observed on all the low-angle thrust faults, except for fault F8. Additionally, two fault lenses, forming duplexes, were documented along faults F2 and F4, displaying a transport direction towards NNW and NW (Figure 6.38d). Hence, the thrust faults on the south side exhibit a W to WNW direction of transport, whilst a NNW-NW direction of transport is displayed by the faults situated on the west side.

In summary, the hinterland-directed thrust faults and fault-propagation-fold structures display a main direction of transport towards N and NNW in the southern part of the study area, with the exception of Fault 2b and 3 at Limovnstangen. Towards the north, the direction of transport shifts towards approximately NW (Borgenvika) to approximate NW-WNW at Evangelieholmen.

Age of phase 4

The hinterland-directed low-angle thrust faults cut through the steep fold limbs of the tight- to isoclinal upright folds (D2) which show that these post-dates D2. The same can be concluded for D1-structures which also pre-date the fold-propagation-folding. Regarding the foreland-directed thrusts, a time relationship was not identified based on cross-cutting of the faults. However, the fault-propagation-fold structures and the low-angle thrusts related to the hinterland-directed transport cannot be documented to have been affected by the foreland-directed transport. Additionally, back-thrusting is a result of the main SSE-directed transport in the Oslo Region, hence the back-thrusting post-date D3.

Further discussions

Back-thrusts are common in the study area, but most extensive at Evangelieholmen. There might be a connection between the presence of the tight- to isoclinal upright folds (D2), which are isolated to Evangelieholmen, and the extensive back-thrusts seen here. Further, the back-thrusts display a shift in transport direction from the southern part of the area towards NW-WNW at Evangelieholmen. According to Fossen and Gabrielsen (2005) do back-thrusts often evolve in connection to ramps due to geometrical differences. Whether there is a thrust ramp present or not is difficult to say, but it is clear that Evangelieholmen is markedly different in terms of structural style compared to the rest of the study area.

7.5 Comparison of structural style with the Oslo Region

Four separate deformational phases were based on the structural analysis identified in the study area. D1 is the oldest and comprises structures (thrusts and folds) associated with bedding-parallel shortening. D2 is characterized by tight- to isoclinal upright folds. Foreland-directed thrust faults and large open, upright folds are defined as D3, whilst back-thrusts and associated folds distinguish D4.

Figure 7.9 illustrates the four main deformational phases identified in the study area. These have been put in context to previous work regarding Caledonian deformation and the associated time of deformation. The structures described by these authors have been placed in an approximate order according to time of development. Hence, authors listed on the top are meant to illustrate that these structures are late-Caledonian and post-date the deposition of the Ringerike Group, but the order amongst the authors is arbitrary. The deformational phases (D1, D2, D3 and D4) connected to the study area are placed according to age.

In the middle left column in Figure 7.9 the four deformational phases (D1, D2, D3 and D4) have been positioned in context to the stratigraphy in the Ringerike area. This is based on observations during the field work. D1 and D2 were documented affecting the uppermost Sælabonn Formation and the Rytteråker Formation. Therefore, lower and upper boundaries have been placed in context to D1 and D2. Regarding D3 and D4 only a minimum lower boundary could be demonstrated attributed to the Verkensvika syncline, in which the Vik Formation has been folded. Because D4 post-dates D3 it is positioned at the top.

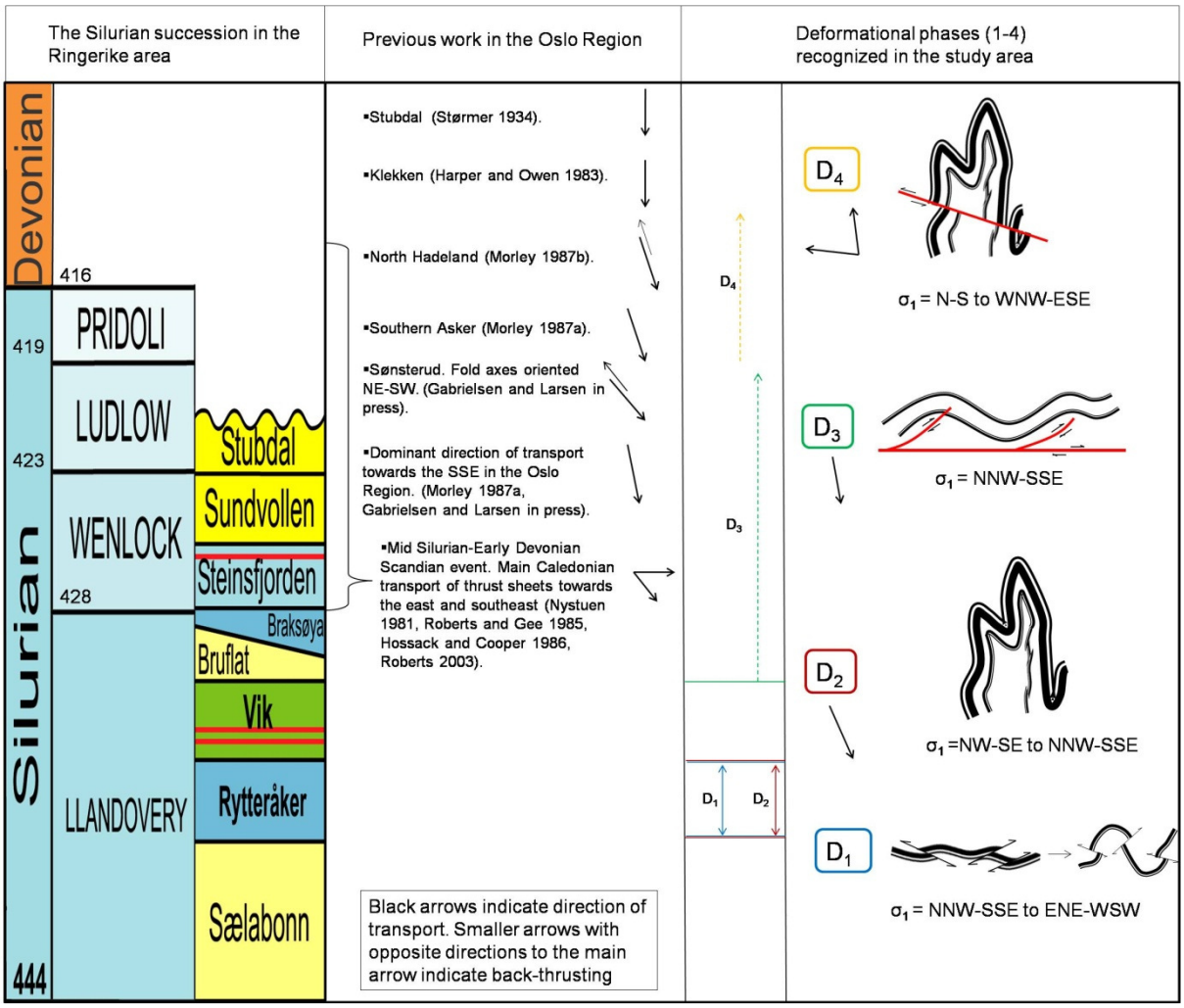

Figure 7.9: From left to right: The Silurian stratigraphy in the Ringerike area. The Devonian period is not to scale. Modified after Larsen and Olaussen (2005). In the middle left column Caledonian structures in the Oslo Region are added. Smaller arrows with opposite direction indicate back-thrusting. However, in some instances the direction of back-thrusting is not stated by the authors, so the arrows only state that back-thrusts have been documented. All the structures added, post-date the deposition of the Upper Silurian Ringerike Group (the order amongst the authors is random). In the middle right column, the four deformational phases recognized in the study area are tied to the stratigraphy based on observations in the study area. Stippled arrows are extrapolated due to the lack of an upper limit observed in the study area. In the right column there are shown four principal sketches and the associated transport directions (black arrows) representing the deformational phases identified in the study area. The orientation of the maximum stress axis connected to each phase is placed below the illustrations.

The regional direction of transport of nappes over the Baltic craton was towards E and SE (Bockelie and Nystuen 1985, Roberts and Gee 1985, Hossack and Cooper 1986). (Figure 7.9)

The dominant direction of transport in the Oslo Region is towards SSE (Morley 1987a, Gabrielsen and Larsen in press). Transport directions towards S, and NE-SW trending structures have also been inferred, as seen in Figure 7.9 (Størmer 1934, Harper and Owen 1983, Larsen and Olaussen 2005). Additionally, back-thrusts are also a dominant feature and have been recognized in several places in the Oslo Region (Morley 1987a, 1987b, 1994, Gabrielsen and Larsen in press).

The Osen-Røa detachment underlies the entire Cambro-Silurian succession in the Oslo Region and can be traced southwards to Langesund (Hossack and Cooper 1986, Morley 1986a). Attributed to decreasing transport towards the S and SE and to differences in lithology, which is one of several important factors, the structural style varies both laterally and vertically within the Oslo (Morley 1987a, Gabrielsen and Larsen in press).

According to Morley (1987a) there is an increase in competent units upwards in the Cambro-Silurian succession. This is reflected by several thrust faults and associated folds dominate the lower part of the succession (Cambro-Middle Ordovician) in the northern Oslo Region. The upper part of the succession (Middle Ordovician-Silurian) is characterized by broader buckle folds, which accommodates most of the shortening, but also layer-parallel faulting or thickening and cleavage (Morley 1987a). On a regional scale the northern part of the Oslo Region is characterized by imbricate zones, whilst the southern part is dominated by triangle zones and pop-up structures (Morley 1986b). An upper detachment level is suggested by Morley (1987a) to separate the Cambro-Middle Ordovician from the overlying Middle-Ordovician-Silurian succession due to the contrasting style in deformation.

The study area is situated approximately south-southwest of the Klekken fault (Figure 6.1) which trend NE-SW (Figure 7.9), as described by Harper and Owen (1983). North of this fault, in its hanging wall, there is an imbricate structure with steep north-dipping thrust faults. In the footwall to the south of this fault the strata dips towards the SE and is

characterized by gentle deformation (Harper and Owen 1983). The deeper structure of the Klekken area has been suggested to be a triangle zone (Gabrielsen and Larsen in press). According to Morley (1987a) there is an evident decrease in shortening in the Ringerike district, south of the Klekken fault.

Southwards at Sønsterud (Figure 7.9), ramps have been identified with complex deformation (Gabrielsen and Larsen in press). According to the authors, these ramps most likely evolved where the Ringerike sandstone was buckle folded. The structures are possibly connected to triangle-zones and pop-up structures. Additionally, there were recognized fold axes trending NE-SW and back-thrusts post-dating the other structures (Gabrielsen and Larsen in press).

D1

An early phase of bedding-parallel shortening, which pre-dates the main SSE-directed main thrust and fold event in north Hadeland (Figure 7.9) has been documented by Morley (1987b). The bedding-parallel shortening event involves thrust-wedging and pressure-dissolution cleavage in limestone beds. The main thrust event involved imbrications and associated folding, associated with the structural style north of the Klekken fault. Further, all structures are assumed to be part of the same deformational event (Morley 1987b). The structural style in north Hadeland is different from the study area. However, an early phase of bedding-parallel shortening is common for both areas. This supports that D1 is associated with the early stages of deformation in context to the main thrust event in the Ringerike area.

D1 structures were observed in the uppermost Sælabonn Formation (Steinsåsen member) and Rytteråker Formation. D1 was not documented in the middle (Djupvarp member) Sælabonn Formation or in the Vik Formation (Figure 7.9). Only a section of the lowermost part of the Vik Formation is exposed in the study area, therefore it is difficult to state if it is affected by the bedding-parallel shortening or not.

D2

A similar structural style compared to D2 in the study area has been documented between Nordre Horn and Pålsrud in Modum. This is described by Gabrielsen and Larsen (in press). According to the authors, this structural style is representative only for a small area and is characterized by disharmonic folds with upright (steep to vertical) axial planes and ENE-WSW trending fold axes. Also, similar to Evangelieholmen, the fold limbs have been cut by steep reverse faults and frequent back-thrusts have been identified (Gabrielsen and Larsen in press). This could suggest that the structural style, only documented at Evangelieholmen in the study area, is not a coincidence, but perhaps was controlled by a specific structural element.

D3

According to Morley (1986b) do thrust faults and amount of shortening decrease towards the higher levels of the Cambro-Silurian succession. Lower Silurian thrust faults (north-western Oslo fjord) are recognized by Morley (1986b) to have developed attributed to space problems within the folds as they got compressed and subsequently cut through the folds. Further, the thrusts faults display small amount of displacement, normally in the range of a few meters Morley (1986b).

Structures identified as D3 in the study area are thrust faults (S3) and large open, upright folds (F3), which corresponds well to Morley's (1986b) descriptions. However, whether the thrusts developed due to compression of the folds or not, cannot be inferred with certainty. aThe thrust faults display a transport direction towards S and SSE and the Verkensvika syncline displays a vergence towards the SSE. The direction of transport is consistent with the general transport direction seen in the Oslo Region as a response to the translation of the Osen-Røa nappe of Nystuen (1981) and the associated deformation of the Cambro-Silurian succession. The folding of the Vik Formation gives a minimum age of deformation (Figure 7.9).

D4

Figure 7.10 show a NNW-SSE directed cross-section from southern Asker, by Morley (1987a). Here a pop-up structure is displayed, exhibiting both fore- and back-thrusts. The back-thrusts display a transport direction towards the NNW (Figure 7.9). In comparison to the majority of back-thrusts identified in the study area, these in southern Asker exhibit steeper dips. The deformational intensity is also higher compared to the study area. Among the exposed thrust faults in the study area, back-thrusts are the most dominant.

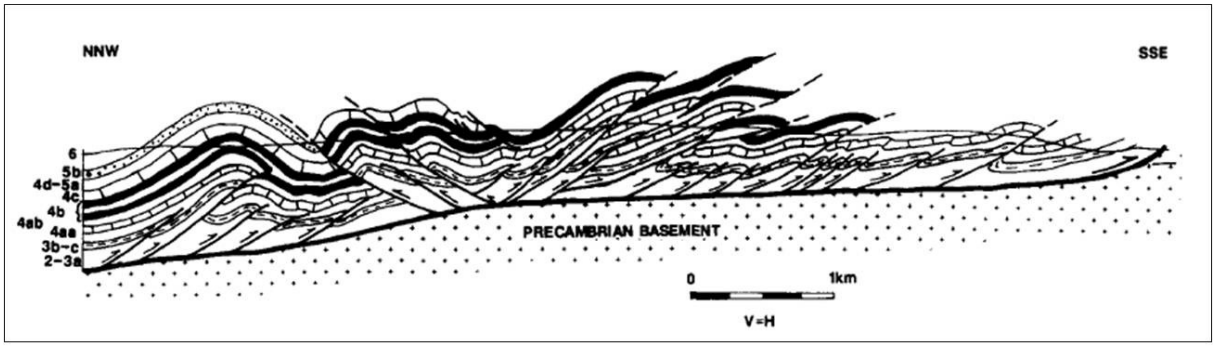

Figure 7.10: Figure from Morley (1987a) displaying a NNW-SSE directed cross-section through southern Asker. The structures involve Cambrian and Ordovician strata.

Deformational phases D1, D2, D3 and D4 were identified in the Lower Silurian (Sælabonn-, Rytteråker- and Vik formations) succession in the study area. The main Caledonian deformational event, known as the *Scandian* phase, took place during Mid Silurian-Early Devonian. This shows that the four separate deformational phases identified in the study area developed in relation to the *Scandian* phase.

8 Conclusion

The main objective of this thesis is to study the geological structures with focus on back-thrusts in the Sælabonn-Rytteråker area. Further, to establish the relationship between the structures and finally, to place them in context to the development of the Ringerike area.

Based on analysis of field data have four separate deformational phases, D1, D2, D3 and D4 (in chronological order) been identified in the study area (Figure 7.9).

Thrust faults (S1) and folds (F1) connected to deformational phase 1 (D1) are associated with bedding-parallel shortening ($\sigma_1 = \sigma_H$). Thrust faults (S1) indicate a maximum stress axis (σ_1) oriented NW-SE to ENE-WSW, whilst associated folds (F1) display a maximum stress axis (σ_1) oriented NW-SE to NNW-SSE.

The development of tight- to isoclinal, disharmonic folds (F2) with upright axial planes are defined as deformational phase 2 (D2). The NE-SW to ENE-WSW trending fold axes, as well as the overall vergence displayed by Evangelieholmen indicate a direction of transport towards SE-SSE.

Structures connected to deformational phase 3 (D3) are foreland-directed thrust faults (S3) and large open and upright folds (F3) with wavelengths in the order of hundreds of meters. These structures display a main transport direction towards SSE, but also towards the S at Limovnstangen.

Deformational phase 4 (D4) comprise back-thrusts which post-date the other structures. Structures connected to this phase are low-angle thrust faults and fault-propagation-folds. The transport direction of the faults shifts gradually from N-NNW in the southern part of the study area to WNW-NW in the northernmost part.

The transport directions displayed by the structures comprising phases D1-D3 are consistent with the main tectonic transport direction displayed in the Oslo Region (e.g Gabrielsen and

Larsen in press). Back-thrusts situated in the southern part of the study area displays in general an opposite direction of transport compared to the regional SSE-direction, which has been documented elsewhere in the Oslo Region (e.g Morley 1986a). However, the NW-WNW directed thrusts in the northern part deviate from this trend.

The generally gentle deformational style, characterized by large open folds as displayed in the study area, is consistent with the general structural style in the upper Cambro-Silurian succession in the Oslo Region as described by (Morley 1987a). Back-thrusts are however, the most dominant of the exposed thrust faults in the study area.

All structures are situated in the Lower Silurian succession at Ringerike. Therefore it can be stated that all phases (D1, D2, D3 and D4) are related to the *Scandian* phase which corresponds to the main Caledonian deformational event (e.g Roberts 2003).

9 References

Allen, P.A. and Allen, J.R. 2005. *Basin analysis. Principles and Applications*. Second ed: Blackwell Science Ltd.

Allmendinger, R.W. 2010. *StereoWin*^{TM} 2010 [Accsessed: 09.4 2010]. Available at http://www.geo.cornell.edu/geology/faculty/RWA/programs.html.

Andersen, T. 1993. The role of extensional tectonics in the Caledonides of south Norway: Discussion. *Journal of Structural Geology* 15, 1379-1379.

Baarli, G. 1990. Peripheral bulge of a foreland basin in the Oslo Region during the early Silurian. *Palaeogeography, Palaeoclimatology, Palaeoecology* 78, 149-161.

Bjørlykke, K. 1974a. Depositional history and geochemical composition of Lower Palaeozoic epicontinental sediments from the Oslo region. *Nor Geol Unders* 305, 81.

Bjørlykke, K. 1974b. Geochemical and mineralogical influence of Ordovician Island Arcs on epicontinental clastic sedimentation. A study of Lower Palaeozoic sedimentation in the Oslo Region, Norway. *Sedimentology* 21, 251-272.

Bjørlykke, K. 1978. The eastern marginal zone of the Caledonide orogen in Norway. *Caledonian-Appalachian orogen of the North Atlantic region Geol Surv Can Pap* 78-13, 49-55.

Bockelie, J. and Nystuen, J. 1985. The southeastern part of the Scandinavian Caledonides. *In* Gee, D.G. and Sturt, B.A. (eds). *The Caledonide orogen–Scandinavia and related areas*: John Wiley and Sons, 1, 69–88.

Brøgger, W.C. and Schetelig, J. 1872. *Kartblad Hønefoss. Part of the series Geologisk kart: Rektangel kart. Vol nr. 19-B*. Norges Geologiske Undersøkelse.

Davies, N., Turner, P. and Sansom, I. 2005a. Caledonide influences on the Old Red Sandstone fluvial systems of the Oslo Region, Norway. *Geological Journal* 40, 83-101.

Davies, N., Turner, P. and Sansom, I. 2005b. A revised stratigraphy for the Ringerike Group (Upper Silurian, Oslo Region). *Norwegian Journal of Geology* 85, 217–225.

Davis, G.H. and Reynolds, S.J. 1996. *Structural geology of rocks and regions*. Second ed: John Wiley & Sons, Inc. 776 pp.

DeCelles, P. and Giles, K. 1996. Foreland basin systems. *Basin Research* 8, 105-123.

Dickinson, W.R. 1974. Plate tectonics and sedimentation. *In* Dickinson, W.R. (ed). *Tectonics and sedimentation*: SEPM Special Publication 22, 1-27.

Fossen, H., Dallmann, W. and Andersen, T.B. 2007b. Fjellkjeden går til grunne. Kaledonidene brytes ned; ca. 405-359 Ma. *In* Ramberg, I.B., Bryhni, I. and Nøttvedt, A. (eds). *Landet blir til, Norges geologi*: Norsk Geologisk Forening, 230-257.

Fossen, H. and Gabrielsen, R.H. 2005. *Strukturgeologi*, Bergen: Fagbokforlaget. 375 s. pp.

Fossen, H., Pedersen, R.B., Bergh, S. and Andresen, A. 2007a. En fjellkjede blir til. Oppbyggingen av Kaledonidene; ca. 500 – 405 Ma. *In* Ramberg, I.B., Bryhni, I. and Nøttvedt, A. (eds). *Landet blir til, Norges geologi*: Norsk Geologisk Forening, 178 – 229.

Fossen, H. and Rykkelid, E. 1992. Postcollisional extension of the Caledonide orogen in Scandinavia: Structural expressions and tectonic significance. *Geology* 20, 737-740.

Friend, P.F. and Ori, G.G. 1984. Sedimentary basins formed and carried piggyback on active thrust sheets. *Geology* 12, 475-478.

Gabrielsen, R.H. and Larsen, B.T. in press. Caledonian structural development of the Oslo Region.

Gee, D. 1975. A tectonic model for the central part of the Scandinavian Caledonides. *American Journal of Science* 275, 468-515.

GoogleEarth™. 2010. *GoogleEarth* 2010 [Accsessed: 25.01 2010]. Available at http://earth.google.com/.

GoogleMaps™. 2010. *GoogleMaps* 2010 [Accsessed: 09.4. 2010]. Available at http://maps.google.no/.

Harper, D.A.T. and Owen, A.W. 1983. The structure of the Ordovician rocks of the Ringerike district: evidence of a thrust system within the Oslo region. *Norsk Geologisk Tidsskrift* 63, 111-115.

Heeremans, M., Larsen, B. and Stel, H. 1996. Paleostress reconstruction from kinematic indicators in the Oslo Graben, southern Norway: new constraints on the mode of rifting. *Tectonophysics* 266, 55-79.

Hole_municipality 2009a. *Digital N5-Raster map sheet Rytteråker 1:5000, Series CJ048-5-2*. Statens kartverk.

Hole_municipality 2009b. *Digital N5-Raster map sheet Ullern 1:5000, Series CJ049-5-4*. Statens Kartverk.

Hole_municipality. 2010. *Hole Kommune Karttjeneste* 2010 [Accsessed: 8.3 2010]. Available at http://www.hole.kommune.no/.

Holtedahl, O. 1953. *Norges geologi, Bind I*. Norges geologiske undersøkelse. 164: I Kommisjon hos H. Aschehoug & Co. 1-575 pp.

Hossack, J. and Cooper, M. 1986. Collision tectonics in the Scandinavian Caledonides. *Geological Society London Special Publications* 19, 285.

Kearey, P., Klepeis, K.A. and Vine, F.J. 2009. *Global tectonics*. Third ed: Wiley-Blackwell.

Kirkland, C., Daly, J., Chew, D. and Page, L. 2008. The Finnmarkian Orogeny revisited: An isotopic investigation in eastern Finnmark, Arctic Norway. *Tectonophysics* 460, 158-177.

Kiær, J. 1908. *Das Obersilur im Kristianiagebiete: eine stratigraphisch-faunistische Untersuchung*, Christiania: Dybwad.

Kiær, J. 1926. Tyrifjorden. *Norsk Geografisk Tidsskrift* 1, 65-99.

Kjerulf, T. 1862. Jordbunden i Ringeriget. *Polytekninsk Tidsskrift,* 1862, 1-15.

Kjerulf, T. 1879. *Udsikt over det sydlige Norges geologi*, Christiana: W.C. Fabritius 262 pp.

Larsen, B.T. and Olaussen, S. 2005. *The Oslo Region. A study in classical Palaeozoic geology. Field guide to NGF's Centennial field trip, 26. – 28 May 2005*: Norsk Geologisk Forening.

Larsen, B.T., Olaussen, S., Sundvoll, B. and Heeremans, M. 2007. Vulkaner, forkastninger og ørkenklima. Osloriften og Nordsjøen i karbon og perm; 359-251 Ma. *In* Ramberg, I.B., Bryhni, I. and Nøttvedt, A. (eds). *Landet blir til, Norges geologi*: Norsk Geologisk Forening, 284-327.

Larsen, B.T., Olaussen, S., Sundvoll, B. and Heeremans, M. 2008. The Permo-Carboniferous Oslo rift through six stages and 65 million years. *:* 31, 52-58.

The Millennium Atlas: Petroleum Geology of the Central and Northern North Sea. 2003. Edited by Evans, D., Graham, C., Armour, A. and Bathurst, P., London: Geol. Society of London.

Morley, C. 1986a. The Caledonian thrust front and palinspastic restorations in the southern Norwegian Caledonides. *Journal of Structural Geology* 8, 753-765.

Morley, C. 1986b. Vertical strain variations in the Osen-Røa thrust sheet, North-western Oslo Fjord, Norway. *Journal of Structural Geology* 8, 621-632.

Morley, C. 1987a. Lateral and vertical changes of deformation style in the Osen-Røa thrust sheet, Oslo region. *Journal of Structural Geology* 9, 331-343.

Morley, C. 1987b. The structural geology of north Hadeland. *Norsk Geologisk Tidsskrift* 67, 39-49.

Morley, C. 1994. Fold-generated imbricates: examples from the Caledonides of Southern Norway. *Journal of Structural Geology* 16, 619-631.

Neumann, E., Olsen, K., Baldridge, W. and Sundvoll, B. 1992. The Oslo rift: A review. *Tectonophysics* 208, 1-18.

NGU. 2010. *N250 Berggrunn-raster, Berggrunnsgeologidatabasen* Norges Geologiske Undersøkelse 2010 [Accsessed: 01.03. 2010]. Available at http://www.ngu.no/kart/bg250/.

Norkart. 2010. *Norgei3D* Norkart Virtual Globe 2010 [Accsessed: 27.2. 2010]. Available at http://www.norgei3d.no/.

Nystuen, J. 1981. The late Precambrian" sparagmites" of southern Norway; a major Caledonian allochthon; the Osen-Roa nappe complex. *American Journal of Science* 281, 69.

Nystuen, J. 1983. Nappe and thrust structures in the Sparagmite Region, southern Norway. *Norges geologiske undersøkelse* 380, 67-83.

O'leary, D., Friedman, J. and Pohn, H. 1976. Lineament, linear, lineation: some proposed new standards for old terms. *Bulletin of the Geological Society of America* 87, 1463.

Oftedahl, C. 1943. Overskyvninger i den norske fjellkjede. *In* Gaarder, T. (ed). *Naturen*: Bergens Museum, 67, 143-150.

Osmundsen, P., Eide, E., Haabesland, N., Roberts, D., Andersen, T., Kendrick, M., Bingen, B., Braathen, A. and Redfield, T. 2006. Kinematics of the Hoybakken detachment zone and the More-Trondelag Fault Complex, central Norway. *Journal of the Geological Society* 163, 303.

Ramsay, J. 1967. *Folding and fracturing of rocks*. International series in the earth and planetary sciences: McGraw-Hill Book Company.

Roberts, D. 2003. The Scandinavian Caledonides: event chronology, palaeogeographic settings and likely modern analogues. *Tectonophysics* 365, 283-299.

Roberts, D. and Gee, D. 1985. An introduction to the structure of the Scandinavian Caledonides. *In* Gee, D.G. and Sturt, B.A. (eds). *The Caledonide orogen–Scandinavia and related areas*: John Wiley and Sons, 1, 55–68.

Roberts, D. and Sturt, B. 1980. Caledonian deformation in Norway. *Journal of the Geological Society* 137, 241.

Schiøtz, O.E. 1902. Den sydøstelige Del af Sparagmit-Kvarts-Fjeldet i Norge. *Norges geologiske undersøkelse* 35, 1-131.

Sippel, J., Saintot, A., Heeremans, M. and Scheck-Wenderoth, M. 2009. Paleostress field reconstruction in the Oslo region. *Marine and Petroleum Geology*.

Strøm, K.M. 1940. Tyrifjord Geomorphology. Relation of a Lake Basin and its Surroundings to the Geological Structure of the Region. *Norsk Geografisk Tidsskrift* 8, 85-93.

Sturt, B.A., Pringle, I.R. and Ramsay, D.M. 1978. The Finnmarkian phase of the Caledonian orogeny. *Journal of Geological Society* 135, 597-610.

Størmer, L. 1934. Spor av kaledonisk overskyvning i Nordmarka. *Norsk Geologisk Tidskrift* 13 (1-4), 116-128.

Størmer, L. 1953. The Middle Ordovician of the Oslo region. Introduction to stratigraphy. *In* Kolderup, N.H. (ed): Norsk Geologisk Tidsskrift, 31, 37-141.

Størmer, L. 1967. Some aspects of the Caledonian geosyncline and foreland west of the Baltic Shield. *The Quarterly Journal of the Geological Society of London* 123, 183–214.

Sundvoll, B., Larsen, B. and Wandaas, B. 1992. Early magmatic phase in the Oslo Rift and its related stress regime. *Tectonophysics* 208, 37-54.

Sundvoll, B. and Larsen, B.T. 1994. Architecture and early evolution of the Oslo Rift. *Tectonophysics* 240, 173-189.

Thompsen, E., Jin, J. and Harper, D.A.T. 2006. Early Silurian brachiopods (Rhynchonellata) from the Sælabonn Formation of the Ringerike district, Norway. *Bulletin of the Geological Society of Denmark* 53, 111–126.

Trønnes, R. and Brandon, A. 1992. Mildly peraluminous high-silica granites in a continental rift: the Drammen and Finnemarka batholiths, Oslo Rift, Norway. *Contributions to Mineralogy and Petrology* 109, 275-294.

Turner, P. 1974. Lithostratigraphy and facies analysis of the Ringerike Group of the Oslo Region. *Norges Geologiske Undersoekelse* 314, 101-131.

Van der Pluijm, B.A. and Marshak, S. 2004. *Earth structure: an introduction to structural geology and tectonics*. Edited by Wiegman, L.A.W. Second ed: W.W. Norton & Company. 656 pp.

Worsley, D., Aarhus, N., Bassett, M., Howe, M., Mørk, A. and Olaussen, S. 1983. *The Silurian succession of the Oslo region*. Edited by Roberts, D. Norges geologiske undersøkelse. 384: Universitetsforlaget.

Zwaan, K.B. and Larsen, B.T. 2003. *Berggrunnskart HØNEFOSS 1815 III, M 1:50 000, foreløpig utgave*. Norges Geologiske Undersøkelse.